INFORMATION TO USERS

This was produced from a copy of a document sent to us for microfilming. While the most advanced technological means to photograph and reproduce this document have been used, the quality is heavily dependent upon the quality of the material submitted.

The following explanation of techniques is provided to help you understand markings or notations which may appear on this reproduction.

1. The sign or "target" for pages apparently lacking from the document photographed is "Missing Page(s)". If it was possible to obtain the missing page(s) or section, they are spliced into the film along with adjacent pages. This may have necessitated cutting through an image and duplicating adjacent pages to assure you of complete continuity.

2. When an image on the film is obliterated with a round black mark it is an indication that the film inspector noticed either blurred copy because of movement during exposure, or duplicate copy. Unless we meant to delete copyrighted materials that should not have been filmed, you will find a good image of the page in the adjacent frame. If copyrighted materials were deleted you will find a target note listing the pages in the adjacent frame.

3. When a map, drawing or chart, etc., is part of the material being photographed the photographer has followed a definite method in "sectioning" the material. It is customary to begin filming at the upper left hand corner of a large sheet and to continue from left to right in equal sections with small overlaps. If necessary, sectioning is continued again—beginning below the first row and continuing on until complete.

4. For any illustrations that cannot be reproduced satisfactorily by xerography, photographic prints can be purchased at additional cost and tipped into your xerographic copy. Requests can be made to our Dissertations Customer Services Department.

5. Some pages in any document may have indistinct print. In all cases we have filmed the best available copy.

University
Microfilms
International

300 N. ZEEB RD., ANN ARBOR, MI 48106

8217400

Calabro, David Charles

THE ELECTRONIC STRUCTURE OF COORDINATED OLEFIN, MU-ALKYLIDENE, AND CARBONYL LIGANDS AS PROVIDED BY PHOTOELECTRON SPECTROSCOPY

The University of Arizona PH.D. 1982

University
Microfilms
International 300 N. Zeeb Road, Ann Arbor, MI 48106

THE ELECTRONIC STRUCTURE OF COORDINATED OLEFIN, μ-ALKYLIDENE, AND CARBONYL LIGANDS AS PROVIDED BY PHOTOELECTRON SPECTROSCOPY

by

David Charles Calabro

A Dissertation Submitted to the Faculty of the

DEPARTMENT OF CHEMISTRY

In Partial Fulfillment of the Requirements
For the Degree of

DOCTOR OF PHILOSOPHY

In the Graduate College

THE UNIVERSITY OF ARIZONA

1 9 8 2

THE UNIVERSITY OF ARIZONA
GRADUATE COLLEGE

As members of the Final Examination Committee, we certify that we have read the dissertation prepared by DAVID CHARLES CALABRO

entitled THE ELECTRONIC STRUCTURE OF COORDINATED OLEFIN, μ-ALKYLIDENE, AND CARBONYL LIGANDS AS PROVIDED BY PHOTOELECTRON SPECTROSCOPY

and recommend that it be accepted as fulfilling the dissertation requirement for the Degree of DOCTOR OF PHILOSOPHY.

Gregory O. Nelson	12/2/81 Date
Robert D. Feltham	12/2/81 Date
Mindy C. Keller	Dec. 2, 1981 Date
Dennis L. Lichtenberger	2 Dec 81 Date
Stephen D. Kevan	Dec 2, 1981 Date

Final approval and acceptance of this dissertation is contingent upon the candidate's submission of the final copy of the dissertation to the Graduate College.

I hereby certify that I have read this dissertation prepared under my direction and recommend that it be accepted as fulfilling the dissertation requirement.

Dennis L. Lichtenberger	2 Dec 81
Dissertation Director	Date

STATEMENT BY AUTHOR

This dissertation has been submitted in partial fulfillment of requirements for an advanced degree at the University of Arizona and is deposited in the University Library to be made available to borrowers under rules of the Library.

Brief quotations from this dissertation are allowable without special permission, provided that accurate acknowledgment of source is made. Requests for permission for extended quotation from or reproduction of this manuscript in whole or in part may be granted by the head of the major department or the Dean of the Graduate College when in his judgment the proposed use of the material is in the interests of scholarship. In all other instances, however, permission must be obtained from the author.

SIGNED: David Calabro

To Chelo

ACKNOWLEDGMENTS

Many thanks are due to the people who aided my growth during this study in many different ways. Chelo, whose patience and enduring faith in me were indispensible. Dennis Lichtenberger, who through our frequent and informal interactions, was much more of an educator than a director. Finally, the assistance, conversations and friendships of Charles Blevins, Andrew Campbell and John Hubbard were bonuses that I was very fortunate to receive.

TABLE OF CONTENTS

Page

LIST OF ILLUSTRATIONS

LIST OF ILLUSTRATIONS--Continued

LIST OF ILLUSTRATIONS--Continued

LIST OF TABLES

ABSTRACT

This dissertation describes a study of the electronic structure of some selected cyclopentadienyl metal olefin, μ-alkylidene and carbonyl complexes. While most studies of this type are largely the theoretical in nature, this work relies on the experimental observations which result from the application of photoelectron spectroscopy to the measurement of the important molecular ionization energies of these compounds.

The first part of the discussion is a study of metal-olefin bonding in the $CpM(CO)_2L$ ($L = C_2H_4$, C_3H_6) compounds. Of particular interest are the observed changes in ionization energy of the olefin pi orbital upon coordination. These results also allow a comparison of the coordination of CO and C_2H_4.

The valence ionizations of μ-CH_2-$[(C_5H_4CH_3)Mn(CO)_2]_2$ are also presented. This example of the increasingly important μ-alkylidene compounds, provides evidence of a 3C-6e configuration with a net Mn-Mn single bond.

The final chapter describes a study of the valence electronic structure of the $CpM(CO)_2$ (M = Co, Rh; Cp = η^5-$C_5H_5^-$ and η^5-$C_5(CH_3)_5^-$) system. This group of four closely related molecules

demonstrates how photoelectron spectroscopy can be used to monitor the electronic effects of specific chemical modifications.

The intent throughout is to not only present a detailed analysis of the specific compounds chosen for this study, but to also further demonstrate the applicability of photoelectron spectroscopy to a broad spectrum of problems concerning the structural and electronic make-up of organometallic molecules.

CHAPTER 1

Introduction

The interface of organic and inorganic chemistry has attracted a steadily increasing amount of attention since the early 1950's. This sustained effort has made organometallic chemistry one of the most important and rapidly developing areas of modern chemistry. The driving force for the growth of organometallic chemistry has been the continued importance of organic synthesis. Metal-assisted organic synthesis provides a whole new set of parameters with which the synthetic chemist has introduced many previously unknown and hard to obtain compounds. However, more importantly, it enables many important organic reactions to be carried out catalytically. Hence, two vitally important chemical endeavors (organic synthesis and catalysis) come together in organometallic chemistry.

This rapid growth period has involved a major research effort at uncovering the rich and varied chemistry of the metal-carbon bond. Much of this effort has dealt with defining the many parameters which produce this chemistry. The application of improved spectroscopic and crystallographic methods to organometallic compounds has directed much work toward a better understanding of basic structure - reactivity relationships. While a great deal of descriptive chemistry has been reported, the kinetics and mechanisms of many important organometallic reactions

remain an area of much speculation. The complexity of these systems and the fact that many proposed reaction intermediates have never been observed challenge our ability to explain many experimental results and to predict reaction products.

A key requirement to an improved explanation of the chemistry of organometallic compounds is a better understanding of the basic orbital interactions which constitute the molecular orbital descriptions of organometallic molecules. While several longstanding qualitative bonding models exist, a quantitative assessment of the relative importance of various orbital interactions is lacking. This has been due to the absence of experimental methods which are capable of providing this information.

In the late sixties the ability for studying the ionization of valence orbitals came on the scene with the birth of ultraviolet photoelectron spectroscopy (UPS).[1-4] By studying these ionizations in the gas phase the problems of solid state and charging effects are avoided and meaningful observations on valence elecronic structure can be made. Since most technical phenomena are the result of valence orbital interactions, a technique which is sensitive to these interactions can potentially provide correlations between electronic structure and molecular properties.

There have been two major applications of UPS. The theoretician may, to a first approxiation, view a photoelectron spectrum as an experimentally measured molecular orbital diagram. It measures the

energies required to attain various positive ion states as the ionization energy of each molecular orbital within the ionizing range of the radiating source. The most common theoretical approximation of ionization energies is Koopmans' Theorem which equates ground state orbital eigenvalues with ionization energies.[5] While the deficiencies of the theorem have been long recognized,[6] it was generally felt to be a good approximation for valence ionizations. The growth of valence photoelectron spectroscopy has shown this not be be valid in many cases (see Appendix A). Considerable theoretical effort has gone into deriving more reliable ways of relating orbital eigenvalues with ionization energies. Photoelectron spectroscopic data furnishes a valuable empirical standard for comparing the relative validity of these calculational methods.

The largest impact of photoelectron spectroscopy is its ability to directly observe changes in the energy of molecular orbitals. Besides changes in ionization energies, band shape analysis can sometimes be used to indicate orbital composition and relative bonding, nonbonding character. The application of these tools and others to a better characterization of the electronic structure of organometallic compounds will be the major focus of this study. This aspect of the dissertation will concern itself with the specific results and interpretations presented. A secondary, but perhaps equally important, focus will be the experimental aproaches used in obtaining these results and arriving at our interpretations of them.

Unlike more commonly used spectroscopic techniques, a single photoelectron spectrum frequently does not furnish a great deal of interpretable data unless it is compared with the spectra of related compounds. Much of the information uncovered here became apparent only as a result of the comparisons made possible by the particular experiments which were performed. The approach which is used throughout this study is to examine the photoelectron spectra of a series of closely related compounds in which changes in electronic structure can be attributed to specific chemical differences. This is apparent in the first two systems discussed, both of which have the $CpMn(CO)_2$ fragment in common.

Chapter three approaches the general area of metal-olefin bonding with a valence ionization study of a series of $CpMn(CO)_2$(olefin) compounds. Various methylated and non-methylated cyclopentadienyl ring and olefin ligands are used to induce specific shifts in the valence ionizations. The information gained from these shifts is used in making peak assignments and a comparison of the relative coördinating abilities of CO and C_2H_4. Chapter four describes the HeI UPS of the dinuclear μ-$CH_2[(MeCp)Mn(CO)_2]_2$ compound. These results are shown to be in good agreement with a Fenske-Hall molecular orbital diagram of this molecule.

Important background material for Chapters three and four is provided by the valence electronic structure study of the $CpM(CO)_3$; M = Mn and Re, system in Appendix B. In particular, the relative ordering of

the mostly metal d ionizations and a bandshape analysis of the predominantly ring pi ionization are discussed.

The final chapter describes a UPS study of the $CpM(CO)_2$ and $Me_5CpM(CO)_2$ (M = CO, Rh) compounds. These results compliment earlier gas-phase evidence for the distortion of coordinated cyclopentadienyl rings from five-fold symmetry (Appendix B). The considerable electronic structure differences between these first and second row analogues are also discussed and attributed to periodic trends in electron relaxation effects.

The overall strategy will be to make small chemical changes, and then try to determine what changes in electronic structure have resulted.

CHAPTER 2

EXPERIMENTAL

Photoelectron Spectrometer

All UPS spectra were measured using a McPherson ESCA 36 electron spectrometer.

HeI. Samples were run from a variable temperature sample cell designed by J. L. Hubbard. Spectra of the mononuclear Mn compounds were obtained at room temperature, while the Re compounds required heating to 50-60°C. A temperature of 80°C was required to obtain a convenient vapor pressure of μ-CH_2-$[MeCpMn(CO)_2]_2$ for data collection. All other samples were run at room temperature. The argon $^2P_{3/2}$ ionization at 15.76 eV was used as an internal lock during data acquisition to ensure that spectral drift was less than ±0.05 eV during time-averaging of repetitive scans. The resolution (FWHM of $Ar^2P_{3/2}$ ionization) was less than 0.025 eV. Resolution was maintained at 0.017 eV during observation of the vibrational structure in the ionizations of the rhenium complexes.

HeII. Samples were handled similarly in the HeII studies. The HeII radiation source was a differentially pumped, charged particle oscillator type lamp based on designs previously described.[7] The He^+ ionization at 24.6 eV was used as an internal lock.

Data Analysis

Peak positions and relative intensities were obtained by a previously described[8] asymmetrical Gaussian curve-fit with the functional form:

$$C(E) = Ae^{-k[(E-P)/W]^2}$$

where C(E) = electron counts at binding energy E; A = peak amplitude; P = peak position (vertical I.P.); $W = W_h$, the half-width for E > P, or W_1, the half-width for E < P; k = 4 ln 2.

Molecular Orbital Calculations

Orbital eigenvalues were calculated by both the extended Hückel[9] and Fenske-Hall[8,10] methods. The general fragment analysis techniques used for $C_5H_5Co(CO)_2$ are typical. Initially, independent calculations were performed on the $C_5H_5^-$ and $Co(CO)_2^+$ fragments. The eigenvectors from these calculations were then used in the overall $C_5H_5Co(CO)_2$ calculation. The atomic basis functions used were taken from Richardson[11a] (Co 1s through 3d with 4s and 4p exponent of 2.0) and Clementi[11b] (double zeta carbon and oxygen functions with the 1s and 2s reduced to single zeta form). An exponent of 1.2 was used for the hydrogen atom. The atomic coordinates and basis functions for the $CpMn(CO)_2$ fragment were taken from reported calculations.[8,12,13] The bond distances and angles of the coordinated olefins were taken from the crystal structures of several $CpMn(CO)_2$(olefin) complexes.[14] The coordinated olefin

geometry (figure 5) was set at a typical C=C bond length of 1.40Å with the four hydrogen atoms bent away from the metal by 12°.[15] The $CpMn(CO)_2$ and CH_2 fragments of μ-CH_2-$[(C_5H_5)Mn(CO)_2]_2$ were oriented according to the crystal structure of this complex.[16] The atomic positions of $C_5H_5Co(CO)_2$ were set according to the crystal structure of $C_5(CH_3)_5Co(CO)_2$.[17]

Preparation of Compounds

All manipulations were carried out using standard Schlenk techniques. Solvents were dried and stored in a dry nitrogen atmosphere until use. Samples were characterized by reported ν_{CO} frequencies and purified by chromatography and/or sublimation. Unless described below, all compounds were prepared according to reported methods. The literature references for these syntheses are given in Table I. $(\eta^5\text{-}C_5H_5)Mn(CO)_3$ was purchased from Strem Chemical Company and $(\eta^5\text{-}C_5H_4CH_3)Mn(CO)_3$ was a gift from Ethyl Corporation. A sample of μ-CH_2-$[(C_5H_4CH_3)Mn(CO)_2]_2$ was kindly furnished by Professor W. A. Herrmann of the University of Regensburg. Infrared spectra were taken in hexane on a Perkin-Elmer 398 spectrometer, ^1H NMR spectra were recorded in CCl_4 on a Varian EM306L instrument. Elemental analyses were obtained from the University of Arizona Analytical Center.

$\underline{\eta^5\text{-}C_5(CH_3)_5Mn(CO)_2(C_2H_4)}$. After purging with argon, a Hanovia-type photochemical reactor was charged with 150 ml of THF containing 0.15 g (0.55 mmoles) $C_5(CH_3)_5Mn(CO)_3$. The pale yellow solution was irradiated for 90 minutes at 0°, at which time the IR indicated complete

loss of the tricarbonyl starting material with a color change to deep red. After bubbling ethylene through the solution for 45 minutes, the now golden yellow solution showed no IR peaks for the $CH_3C_5H_4Mn(CO)_2(THF)$ intermediate. Evaporation to dryness and multiple sublimations at 45° (0.1 mm) gave the bright yellow product (66%).

Analysis: Calcd. for $C_{14}H_{19}O_2Mn$: C, 61.35; H, 6.93; O, 11.68; Mn, 20.05. Found: C, 61.78; H, 7.03; O, 11.59; Mn, 19.6 ± 1.

^1H NMR (CCl_4): δ 1.69 (singlet). IR (hexane, cm^{-1}) 1958(S), 1989(S).

$\underline{\eta^5\text{-}C_5(CH_3)_5\ Rh(CO)_2}$. $LiC_5(CH_3)_5$ was prepared in situ by reacting 0.5 ml (3 mmoles) distilled $C_5(CH_3)_5H$ with 1.2ml 2.4M (n-butyl)Li in 5 ml hexane at 0°. After warming to room temperature and stirring overnight, this milky white solution was charged with 0.15 g (0.39 mmoles) $Rh_2Cl_2(CO)_4$ to give an immediate dark solution. After stirring for 3.5 hours solvent was removed and the purple/black residue was eluted through a fluorosil column using methanol. A dark band was collected, solvent evaporated and the residue sublimed at 40-50° to give red-orange crystals. The product decomposed at 79-80° and exhibited the reported ν_{CO} peaks (KBr) at 2000 cm^-(s) and 1939 cm^-(s).[24]

Table I - Literature References for Sample Preparation

Compound	Reference
$C_5(CH_3)_5H$	18
$(\eta^5\text{-}CH_3C_5H_4)Mn(CO)_2(C_2H_4)$	19
$(\eta^5\text{-}CH_3C_5H_4)Mn(CO)_2(C_3H_6)$	19
$(\eta^5\text{-}C_5H_5)Co(CO)_2$	20
$(\eta^5\text{-}C_5(CH_3)_5)Co(CO)_2$	17, 21
$(\eta^5\text{-}C_5H_5)Rh(CO)_2$	22
$Rh_2Cl_2(CO)_4$	23

CHAPTER 3

METAL-OLEFIN ORBITAL INTERACTIONS IN $CpMn(CO)_2$(olefin)

Interactions that are basically pi in symmetry between metals and coordinated molecules are a common occurrence in inorganic and organometallic chemistry. The most important examples are perhaps the interactions of metals with unsaturated hydrocarbons and other carbon-containing species. The Dewar-Chatt-Duncanson model has provided a long-standing qualitative picture of the bonding in olefin-type systems.[25] However, recent theoretical treatments have called attention to a number of other potentially significant considerations.[26-30] For instance, in one study the classical donation from the olefin pi orbital to the empty metal dz^2 orbital is found to be accompanied by a comparable interaction with the dx^2-y^2 orbital.[27] The prediction of considerable metal interaction with the olefin σ and σ^* orbitals has also appeared.[28,29] There is considerable disagreement between different theoretical methods as to the relative importance of the different bonding interactions. Experimental information relating to these interactions is obtainable from high-resolution valence photoelectron spectroscopy of particular metal-olefin complexes. The application of this technique to the study of the electronic structure of coordinated olefins has been receiving

increasing attention. Early studies reported the HeI spectra of ethylenes adsorbed on metal surfaces[31] and coordinated to $(\eta^5\text{-}C_5H_5)_2Mo$ (and W)[32] and $Fe(CO)_n$.[33-37] More recently the gas phase HeI and HeII spectra of some Rh and Ir complexes have been reported.[38] Many of the systems that have been studied have been hampered either by instability and decomposition of the molecules or by the overlap of key ionization features.

This chapter describes a study of the valence ionizations of $MeCpMn(CO)_2(C_2H_4)$, $MeCpMn(CO)_2(C_3H_6)$, and $Me_5CpMn(CO)_2(C_2H_4)$, where MeCp = $\eta^5\text{-}C_5H_4CH_3$ and Me_5Cp = $\eta^5\text{-}C_5(CH_3)_5$. The stability and volatility of these systems make them attractive for the gas phase photoelectron study of coordinated olefin ionizations. The possibility of different methyl substitutions on the olefin and cylopentadienyl ring is also important. As we have shown, ring methylation causes large shifts in the valence ionizations which are dependent on the orbital character of the band.[39] Knowledge of these shifts allows predictable variations in the available UPS spectral window, which is useful in uncovering specific ionization features that are otherwise obscured by overlapping peaks. Peak assignments and interpretations in this study are aided by HeI/HeII intensity ratio changes and molecular orbital calculations. Particular attention is given to changes in the metal d ionizations in going from the parent tricarbonyl to the olefin complexes, and to the ionization energy shift of the predominantly olefin pi orbital upon coordination. A direct comparison of CO and C_2H_4 bonding capabilities in these complexes is provided by these results. It is also shown that distortions of the coordinated olefin, as well

as the relative pi-donation/pi*-acceptance, are important in explaining the observed shifts in the ionization energy of the olefin pi orbital. These distortions represent a movement toward a metallocyclopropane-type geometry from the classical Dewar-Chatt-Duncanson extreme.

Ionization Band Assignments

The valence photoelectron spectra of $MeCpMn(CO)_3$, $MeCpMn(CO)_2(C_2H_4)$, $MeCpMn(CO)_2(C_3H_6)$ and $Me_5CpMn(CO)_2(C_2H_4)$ are shown in figure 1. The similarities and differences in the photoelectron spectra of this series of closely related compounds are important to the interpretation of the ionizations. Each spectrum has a broad band of overlapping ionizations from about 11-16 eV ionization energy. The ionizations expected to occur in this region are associated with the carbonyl 5σ and 1π orbitals and the cyclopentadienyl $a_2''(\pi)$ and certain sigma orbitals. The most noticeable changes occur on the leading edge of this region. For each of the MeCp complexes there is a visible shoulder at about 12 eV that has been attributed to ionization from an orbital of the ring methyl group (Appendix B). For the propylene complex there is an additional inflection at about 11-11.5 eV that is presumably due to the methyl group of this olefin. In the spectrum of the Me_5Cp complex this shoulder now appears as a major ionization feature that has shifted to lower binding energy, consistent with the electron-donating effect of the five cyclopentadienyl methyl groups.[39]

The most significant changes are observed in the valence ionization features occuring below 11 eV. This region is shown in greater

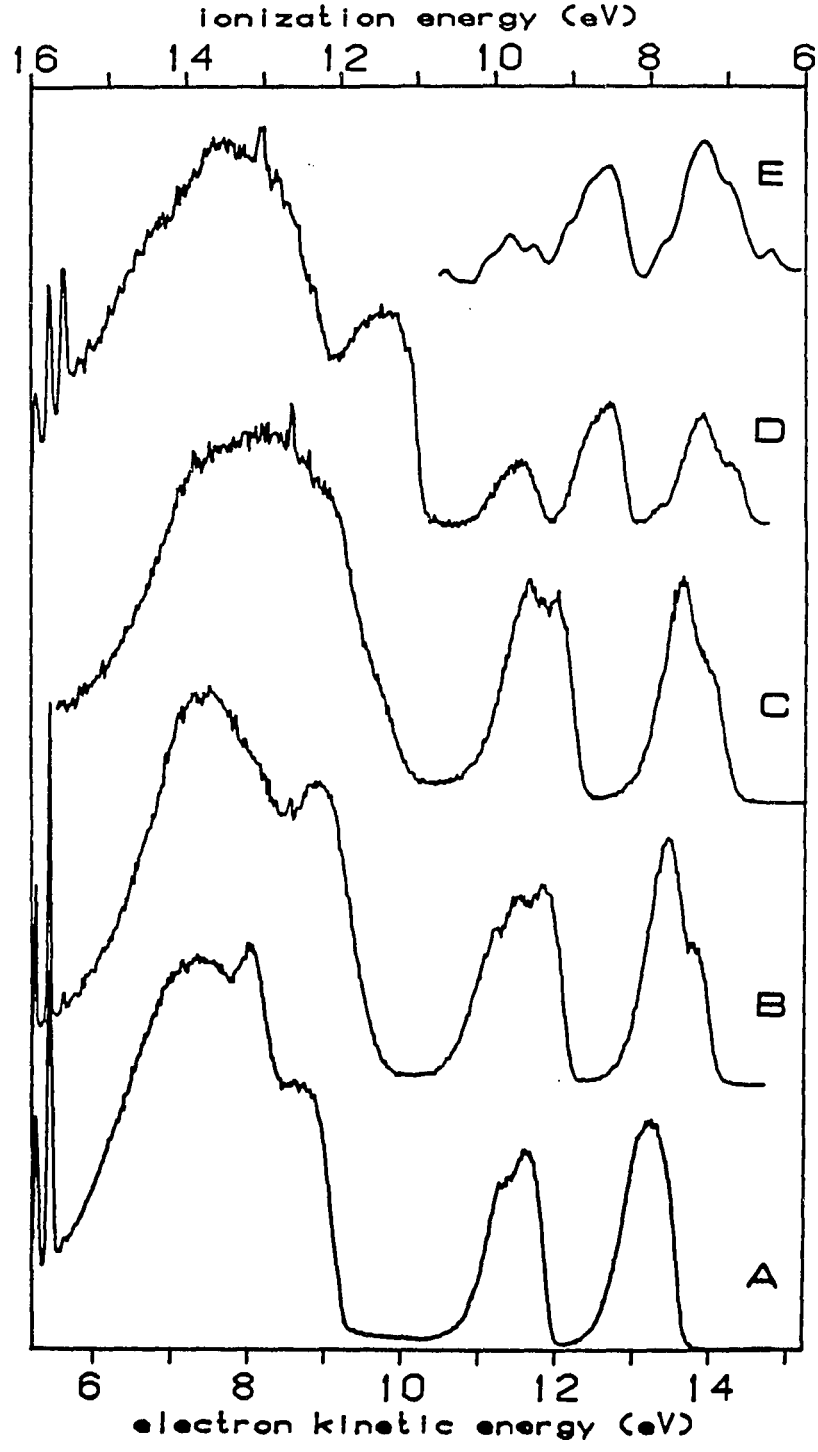

Figure 1 - HeI Photoelectron Spectra of A) $MeCpMn(CO)_3$, B) $MeCpMn(CO)_2(C_2H_4)$, C) $MeCpMn(CO)_2(C_3H_6)$, D) $Me_5CpMn(CO)_2(C_2H_4)$ and E) HeII Spectra of $Me_5CpMn(CO)_2(C_2H_4)$

detail along with the curve analysis of these bands in figure 2. The vertical ionization energies, shapes, and relative intensities of each band are compiled in Table II. The fit bands are labeled a, b, c, d, and e starting from low ionization energy. A number of very significant changes occur in these ionizations. Consider first comparison of the spectrum of $MeCpMn(CO)_3$ with that of $MeCpMn(CO)_2(C_2H_4)$. Previous comparisons of the ionizations of metal-CO and metal-C_2H_4 complexes found very little differences in the predominantly metal ionizations.[32-36] We observe distinct differences in these ionizations which will be important in interpreting the olefin interactions. For instance, the broad, unresolved peak at about 8 eV in the spectrum of $MeCpMn(CO)_3$ becomes a pair of partially resolved peaks with an intensity pattern of approximately 1:2 in the spectrum of $MeCpMn(CO)_2(C_2H_4)$. The order of the 1:2 intensity peaks is opposite to that concluded for the first band of the $MeCpMn(CO)_3$ complex (Appendix B). The ionization band in the region from 9-10 eV is considerably more broad in the spectrum of the ethylene complex than in the spectrum of the tricarbonyl complex. The shape of this band for the tricarbonyl complex, shown in detail in figure 2A, is generally characteristic of the predominantly cyclopentadienyl e_1'' ionizations for these complexes (Appendix B). The curve analysis of the corresponding band in the olefin complex (figure 2B) suggests that a similarly shaped ionization may be present in this region along with an additional overlapping band. The intensities are consistent with bands c and d being associated with the MeCp e_1'' ionization. The low intensity band e at 10.11 eV must then be assigned to

Table II - HeI Ionization Data for $(CH_3)_nC_5H_{5-n}Mn(CO)_2L$

where L = CO, C_2H_4, C_3H_6; n = 1,5

		Ionization Energy (eV)	W_h	W_l	Relative Amplitude	Relative Area	
$CH_3C_5H_4Mn(CO)_3$	a	7.89	0.65	0.38	1.0	1.0	1.0
	b	8.23	0.65	0.38	0.50	0.50	
	c	9.57	0.57	0.36	0.96	0.87	0.93
	d	10.00	0.57	0.36	0.57	0.52	
$CH_3C_5H_4Mn(CO)_2(C_2H_4)$	a	7.38	0.66	0.33	1.0	1.0	1.0
	b	7.78	0.66	0.33	1.55	1.55	
	c	9.32	0.70	0.36	1.49	1.61	1.27
	d	9.78	0.70	0.36	0.85	0.90	
	e	10.11	0.70	0.36	0.49	0.52	
$CH_3C_5H_4Mn(CO)_2(C_3H_6)$	a	7.19	0.61	0.35	1.0	1.0	1.0
	b	7.59	0.61	0.35	1.40	1.40	
	c	9.16	0.66	0.36	1.58	1.69	1.36
	d	9.58	0.66	0.36	0.90	0.96	
	e	9.75	0.95	0.38	0.45	0.62	
$(CH_3)_5C_5Mn(CO)_2(C_2H_4)$	a	6.94	0.61	0.32	1.0	1.0	1.0
	b	7.34	0.61	0.32	1.60	1.60	
	c	8.48	0.42	0.28	2.03	1.55	0.94
	d	8.81	0.42	0.28	1.15	0.88	
	e	9.67	0.71	0.40	1.0	1.19	0.46

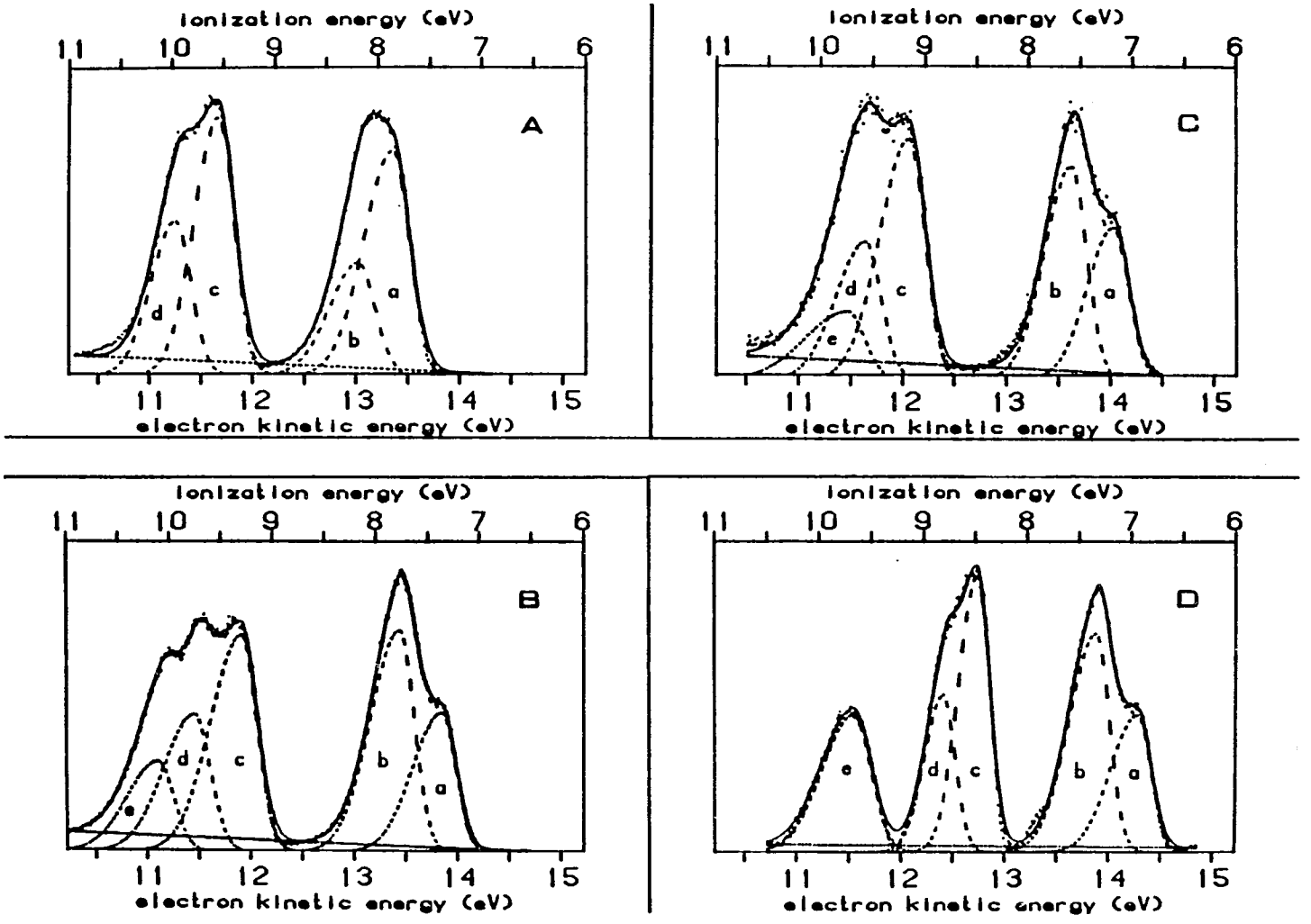

Figure 2 - Low Energy (11 → 6 eV) HeI Spectra of A) $MeCpMn(CO)_3$, B) $MeCpMn(CO)_2(C_2H_4)$, c) $MeCpMn(CO)_2(C_3H_6)$ and D) $Me_5CpMn(CO)_2(C_2H_4)$

the predominantly olefin pi ionization. This is in the vicinity of the pi ionization of free ethylene which occurs at 10.51 eV. However, it should be noted that coordination of a $2e^-$ donor molecule to a metal normally shifts ionization of the ligand donor orbital to higher ionization energy. In previous photoelectron spectra of a single olefin coordinated to a metal center, the ionizations assigned to the olefin donor orbital are stabilized by 0.05 to 1.15 eV on coordination.[32,36] A destabilization of 0.4 eV in the present case should be considered unusual. Also, the fact that the bands in this region are overlapping introduces uncertainty in their true shapes, intensities, and positions. We felt that additional experimental information must be obtained to confirm these results.

One approach is to perturb the electronic structure of the system in a well-defined way and observe the effect on each valence ionization. The change in a particular valence ionization will then give information on the associated orbital character. For example, the electronic structure of the analogous propylene complex may be considered a simple perturbation of the electronic structure of the ethylene complex. The methyl group on the propylene alters the olefin electronic structure through a combination of inductive and hyperconjugative effects as described in a UPS study of the effects of ring methylation in $CpMn(CO)_3$.[39] The first ionization of free propylene (9.85 eV) is sufficiently lower than the first ionization of free ethylene (10.51 eV) to alter the interactions with the metal and shift the valence ionizations of the complexes. Comparison of spectra B and C in figures 1 and

2 show the effects of these perturbations. The most visible change from the ethylene to the propylene complex spectrum is a narrowing and change in contour of the band between 9 and 10 eV. The curve analysis indicates that this is a result of fit band e shifting closer to bands c and d. The data in Table III show that band e experiences the largest destabilization (0.36 eV), consistent with assigning it to the olefin pi ionization. The splitting and intensity pattern of the metal ionizations remains much the same but they are shifted 0.19 eV to lower binding energy by the destabilized olefin levels. Bands c and d, assigned to orbitals which correlate predominantly with the e_1'' HOMO of the free cyclopentadienide anion, (Appendix B) are similarly shifted 0.18 eV to lower binding energy.

The problem remains that the olefin pi ionization has not been clearly resolved in these complexes, leaving some uncertainty concerning its precise ionization energy and intensity. The propylene complex is helpful in supporting band assignment, but the pi ionization band is shifted further under the predominantly cyclopentadienyl e_1''-type ionizations. This observation indicates that methylation of the cyclopentadienyl ring, rather than the olefin, should be helpful in separating these bands. The need to selectively separate overlapping bands in complexes of this type is what originally prompted our study of ring methylation, and led to the synthesis of $Me_5CpMn(CO)_2(C_2H_4)$. The valence ionization spectrum of this complex is shown in figures 1 and 2. A clearly visible olefin pi ionization is observed for this complex. The

Table III. Observed Effects of Ring and Olefin Methylation[a]

	$MeCpMn(CO)_2(C_2H_4)$ ↓ $Me_5CpMn(CO)_2(C_2H_4)$	$MeCpMn(CO)_2(C_2H_4)$ ↓ $MeCpMn(CO)_2(C_3H_6)$
Metal 1a', 2a', a" shifts[b]	0.44	0.19
Ring e_1" shift	0.85	0.18
Olefin pi shift (band e)	0.44	0.36

a) Destabilization of ionization energies in eV

b) The 1a', 2a' and a" shift by the same amount

Me_5Cp e_1"-type ionization (c and d) has the characteristic shape for this band and has shifted 0.85 eV to lower binding energy compared to the corresponding MeCp ionization (Table III). The olefin pi ionization (9.67 eV) has shifted 0.44 eV. The predominantly metal d ionizations have shifted 0.44 eV also, and retain the same splitting and intensity pattern.

The olefin pi ionization is characterized as rather low intensity and broad. The HeII valence photoelectron spectrum of $Me_5CpMn(CO)_2(C_2H_4)$ is shown in figure 1E. The relative increase in intensity of the first band compared to the next two may be attributed to the high metal d character of the first ionization.[40,41] The relative intensity of the Me_5Cp and ethylene pi ionizations does not change appreciably, as one would expect for the similar carbon character and nodal characteristics of these orbitals.

The experimental observations described above present two specific challenges for our understanding of the bonding of olefins to metal centers. First, what do the shifts and band contours of the metal and cyclopentadienyl ionizations indicate about the relative strengths of separate olefin orbital interactions with the metal center? Second, why does the olefin pi ionization, which forms the $2e^-$ donor bond to the metal center, occur at <u>lower</u> binding energy for the coordinated olefin than for the free olefin? Before addressing these points in detail, it is necessary to be familiar with the relevant molecular orbitals of $CpMn(CO)_2(C_2H_4)$. These will provide a basis for the interpretation of the spectral changes which occur throughout this series of compounds.

Orbital Interactions of C_2H_4 with $CpMn(CO)_2$

The $CpMn(CO)_2$ fragment is able to coordinate many different kinds of ligand molecules,[42] partly because it possesses both donor and acceptor orbitals that are energetically and spatially favorable for bonding interactions. The bonding capabilities of the $CpMn(CO)_2$ fragment have been described previously and applied to a large number of $CpMn(CO)_2L$ compounds.[8,12,13,43,44] These compounds may be considered pseudo-octahedral if the cyclopentadienyl ring is viewed as occupying three coordination sites. The most convenient coordinate system for describing the orbital interactions of $CpMn(CO)_2$ places the vacant coordination site along the z axis, with the x axis bisecting the two carbonyls as shown in figure 3. We have placed a C_2H_4 ligand in the vacant coordination site to illustrate how it interacts with the valence orbitals of the $CpMn(CO)_2$ fragment. The orbitals shown are calculated eigenvectors of the fragment and not the ethylene complex. The LUMO of the fragment is the 3a' orbital, which is high in dz^2 character and is a good acceptor orbital for incoming ligands along the vacant z axis. The three highest occupied orbitals of $CpMn(CO)_2$ are the 1a', a" and 2a' orbitals shown in figure 3. The 1a' and a" both possess pi symmetry with respect to the vacant coordination site. The 1a' orbital is high in dxz character. The a" is mostly dyz in nature and is hybridized toward the vacant site. Thus the a" orbital is the most effective pi donor orbital and molecules with single pi acceptor orbitals, like olefins, tend to align for interaction with this orbital.[42,44] The remaining HOMO of the fragment is the 2a' orbital which is high in

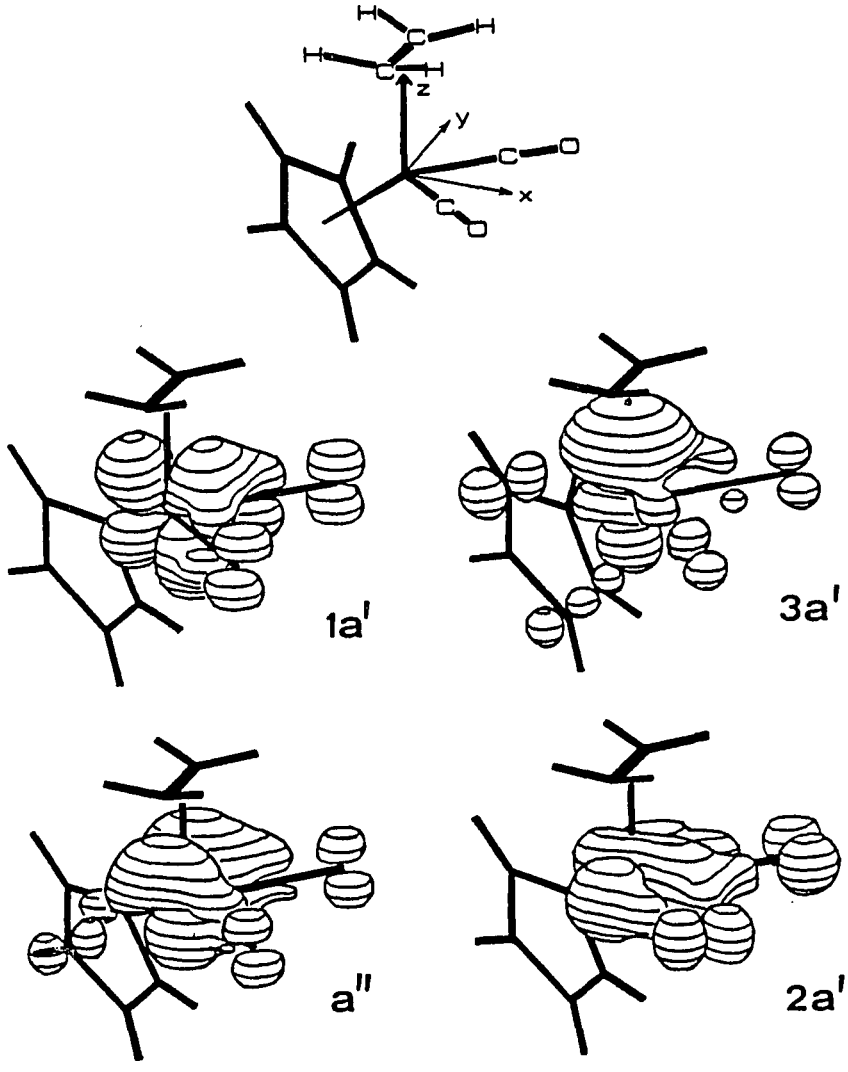

Figure 3 - Three-Dimensional Fenske-Hall Orbital Surface Plots of the Valence Molecular Orbitals of the $CpMn(CO)_2$ Fragment Showing Their Positions Relative to an Ethylene Ligand. The Contour Shown is for a 0.05 Value of the Wavefunctions.

dx^2-y^2 character (some dz_2 also) and has primarily delta symmetry with respect to the vacant site. The correlation of these occupied orbitals with the normal t_{2g} orbitals in octahedral symmetry can be seen.

Coordination of the olefin to $CpMn(CO)_2$ primarily involves the formation of a $2e^-$ donor bond between the olefin pi donor orbital and the empty 3a' orbital of the fragment, and the orientation of the olefin to give optimum overlap between its pi* acceptor orbital and the most effective fragment donor orbital (a"). The olefin has no other comparable acceptor orbitals to interact with the less favorable la' donor. The remaining 2a' fragment orbital has no significant delta overlap with the olefin, but it may have some interaction with the olefin pi orbital. The strength of these interactions will affect the ionization energies of the metal d and olefin pi orbitals observed in the photoelectron spectrum.

Metal and Ring Ionizations

The HeI spectra of the olefin complexes in figures 1 and 2 show a considerably different bandshape in the metal ionization region (7.0 - 8.0 eV) than that of the $MeCpMn(CO)_3$ analogue. The ionization energy shifts are summarized in Table IV. These shifts furnish the information regarding the relative bonding capabilities of CO and C_2H_4. These shifts are also predicted by simple molecular orbital calculations. A comparison of the calculated and observed ionization energies for $MeCpMn(CO)_3$ and $MeCpMn(CO)_2(C_2H_4)$ is presented in figure 4. The predicted values are obtained by applying the calculated shifts between

Table IV - Effects of CO Substitution by Olefin[a]

	$Me_5CpMn(CO)_3$ ↓ $Me_5CpMn(CO)_2(C_2H_4)$	$MeCpMn(CO)_3$ ↓ $MeCpMn(CO)_2(C_2H_4)$	$MeCpMn(CO)_3$ ↓ $MeCpMn(CO)_2(C_3H_6)$
1a' shift	0.88	0.85	1.04
2a', a" shift	0.12	0.11	0.30
Ring e_1" shift	0.26	0.24	0.42

a) Destabilization of ionization energies in eV

$CpMn(CO)_3$ and $CpMn(CO)_2(C_2H_4)$ to the observed ionization energies of $MeCpMn(CO)_3$. This assumes that deviations from Koopmans' Theorem, limitations of the approximate method, etc., are reasonably constant for the two systems and that MeCp compared to Cp is a minor perturbation.[12] Thus if the calculations reasonably represent the different bonding of CO and C_2H_4 to $CpMn(CO)_2$, there should be agreement in the shift of the ionization energies. As can be seen, the theoretical prediction is very good in this case.

Figure 4 shows that the highest occupied, mostly metal d orbitals of $MeCpMn(CO)_3$(1e and a_1) switch their relative ordering in $MeCpMn(CO)_2$-(C_2H_4). The a_1 orbital of the tricarbonyl is greatly destabilized (0.85 eV) when a CO ligand is replaced by C_2H_4, and becomes the 1a' HOMO of $MeCpMn(CO)_2(C_2H_4)$.[45] This destabilization is expected since the 1a' orbital of $MeCpMn(CO)_2(C_2H_4)$ is no longer stabilized by backbonding as it was in the tricarbonyl. The single C_2H_4 pi* acceptor prefers to interact with the a" donor of $CpMn(CO)_2$, as explained above.

The 1e HOMO of the tricarbonyl correlates primarily with the a" and 2a' orbitals of the ethylene complex. These orbitals remain nearly degenerate and experience only a slight shift (0.11 eV) to lower ionization energy. In the absence of unusual olefin orbital interactions with the 2a' orbital (vide infra), the 2a' and a" orbitals can remain nearly degenerate only if the ethylene stabilization of the a" orbital is similar to the carbonyl pi-backbonding stabilization of this orbital. This has been illustrated for a wide range of good and poor acceptor ligands in $CpMn(CO)_2$(ligand) complexes.[8,12,13,32,46] The near

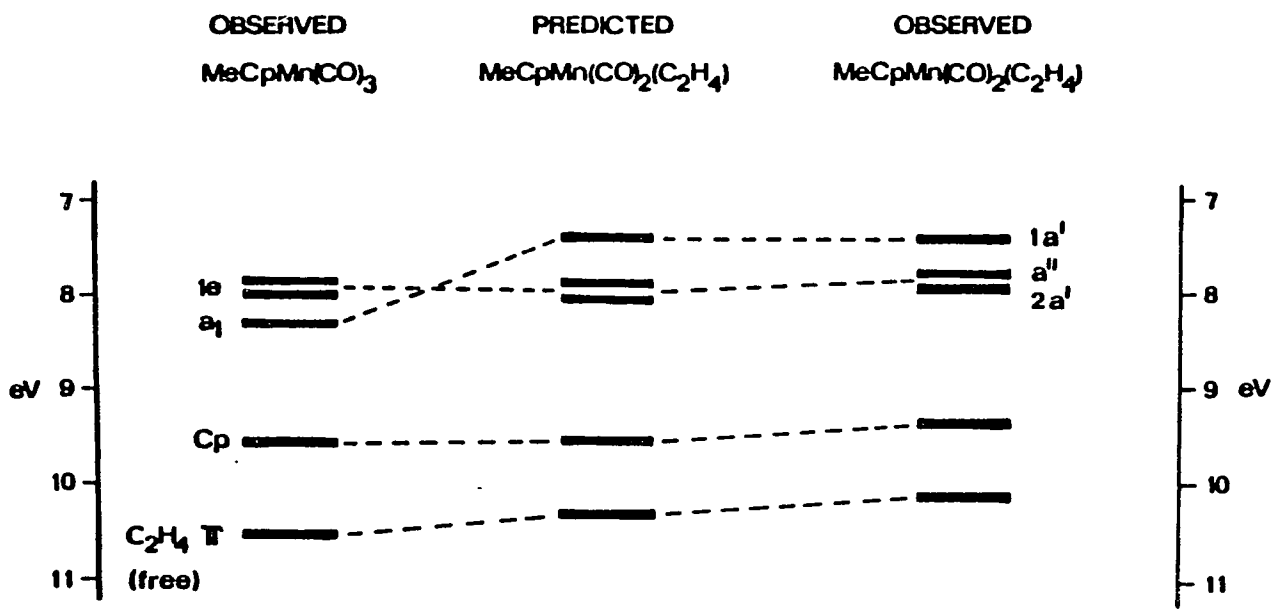

Figure 4 - Predicted Versus Observed Orbital Ionization Energies for $MeCpMn(CO)_2(C_2H_4)$

degeneracy of the a" and 2a' orbitals in this complex indicates that the single C_2H_4 acceptor orbital is comparable in backbonding ability to a single CO acceptor.

The 2a' orbital is the correct symmetry to interact with the olefin pi bond. Although this interaction has been invoked in the discussion of other metal-olefin properties,[47] it does not appear to be important in determining the shifts of the ionizations in these complexes. An interaction of this type would be most directly manifested in a destabilization of the 2a' ionization. One example in which an extra destabilization of the 2a' ionization would be observed is given by comparison of the ethylene and propylene complexes. The greatest difference between ethylene and propylene is the ionization energy of the olefin pi bond, which is 0.66 eV less stable in the case of propylene and would interact more strongly with the 2a' orbital. However, Table III shows that the 1a', 2a', and a" ionizations all shift identically from the ethylene to the propylene complex, indicating that any difference in the 2a' interaction is negligible on the energy scale of these experiments.

The slight decrease in ionization energy of the 2a' and a" orbitals when a CO is replaced by ethylene reflects the slight increase of charge density on the metal center of the ethylene complex compared to the carbonyl complex. This increase is primarily the result of the increased localization of the 1a' orbital on the metal center due to lack of a suitable ethylene a' acceptor orbital. In the case of propylene the greater destabilization of the 2a' and a" ionizations shows that

propylene is a better donor than ethylene, while the remaining degeneracy of these ionizations indicates that the single acceptor of propylene is still comparable to the single acceptor of CO.

Effects of Methylation

The sensitivities of the ionizations to both methylation of the cyclopentadienyl ring and methylation of the olefin are summarized in Table III. The shift of the metal and ring valence ionizations with methylation of the ring is as expected from a previous UPS investigation of the $CpM(CO)_3$ compounds of Mn and Re (Appendix B).[39] Specifically, the shift of the predominantly ring e_1'' ionization (0.85 eV) is about twice as large as the shift of the metal ionizations (0.44 eV). In addition, the olefin pi level allows observation of the shift in a ligand ionization. It is interesting to note that the olefin pi ionization shifts by the same amount as the metal ionizations when the cyclopentadienyl ring is methylated. Similarly, when the olefin is methylated, the olefin pi ionization shifts twice as much as the metal ionizations. In this case the metal and the ring ionizations shift by the same amount.

It has been shown that the shift in the pi ionization of the methylated group is largely due to the hyperconjugation effect, which is accompanied by some charge induction.[39] The shifts in other ionizations are directly due to the resulting charge rearrangement throughout the molecule. Thus the pi ionization of the methylated group is destabilized more than the other ionizations. The similarity of the metal and olefin pi shifts when the ring is methylated, illustrate the very

fluid electron density in these systems. This is apparently another reason that the $CpMn(CO)_2$ fragment is able to form stable molecules with a large number of different ligand types. The fluid electron density is able to accommodate a wide range of different bonding needs.

The Effect of Coordination on the Olefin pi Ionization

Figure 4 shows that the C_2H_4 donor orbital is destabilized upon coordination. In the case of coordinated olefins, there are three distinct factors which affect their pi orbital ionization energies. As pointed out above, such donor orbitals are normally stabilized by bond formation. This can result simply from the overlap of a filled ligand donor orbital with an appropriate metal orbital to give M-L bonding and antibonding combinations. The magnitude of this stabilization depends on both the amount of overlap and the energy separation between the metal and ligand orbitals. A second factor in the orbital energy is the charge redistribution which accompanies olefin coordination. Since olefins possess both donor and acceptor capabilities, the relative dominance of these two interactions will determine the direction of net charge flow in the M-olefin bond. If the olefin behaves primarily as a donor ligand, then it will acquire a partial positive charge upon coordination and charge redistribution will exert a stabilizing influence on the olefin pi orbital. If the olefin acceptor ability dominates, the olefin will experience a build up of negative charge which will have a destabilizing effect on it's pi ionization energy. It is tempting to interpret shifts in the olefin pi ionization energy solely in terms of

these charge transfer mechanisms so as to give an indication of the relative donor/acceptor strength of the olefin ligand.[23,38] This line of reasoning is valid only under certain circumstances (vide infra).

For most other ligand molecules the effects of M-L overlap and the accompanying charge redistribution are sufficient for explaining shifts in the ligand ionization energies upon coordination. However, in the case of olefin ligands the donor and acceptor orbitals are pi bonding and antibonding with respect to the C-C bond. As a result both pi-donation and pi*-acceptance serve to reduce the C=C bond order and lengthen the C-C bond. In addition, some rehybridization of the carbon centers toward sp^3 occurs which partially destroys the σ-π separability. These points have been discussed by other authors.[47] Crystal structures of coordinated olefins in complexes of this type show lengthening of the C=C bond from 1.34 to about 1.40 Å, and a bending of the four substituent groups or atoms away from the metal atom.[15]

Figure 5 shows how the calculated orbital energies and overall strength of the metal-olefin interaction are sensitive to these olefin distortions. In reconstructing the metal-olefin bond we first bring a free ethylene molecule within bonding distance of a $CpMn(CO)_2$ fragment while maintaining the olefin at its free geometry (figure 5b). The calculated relative orbital energies which result at this hypothetical geometry are not in agreement with the observed HeI spectrum. For instance the a" and 2a' orbitals are not approximately degenerate. Also, the C_2H_4 pi orbital has been weakly stabilized. This initial stabilization of the olefin pi orbital corresponds to the normal stabilization of a donor orbital due to M-L overlap. Stepwise relaxation of the olefin

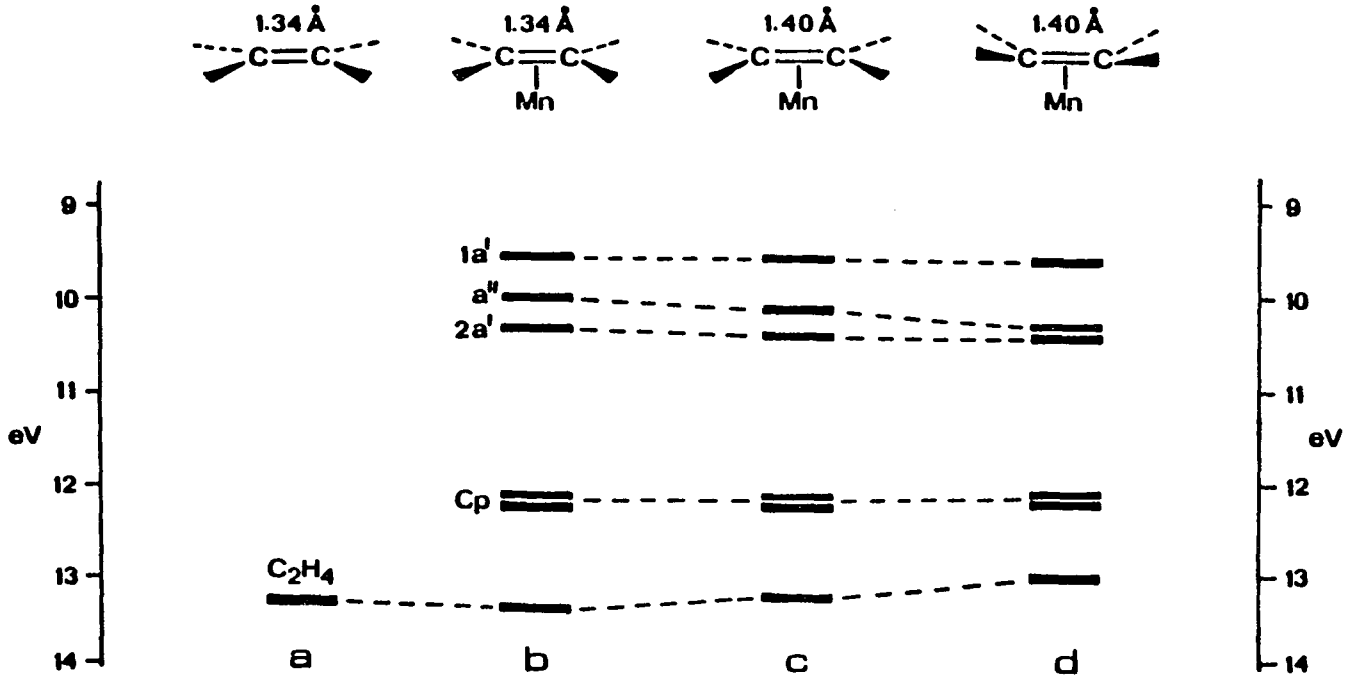

Figure 5 - Stepwise Effects of Olefin Distortions on the Metal d and Olefin pi Orbitals

to its favored coordination geometry is shown in figures 5c and 5d. Lengthening of the C=C bond to 1.40Å (5c) decreases the pi-pi* separation and destabilizes the olefin pi orbital. This improves the pi-donation to the metal and increases pi*-acceptance from the metal into the more stable olefin pi* orbital. This increased backbonding is evidenced by the stabilization of the metal a" donor orbital. These trends are continued with the partial rehybridization of the ethylene carbon atoms such that the four hydrogen atoms are bent away from the metal. This further destabilizes the olefin pi orbital and also strengthens the M-olefin interaction by increasing orbital overlaps. The increased backbonding to the olefin now stabilizes the a" to approximate degeneracy with the 2a' as observed experimentally. Thus the free olefin sacrifices some of its own carbon-carbon bond strength to form a stronger metal-olefin bond. It should be emphasized again that the ability of the eigenvalues of both the extended Hückel and Fenske-Hall calculations to produce the shift in the olefin pi-ionization indicates that excited state, relaxation, and other effects are not of primary importance for this trend.

These results are in agreement with bond energy calculations by Sakaki et. al. on $Pt(PH_3)_2C_2H_4$.[30] They found that olefin distortion causes a strengthening of the M-C and C-H bonds, and a weakening of the C=C bond. As we have shown, our Mn system exhibits the same trends in M-C and C=C bond strengths with olefin distortion. Sakaki also obtained a net transfer of electron density onto the olefin with bond formation in their d^{10} system. The shifts in ionization energies for the d^6

$Mn-C_2H_4$ system do not indicate a net transfer of electron density when the olefin is coordinated.[48] Also, if charge redistribution were significant in this system the non-iterative extended Hückel calculations would not be successful in predicting the correct ionization shifts. Distortion of the olefin upon coordination, and the resulting destabilization of the olefin pi ionization, is enchanced by both pi-donation and pi*-acceptance by the olefin, but does not necessarily require a net charge transfer. Instances in which the donation and acceptance essentially balance may be envisioned as a coordinated olefin effectively experiencing a partial pi → pi* excitation. Several authors have noted the similarity between the geometry of coordinated olefins and the geometry adopted by olefins in their electronically excited state.[49,50]

As can be seen, the relationship between olefin binding energy shifts and metal-olefin interactions is complex. The important factors which determine the ionization energy of the coordinated olefin pi orbital are summarized in Table V. The three columns show how each contributing factor affects the olefin pi ionization energy if the pi-donation and pi*-acceptance interactions are considered individually. For instance, pi-donation has a stabilizing effect on the olefin pi orbital as a result of overlap stabilization and the build-up of positive charge on the olefin, but a destabilizing effect due to a decrease in C=C bond order. The pi*-acceptance has strictly a destabilizing effect on the olefin pi orbital. The pi*-acceptance results in an accumulation of negative charge on the olefin and also reduces the C=C bond order. The

Table V - The Effect of Metal-Olefin Interactions on Olefin Pi Ionization Energy[a]

Orbital Interaction With Metal	Effeect of Metal-Olefin Overlap Energy	Effect of Charge Redistribution	Effect of Decrease in C=C Bond Order
Olefin pi-donation	stabilization	stabilization	destabilization
Olefin pi*-acceptance	0	destabilization	destabilization

a) Stabilization in this sense refers to a shift of the ionization to greater ionization energy

overall shift in olefin pi ionization energy upon coordination is determined by both the relative dominance of the pi-donation/pi*-acceptance interactions and the relative magnitudes of each contributing factor.

The small charge redistribution upon ethylene coordination in $MeCpMn(CO)_2(C_2H_4)$ indicates that, in this system, the pi-donation and pi*-acceptance interactions are approximately of equal importance, resulting in no significant overall charge transfer between the metal and olefin. The observed 0.40 eV destabilization of the ethylene pi orbital in $MeCpMn(CO)_2(C_2H_4)$ from free ethylene results from the combined reduction in C=C bond order of both pi-donation and pi*-acceptance, which more than compensates for the small metal-olefin overlap stabilization. In this compound one cannot conclude that the decrease in olefin ionization energy implies a build-up of electron density on the olefin resulting from a dominant pi*-acceptance interaction.

The $MeCpMn(CO)_2(C_3H_6)$ and $Me_5CpMn(CO)_2(C_2H_4)$ compounds provide convenient perturbations which help illustrate the usefulness of Table V. In $MeCpMn(CO)_2(C_3H_6)$ the coordinated propylene pi orbital has been destabilized by only 0.10 eV relative to free propylene. This molecule has the largest energy separation between the filled metal levels and the olefin pi* level, and therefore has the least amount of pi*-acceptance. In addition, the enhanced pi-donation of propylene due to its electron-donating methyl group, makes propylene an overall stronger donor than acceptor ligand in this system. This can be seen by the increased 2a' shift (0.30 eV) in Table IV. In this case the donor and acceptor charge transfer mechanisms do not cancel, but instead, furnish a stabilizing influence which reduces the overall destabilization of

the propylene upon coordination. The $Me_5CpMn(CO)_2(C_2H_4)$ complex presents a perturbation in the opposite direction. The five ring methyl groups destabilize the mostly ring e_1'' orbital and supply an increased amount of electron density to the metal. This decreases the energy separation between the metal levels and the C_2H_4 pi* orbital which enhances olefin pi*-acceptance, and diminishes olefin pi-donation to the more electron-rich metal. The charge transfer contribution now furnishes a further destabilization which helps to shift the C_2H_4 pi orbital to lower ionization energy by 0.85 eV in $Me_5CpMn(CO)_2(C_2H_4)$.

CHAPTER 4

AN ANALYSIS OF THE THREE-CENTERED BONDING IN μ-CH_2-$[MeCpMn(CO)_2]_2$

Since the first identification of a CH_2 moiety stabilized as a bridging group between two metal centers,[57] such compounds have been increasingly recognized for their importance in organometallic chemistry. The metal-methylene unit may be an intermediate in olefin metathesis reactions, and it recently has been implicated as significant in certain Fischer-Tropsch type reactions.[52-54] A growing number of μ-alkylidene complexes have been synthesized in recent years and an understanding of the stabilities and reactivities of these species is beginning to unfold.[55,56] This chapter reports the HeI valence photoelectron spectrum of μ-$CH_2[MeCpMn(CO)_2]_2$. A recent UPS study of the closely related μ-$CH_2[CpMn(CO)_2]_2$ compound has appeared.[57] These authors concluded, on the basis of CNDO calculations, that there is essentially no net Mn-Mn bond in this dinuclear system in spite of a shorter Mn-Mn distance than found in $Mn_2(CO)_{10}$. The HeI results and Fenske-Hall calculations in this chapter avoid this contradiction by indicating 3C-6e bonding in the three-membered ring with a net Mn-Mn single bond.

It should be noted that an understanding of the ionization features and orbital interactions in μ-$CH_2[MeCpMn(CO)_2]_2$ (MeCp = η^5-$C_5H_4CH_3$) is greatly facilitated by the detailed examinations of $MeCpMn(CO)_2(C_2H_4)$ (Chapter 3) and $MeCpMn(CO)_3$ (Appendix B). The olefin and bridging methylene complexes (figure 6) are intermediate members of a series of 3-member ring molecules from cyclopropane to trinuclear metal clusters. The μ-CH_2-$[MeCpMn(CO)_2]_2$ complex may be visualized as following from the $MeCpMn(CO)_2(C_2H_4)$ complex by replacing one CH_2 of the olefin by a $MeCpMn(CO)_2$ unit. However, as will be seen in the following discussion, the bonding descriptions for the olefin and methylene complexes are considerably different.

Peak Assignments

The 11-6 eV photoelectron spectrum of μ-CH_2-$[MeCpMn(CO)_2]_2$ is shown in figure 7. It is helpful to compare this spectrum with the spectra in the preceding chapter as well as those of other $MeCpMn(CO)_2$(ligand) compounds.[8,12,13] The most intense ionization band centered at $\sim$ 9.2 eV exhibits the familiar band-shape and ionization energy of the predominantly cyclopentadienyl pi ionization observed in a large number of cyclopentadienyl-containing compounds (Appendix B). The lowest energy, broad ionization band in the 6.5-8.0 eV region contains at least four resolvable peaks. This envelope falls in a region where ionization from orbitals which are high in metal d character typically occur in $MeCpMn(CO)_2$(ligand) compounds. The relatively high metal d character of these ionizations is borne out by a reported HeI/HeII

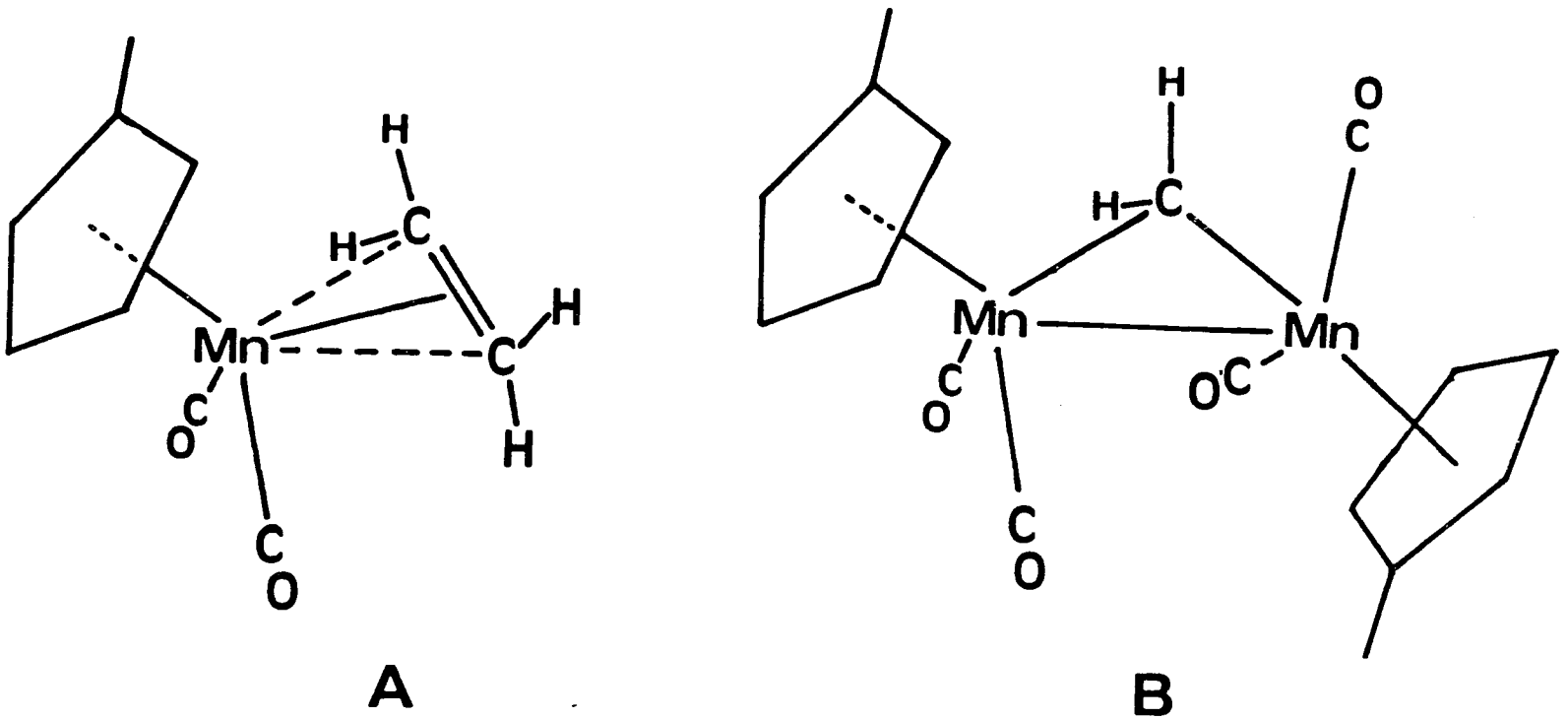

Figure 6 - Perspective Views of A) $MeCpMn(CO)_2(C_2H_4)$ and B) μ-CH_2-$[MeCpMn(CO)_2]_2$

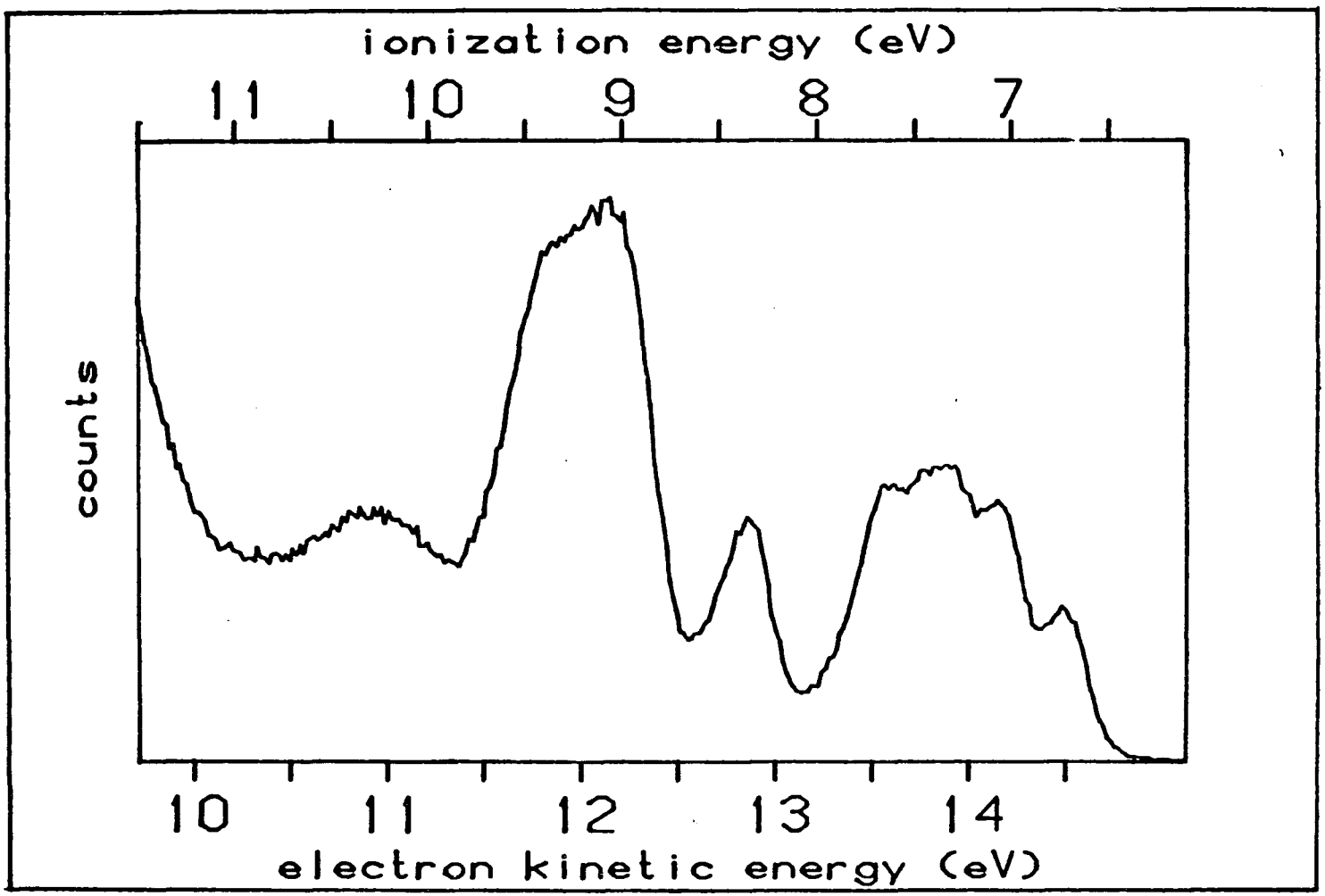

Figure 7 - The 11 → 6 eV HeI Spectrum of μ-CH_2-$[MeCpMn(CO)_2]_2$

comparison of this system.[57] Ionizations from M-M bonding orbitals may also fall in this region. This leaves the peaks at 10.23 eV and 8.34 eV as specific to this complex. The peak at 10.23 eV is similar in position to the ethylene pi ionization of $MeCpMn(CO)_2(C_2H_4)$. It is also similarly low in intensity and very broad. This indicates appreciable bonding character in the orbital.[59] We therefore assign this ionization as primarily associated with the $2e^-$ donor orbital of the methylene which is significantly bonding to the Mn-Mn dimer. A peak in the region of 8.34 eV has not been previously observed in any other $CpMn(CO)_2$(ligand) complexes. We interpret this ionization as being associated primarily with the methylene ligand. One might attempt to ascribe this ionization to a single metal-metal bond. However, the position of this ionization is not consistent with the ionizations of similar dimers like $Mn_2(CO)_{10}$.[58a] Additional evidence for assignment comes from the following consideration of the orbital interactions in this complex.

Molecular Orbital Analysis

Before considering the results of the calculations on the μ-methylene complex, one must remember the nature of the frontier orbitals and bonding capabilities of the $CpMn(CO)_2$ fragments, as discussed for the $CpMn(CO)_2$(olefin) system. Briefly, the fragment has an empty low-lying dz^2 type orbital (3a') directed toward its vacant coordination site that is suitable for forming a dative bond with an electron donor ligand. The three occupied orbitals of the d^6 metal fragment are 1a', 2a' and a". The 1a' and a" are suitable for pi-donation toward the vacant site,

with the a" most effective because it is the least stable and directed for best overlap. The orientation of the $CpMn(CO)_2$ fragments in the bridging methylene complex is shown in figure 8. It is interesting that the vacant site of each $CpMn(CO)_2$ fragment is directed near the center of the Mn-C-Mn triangle, and the a" orbitals are essentially in the plane of this triangle.

The orbitals which are obtained for the dinuclear fragment, that is $[CpMn(CO)_2]_2$ in the absence of the CH_2 group, are shown in figure 9. The frontier orbitals of each $CpMn(CO)_2$ portion simply combine into the corresponding bonding and antibonding combinations. The strongest combination is naturally between the dz^2-type 3a' orbitals, which are each directed toward the same region. The LUMO is the symmetric combination of these obtials. Of the filled metal levels, the strongest interaction is between the a" orbitals. The HOMO is the antisymmetic (antibonding) combination of these orbitals. The net bond order between the metals is zero since the bonding and antibonding combinations are filled in pairs.

As in the bonding of carbenes with metals,[60] the methylene group has a filled orbital (a_1) that can act as a sigma donor to the metal. It also has an emply $p\pi$ orbital (b_1) that can accept pi-electron density from the metal. The interaction of these orbitals with those of the dinuclear $(CpMn(CO)_2)_2$ fragment are shown in figure 10. The LUMO of the dinuclear fragment has the correct symmetry, is relatively low in energy, and has a nearly ideal spatial distribution for accepting electron density from the donor orbital of the methylene

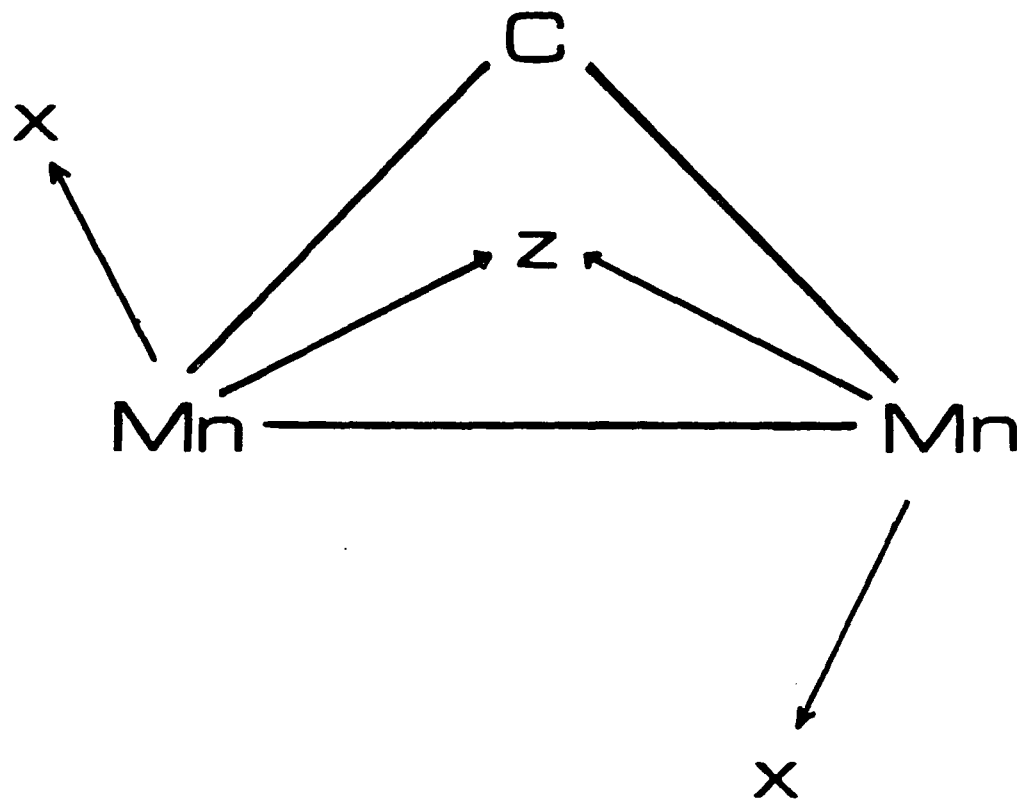

Figure 8 - Local Coordinate Axes Used in the Molecular Orbital Calculations

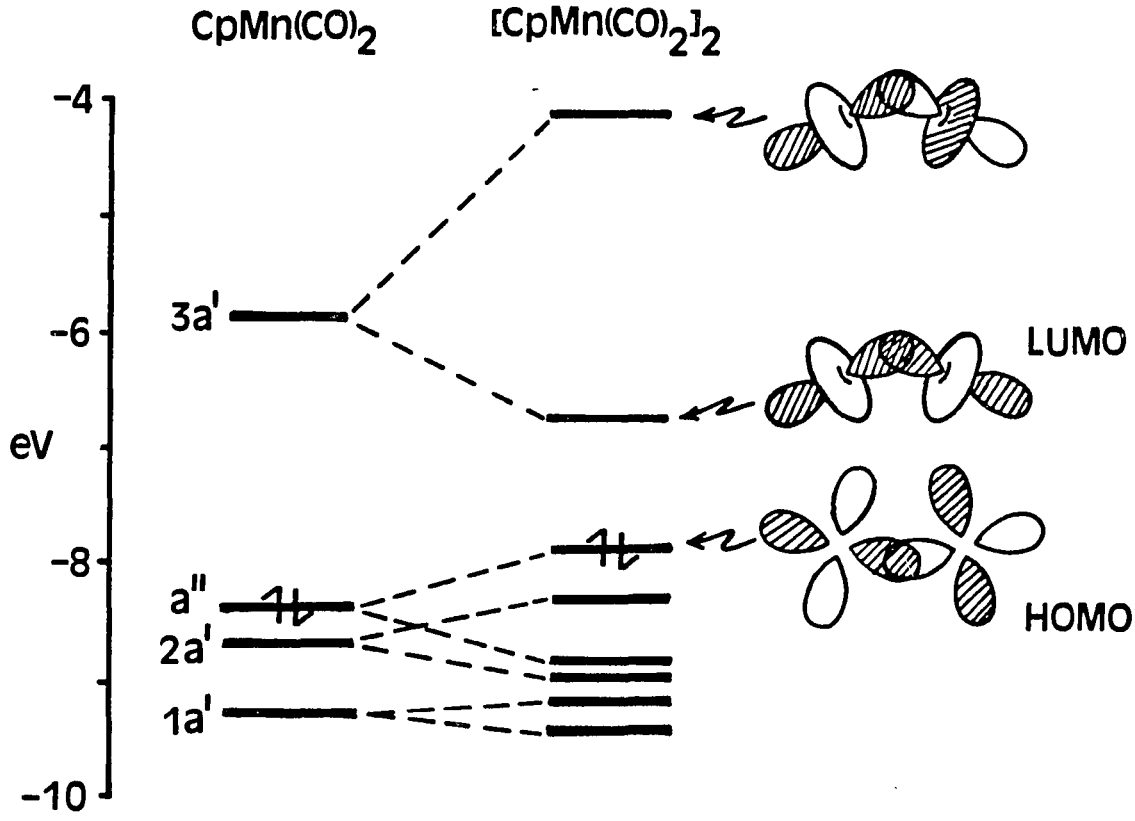

Figure 9 - Valence Molecular Orbital Diagram of the $[MeCpMn(CO)_2]_2$ Fragment

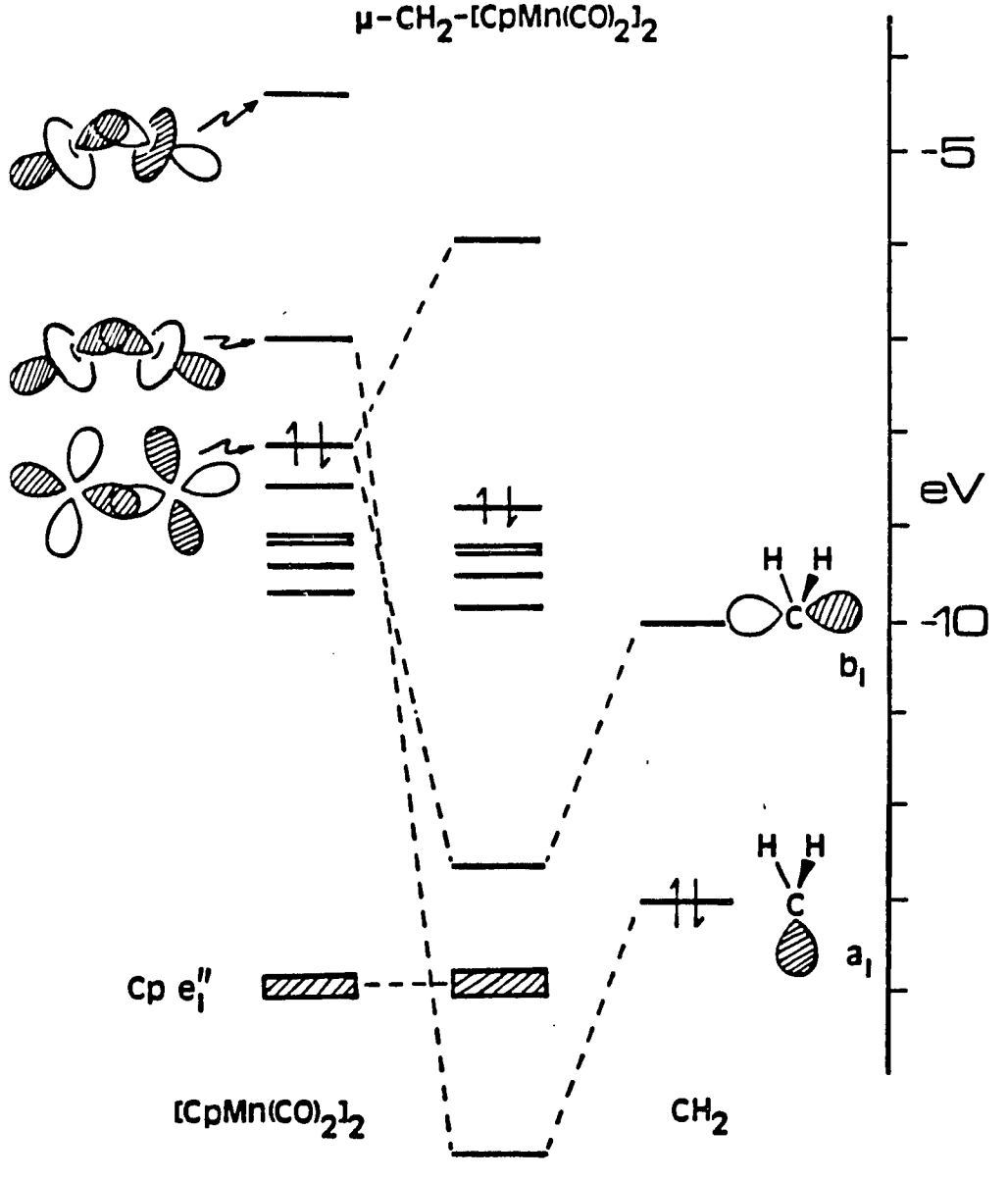

Figure 10 - Molecular Orbital Diagram of μ-CH_2-$[MeCpMn(CO)_2]_2$ The Highest Occupied Orbital is Indicated by an Electron Pair in Each Case

group. Similarly, the HOMO of the dinuclear fragment is well-situated for donating electron density into the empty pπ orbital of the methylene group.

Figure 10 and the calculated methylene carbon charge in Table VI show μ-CH_2 to be an overall better acceptor than donor in this system. It is important to note that these calculations place the originally empty pπ orbital of CH_2 slightly below the filled metal levels. Because of this ordering the donation into this pπ orbital should effectively be described as a charge transfer from the HOMO to the dinuclear fragment of the methylene group. This results in the high negative charge on the methylene carbon.[55a] Also, the HOMO of the dinuclear fragment is antibonding between the metals, and removal of density from this orbital now leaves a net metal-metal bond. The electron donation from the methylene group is not as great as its electron acceptance because of the stability of the methylene donor orbital. Although the molecular orbital resulting from methylene sigma donation remains primarily methylene in character, this donation does serve to strengthen the metal-metal bond since it is placing density in the LUMO of the dinuclear fragment, which is bonding between the two metals. Thus both interactions tend to produce a net metal-metal bond. The bonding in the Mn-C-Mn triangle may be viewed as a 6-electron, 3-center description similar to cyclopropane. This description is similar to that discussed for μ-CH_2-$Os_3(CO)_{10}(\mu\text{-}H)_2$.[55a]

The discussion given above is roughly analogous to that provided by Hofmann in his extended Hückel study of μ-$CH_2[CpRh(CO)]_2$.[61]

Table VI - Mulliken Populations and Atomic Charges

	μ-CH_2-[$CpMn(CO)_2$]$_2$	$CpMn(CO)_2(CH)_2$
methylene carbon atomic charge	-0.526	-0.529
methylene a_1 population	1.367	1.279
methylene b_1 population	1.025	1.022
total metal d- methylene carbon overlap population	0.418	0.385
total overlap population between the frontier orbitals of the $CpMn(CO)_2$ fragments	0.170	

Extended Hückel calculations on these systems give qualitatively similar results although there is more mixing in the molecular orbitals, making it difficult to seprate the individual interactions. There is also considerable uncertainty in the eigenvalues and the relative placement of some of the orbitals, particularly the placement of the methylene orbitals relative to the metal orbitals. This latter point is an important question for the parameter-free calculations. Comparison of figure 10 with the spectrum in figure 7 shows that the calculations account well for the important ionization features of this bridging methylene complex.

Both figures indicate a group of closely spaced levels (mostly metal d) separated from a single level (mostly methylene $p\pi$). The characteristic cyclopentadienyl pi band comes next and is followed by a final low intensity band observed at 10.23 eV. As mentioned earlier, the width of this final band indicates appreciable bonding character, and the molecular orbital analysis indicates that this orbital is totally bonding in the Mn-C-Mn triangle. The band at 8.34 eV is associated with an orbital that has a node at the C atom and between the two metal atoms in the Mn-C-Mn triangle, and this band is considerably sharper.

The relative intensities of the ionization bands are also consistent with the charge transfer from the metals to the methylene. For instance, in the photoelectron spectrum of $MeCpMn(CO)_3$ (Appendix B) the ionization band area in the metal region relative to that in the MeCp region is .93 to 1. These bands represent six metal electrons to

four MeCp electrons. From the orbital analysis of μ-CH_2-[$MeCpCpMn(CO)_2$]$_2$ there are five metal electrons to four MeCp electrons per $MeCpMn(CO)_2$ fragment. If ionization cross-sections do not change we should then see a ratio of .77 to 1 for the area of the first band (overlapping metal ionizatons) to the area of the MeCp band. The ratio determined from the spectrum in figure 7 is .73 to 1. This supports metal to ligand charge transfer and the loss of one filled orbital of predominantly metal character in dimer formation.

Bridging Versus Terminal Methylene Bonding

Carbene ligands normally occupy terminal positions in their bonding to metal complexes. In fact, several terminal metal-carbene complexes of the form $CpMn(CO)_2$(carbene) are known.[62] The preparation of the title compound also suggests the terminal metal-methylene complex, $MeCpMn(CO)_2CH_2$, as a probable intermediate.[56] This is because the bridged dinuclear complex is obtained from the reaction of $MeCpMn(CO)_2$(THF) with CH_2N_2, and there is no reason to suspect the presence of [$MeCpMn(CO)_2$]$_2$. Interconversion between bridging and terminal positions may be important in mechanisms of catalytic hydrocarbon formation at surfaces[54] and in other reactions. It is therefore appropriate to examine those factors that favor the bridging dinuclear geometry over the terminal mononuclear geometry for this particular methylene complex. This comparison is somewhat related to the recent discussions of bridging versus terminal bonding in metal dimers.[63]

The results of Fenske-Hall calculations on a model $CpMn(CO)_2(CH)_2$

complex are presented in figure 11 and Table VI. A typical Mn-C distance of 1.90 Å from the structures of other $CpMn(CO)_2(CR_2)$ compounds was used,[63] and the H-C-H angle was set at 120°. The plane of the CH_2 group was oriented perpendicular to the plane of the MeCp ring, as is found in the structures of other carbene complexes.[43] The molecular orbital diagram of $CpMn(CO)_2(CH)_2$ in figure 11 has many similarities to that of μ-CH_2-$[CpMn(CO)_2]_2$ in figure 10. The methylene a_1 donor interacts with the 3a' LUMO of $CpMn(CO)_2$, while the vacant methylene pπ accepts density from the $CpMn(CO)_2$ a" HOMO. The data in Table VI shows the methylene group to be in remarkably similar environments in the terminal $CpMn(CO)_2(CH_2)$ and bridging μ-CH_2-$[CpMn(CO)_2]_2$ compounds. The calculated charge on the methylene carbon atom is essentially identical in these compounds. The Mulliken populations of the methylene donor and acceptor orbitals change negligibly in going from terminal to bridging configurations. The orbital eigenvalues show some expected shifts for the unoptimized geometry in the model calculations, but the relative ordering of the orbitals is the same in both the mononuclear and dinuclear metal complexes. The overall methylene bonding interaction appears to show no significant preference for either conformation.

Obviously, a significant difference between the two bonding modes is the formation of a Mn-Mn bond in the dimer, which is made possible by the charge transfer to the low-lying pπ orbital of the methylene group. The formation of the metal-metal bond is illustrated by the overlap population between the frontier orbitals (1a', 2a', a", and 3a') of the two $CpMn(CO)_2$ fragments shown in Table VI. The increased stability

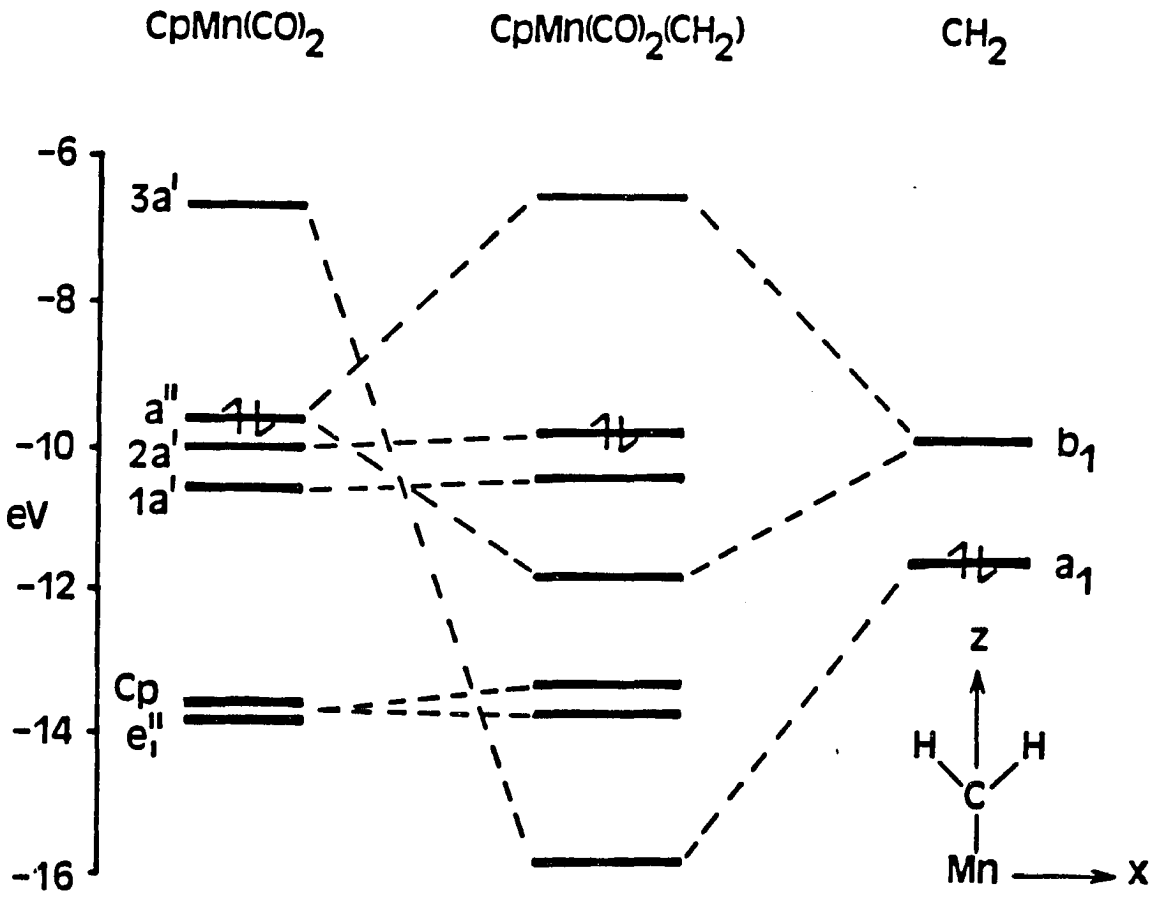

Figure 11 - Calculated Orbital Interactions in $CpMn(CO)_2CH_2$

gained by the additional metal–metal bond formation is apparently the driving force for formation of the dimer complex. In situations where changes in the metal–metal bond interaction are not so severe, there should be a less pronounced preference for the bridging configuration.

CHAPTER 5

EVIDENCE OF CYCLOPENTADIENYL RING DISTORTION AND THE IMPORTANCE OF ELECTRON RELAXATION IN $CpM(CO)_2$ WHERE M = Co AND Rh

This study of the valence ionization energies of group VIII $CpM(CO)_2$ compounds is part of our continuing interest in the electronic structure of cyclopentadienyl-metal carbonyl compounds. This group of compounds is chosen as a result of their generally well-established bonding models and geometrical structures which facilitate UPS interpretations. They also provide a useful standard with which to compare the electronic effects of replacing CO by various other ligands. The results of this chapter will lay the groundwork for future investigations of the $CpRh(C_2H_4)_2$, μ-CH_2-$[CpRh(CO)]_2$ and μ-CO-$[CpRh(CO)]_2$ compounds.

In earlier studies of the group VII $CpM(CO)_3$ system the magnitude of the electronic effect of cyclopentadienyl ring permethylation was determined by shifts in core and valence orbital ionization energies.[39] Since the chemical differences exist between substituted and unsubstituted cyclopentadienyl compounds has received considerable attention,[64] further study is needed to determine to what extent electronic effects contribute to these observed differences. UPS evidence for a geometrical distortion of coordinated cyclopentadienyl rings from

five-fold symmetry in the group VII tricarbonyls is presented in Appendix B. It is important to compare the extent of ring distortion in the noncyclindrically symmetrical $CpM(CO)_2$ system with the cylindrically symmetrical $CpM(CO)_3$ case to determine the relative driving force symmetry exerts in causing ring distortion. A brief presentation of the HeI and HeII spectra of $CpCo(CO)_2$ and $Me_5CpRh(CO)_2$ has appeared.[65] This discussion was limited to a description of some of the low energy molecular orbitals of these molecules without a very detailed attempt at making peak assignments.

In this chapter the HeI and HeII photoelectron spectra of $CpM(CO)_2$ ($Cp = \eta^5\text{-}C_5H_5^-$) and $Me_5CpM(CO)_2$ ($Me_5Cp = \eta^5\text{-}C_5(CH_3)_5^-$) where M = Co and Rh are presented. This system of four closely-related compounds is another example of how UPS can be a very powerful probe of electronic structure when applied to a series of compounds which contain a systematic set of chemical modifications. With careful analysis and the use of various peak assignment techniques, the spectral changes which are observed throughout this series will be attributed to specific chemical changes.

Ionization Band Assignments

This section emphasizes the information provided solely by the ionizations. The 16 → 6 eV valence ionizations of the complexes are shown in the HeI photoelectron spectra in figures 12 and 13. As is common with cyclopentadienyl metal carbonyls, (Chapter 3) the broad, intense band envelop between 15-12 eV is due to ionizations from a

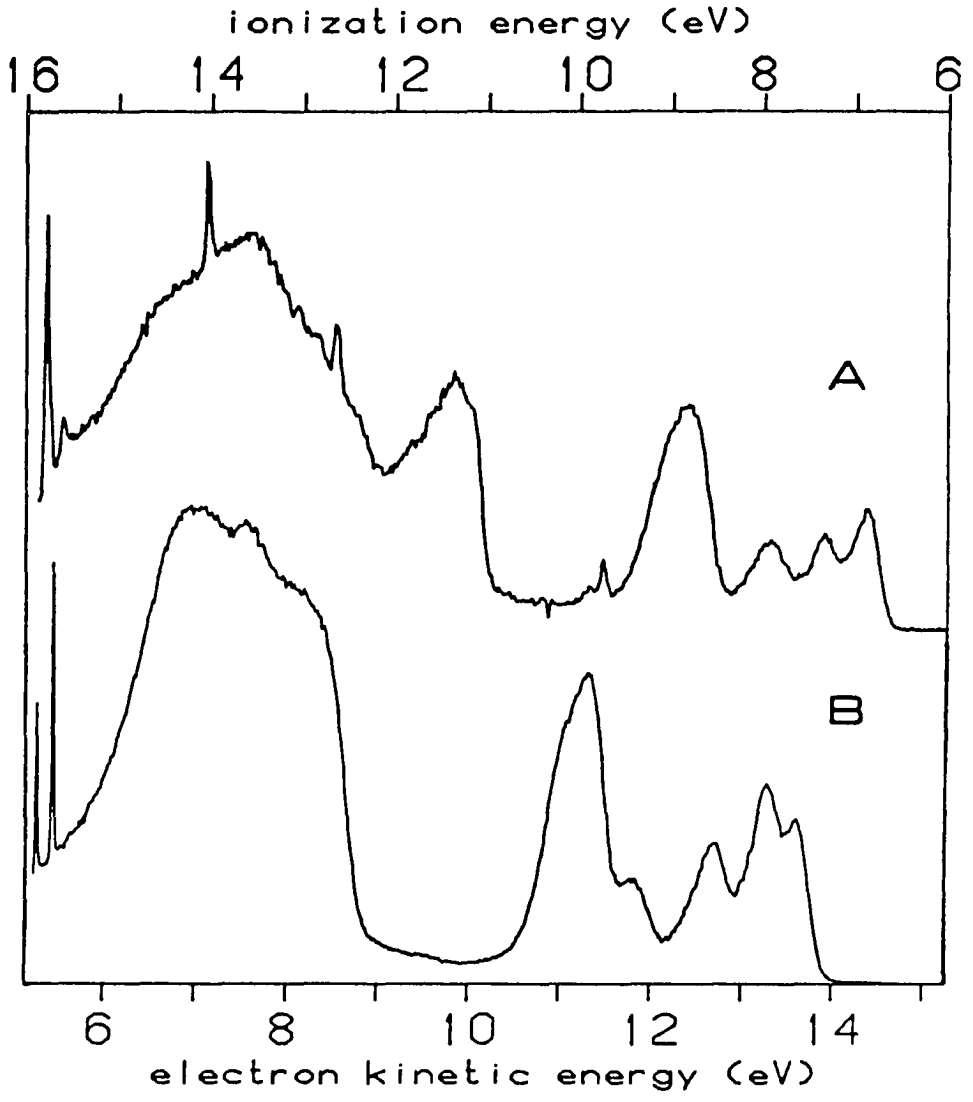

Figure 12 - The HeI Spectra of A) $Me_5CpCo(CO)_2$ and B) $CpCo(CO)_2$

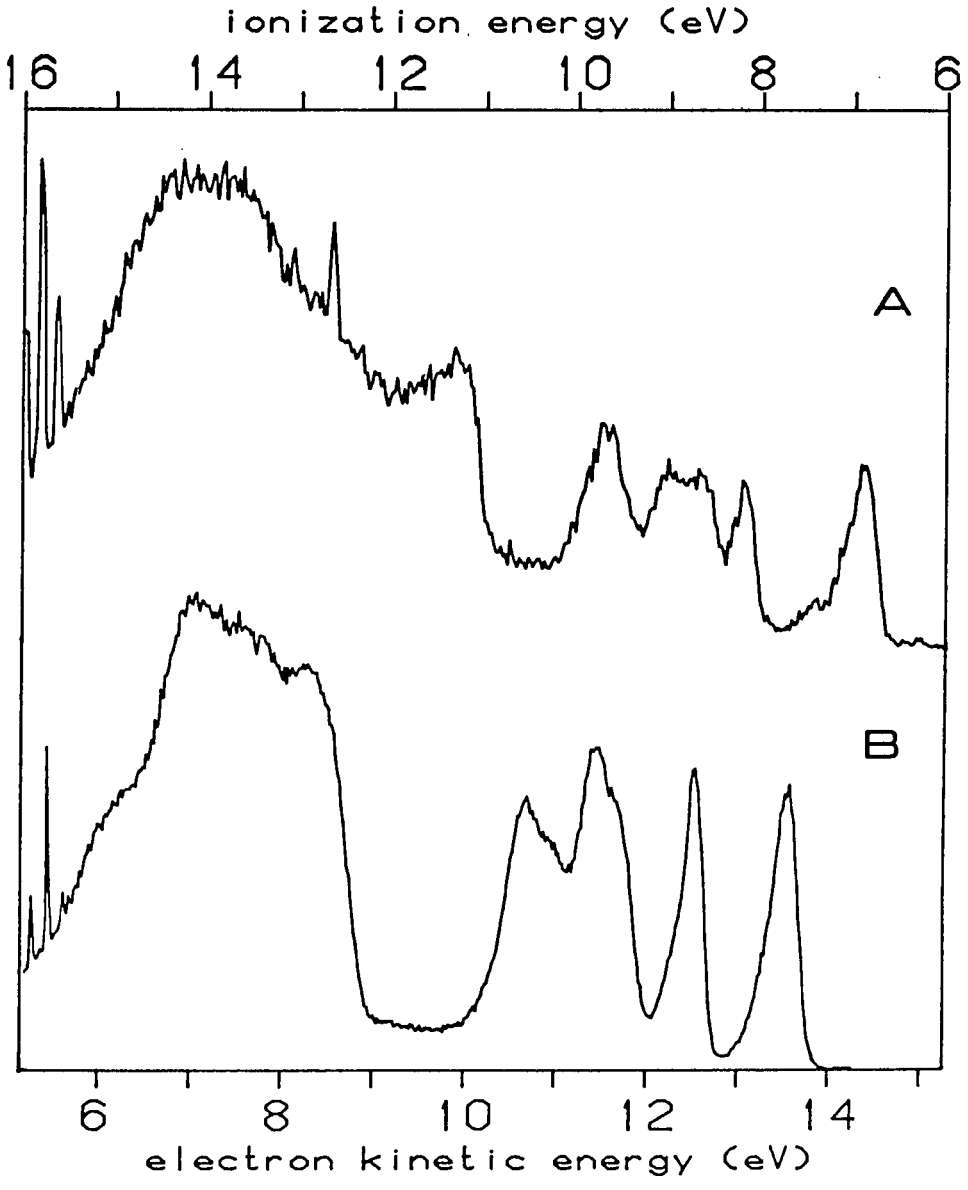

Figure 13 - The HeI Spectra of A) $Me_5CpRh(CO)_2$ and b) $CpRh(CO)_2$

series of closely-spaced ring and CO sigma orbitals and the ring a_2 pi orbital. The permethylated compounds possess a familiar additional peak at $\sim$ 11.5 eV which has been assigned to an ionization from a methyl group orbital in Chapter 3. The ionization energy region below 11 eV furnishes much information energy region below 11 eV furnishes much information on the important valence orbital interactions in these compounds and the changes which take place in this region will be a central focus. The electron-donating effect of the five ring methyl groups can be seen in the pentamethylcyclopentadienyl analogue of both Co and Rh as a general shift to lower ionization energy. The relative shift of each peak with ring methylation will be used as a peak assignment aid since the ionization with the greater ring pi character would be expected to shift the most. It is apparent that significant changes occur when Co is replaced by Rh. These unexpectedly large changes will be an important part of the discussion.

The close-up, low energy HeI and HeII spectra of the Co and Rh analogues are shown in figures 14-17 with the corresponding ionization bandshape analysis in Table VII. From the results on cyclopentadienyl metal carbonyls in Appendix B, it is know that only ionizations from the highest occupied ring pi orbital and orbitals which are high in metal d character occur below 11 eV. In these d^8 compounds these orbitals should derive from the four filled metal d orbitals and a pair of orbitals which original from the e_1'' HOMO of the free cyclopentadienide ring. In the HeI spectrum of $CpCo(CO)_2$ in figure 14 we can see bandshape features which indicate the presence of six ionization peaks. The

Table VII - Results of Curve-Fit Analysis on Valence Ionization Data

	Vertical Ionization Energy (eV)	High Energy Halfwidth (eV)	Low Energy Halfwidth (eV)	Relative Integrated Peak Areas HeI	HeII
$C_5H_5Co(CO)_2$	10.23	0.52	0.35	1.18	0.79
	9.87	0.52	0.35	2.35	1.37
	9.41	0.36	0.44	0.62	0.63
	8.51	0.64	0.30	0.89	1.06
	7.95	0.59	0.24	0.84	1.09
	7.59	0.58	0.30	1.00	1.00
$(CH_3)_5C_5Co(CO)_2$	9.09	0.66	0.37	1.09	0.76
	8.75	0.66	0.37	3.24	3.48*
	7.92	0.53	0.48	1.03	1.49
	7.32	0.38	0.34	0.80	1.62
	6.84	0.41	0.25	1.00	1.00
$C_5H_5Rh(CO)_2$	10.59	0.53	0.34	1.02	0.71
	10.25	0.53	0.34	1.04	0.83
	9.82	0.43	0.32	1.22	0.70
	9.50	0.43	0.32	1.03	1.62
	8.65	0.41	0.16	0.87	1.40
	7.64	0.50	0.22	1.00	1.00
$(CH_3)_5C_5Rh(CO)_2$	9.62	0.58	0.42	1.39	1.97*
	9.01	0.44	0.33	0.72	1.14
	8.61	0.44	0.33	0.83	0.56
	8.11	0.35	0.18	0.52	0.60
	6.78	0.58	0.21	1.00	1.00

* two overlapping peaks

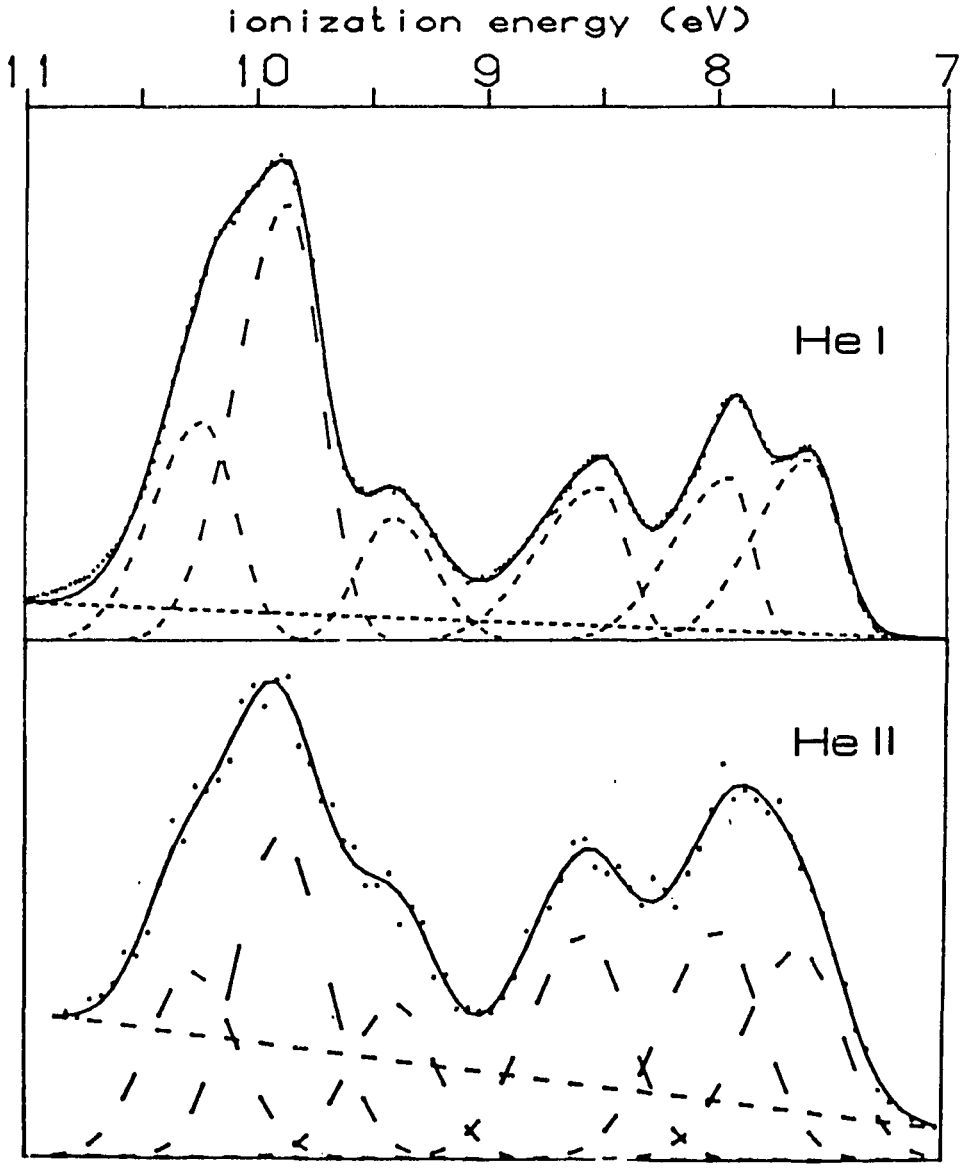

Figure 14 - The HeI and HeII Comparison of $CpCo(CO)_2$

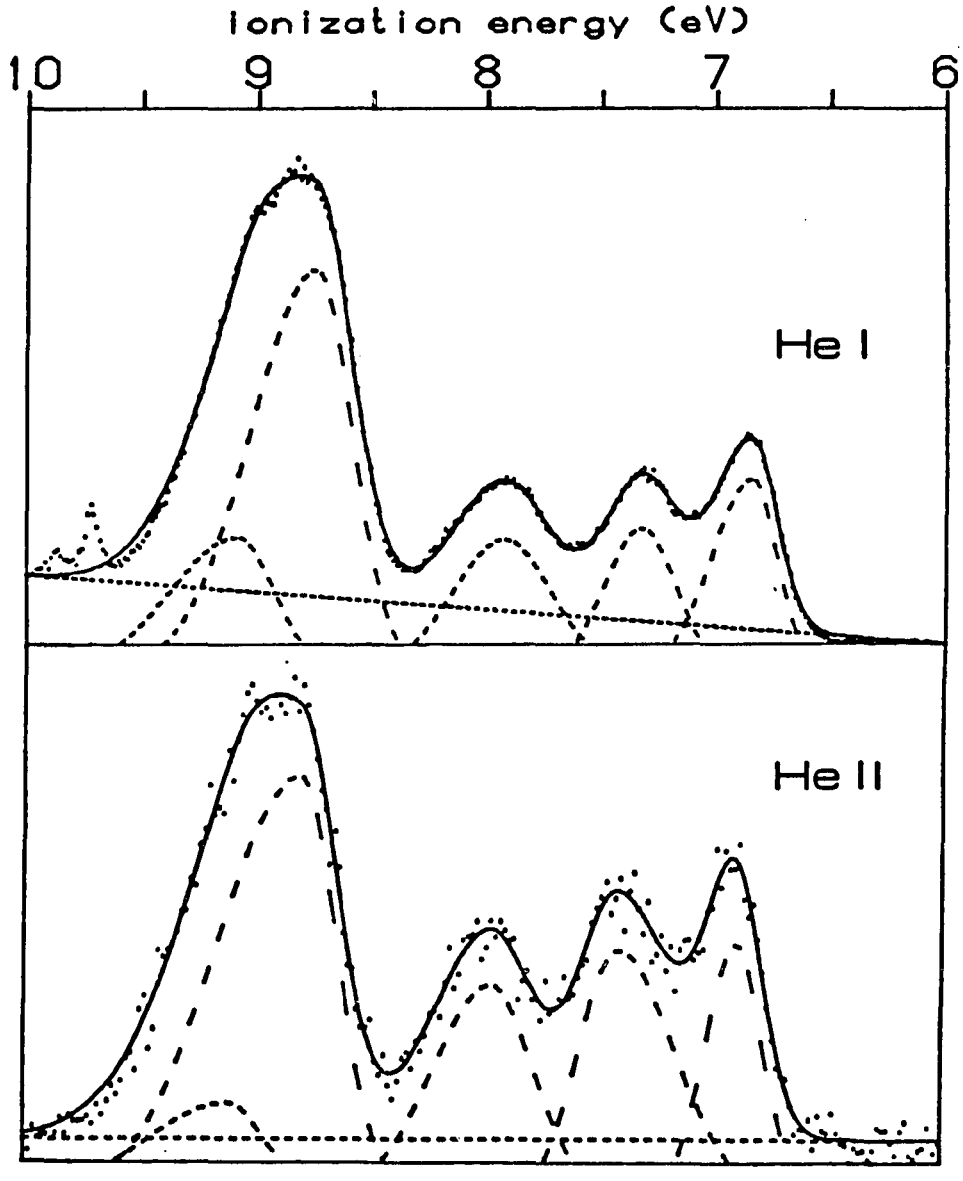

Figure 15 - The HeI and HeII Comparison of $Me_5CpCo(CO)_2$

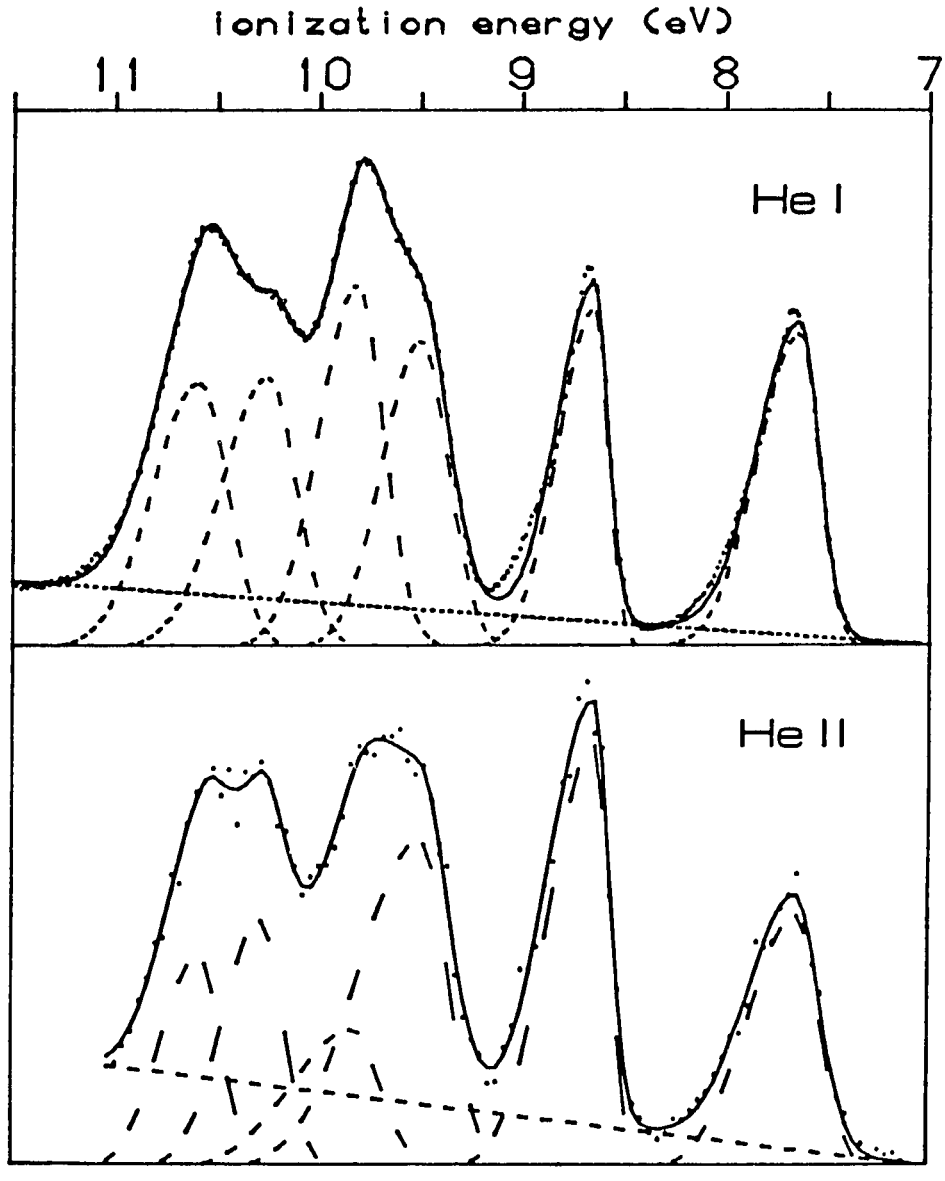

Figure 16 - The HeI and HeII Spectra of $CpRh(CO)_2$

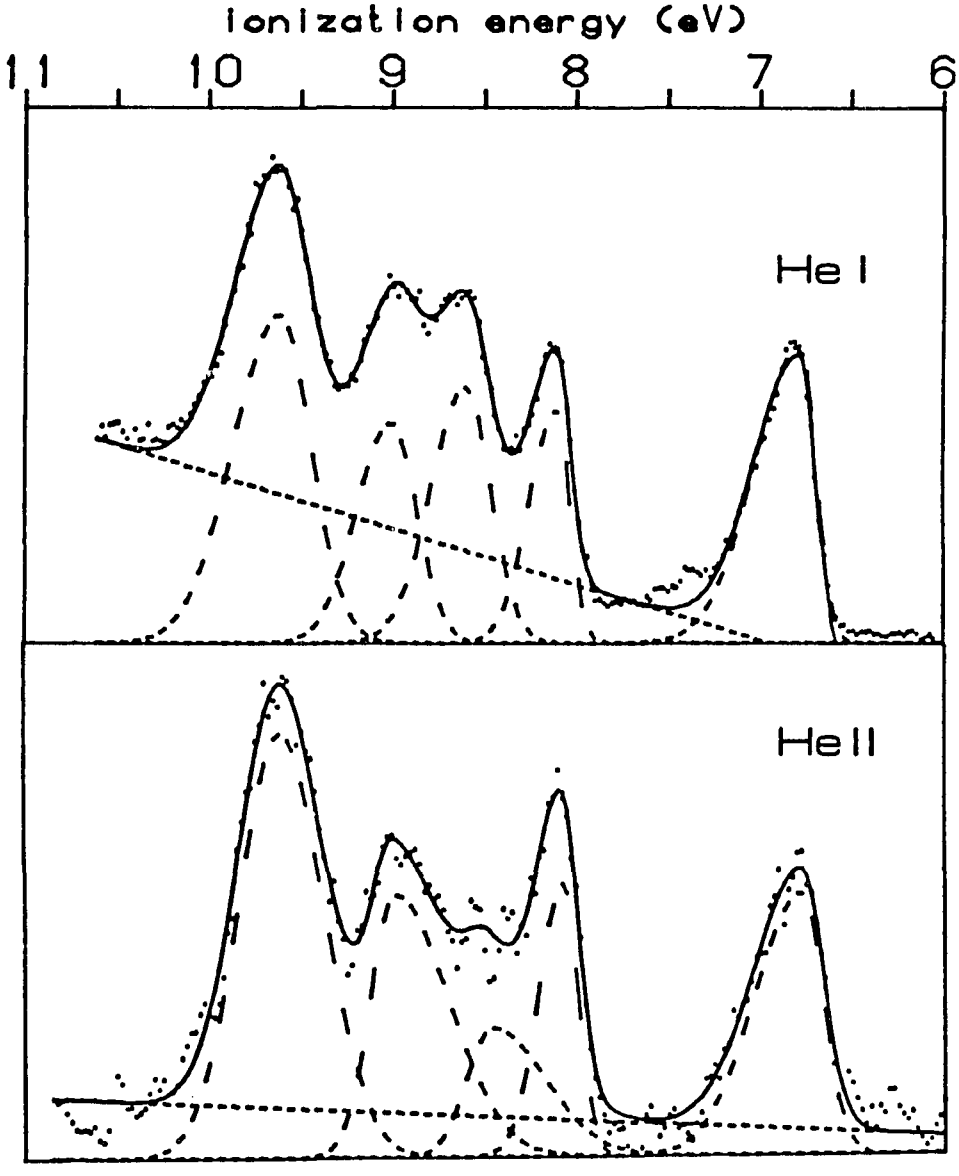

Figure 17 - The HeI and HeII Spectra of $Me_5CpRh(CO)_2$

HeI/HeII comparison of this compound in figure 14 and Table VII show that while the four lowest energy peaks change only modestly in their relative peak areas, all four experience a considerable increase in peak area relative to the ionizations at 10.23 eV and 9.87 eV when going from HeI to HeII. This is an initial indication that the first four ionizations from mainly ring orbitals.

Comparison with the HeI spectrum of $Me_5CpCo(CO)_2$ in figure 15 provides more peak assignment information. In this case we can clearly resolve only four ionization features, although two Gaussians are needed for a reasonable representaton of the band at 8.8 eV. It is apparent by comparison with figure 14 that the loss in resolution in the 8.8 eV band of figure 15 is due to overlap with a third peak, thereby accounting for all six expected ionizations. The third peak under this band most probably corresponds to a 9.41 eV peak of $CpCo(CO)_2$. Assuming this to be the case we have compiled the ionization energy shifts which result from ring methylation in Table VIII. These results show that while all six ionizations shift to lower energy upon ring methylation, the four lowest energy ionizations of $CpCo(CO)_2$ shift much less than the 9.87 and 10.23 eV peaks. This is a further indication that these two peaks are high in ring pi character while the other four are mostly metal d in nature. These unequal peak shifts cause the two ring ionizations of $CpCo(CO)_2$ to move on top of the mostly metal d ionization at 9.41 eV to produce the HeI spectrum of $Me_5CpCo(CO)_2$ in figure 15. It can be seen that the first two ionizations of $CpCo(CO)_2$ move slightly farther apart in $Me_5CpCo(CO)_2$. It will be shown that this results from the

Table VIII - Shifts in Ionization Energy (eV) Resulting from Ring Methylation

$CpCo(CO)_2$	→	$Me_5CpCo(CO)_2$	Δ
10.23		9.09	1.14
9.87		8.75	1.12
9.41		8.75	0.66
8.51		7.92	0.59
7.95		7.32	0.63
7.59		6.84	0.75

$CpRh(CO)_2$	→	$Me_5CpRh(CO)_2$	
10.59		9.62	0.97
10.25		9.62	0.63
9.82		8.61	1.21
9.50		9.01	0.49
8.65		8.11	0.54
7.64		6.78	0.86

fact that the HOMO in these molecules possesses a substantial amount of ring character which causes it to shift slightly more than the other "mostly metal d" when the ring is methylated.

The changes which occur when going to HeII are not as clear-cut for $Me_5CpCo(CO)_2$ as for $CpCo(CO)_2$. The first three ionizations in figure 15 again increase in area relative to the broad, most intense band at 8.8 eV but not to as large a degree as in $CpCo(CO)_2$. In $Me_5CpCo(CO)_2$ this envelope now includes a metal d ionization which partially maintains its overall relative peak area in the HeII specrum. The overall relative peak area in the HeII spectrum. The overall orbital ordering in both of these Co compounds corresponds to four lowest energy orbitals whose major atomic component is metal d, followed by two orbitals which are largely ring pi in character.

This basic orbital ordering changes considerably when Co is replaced by Rh. The HeI and HeII spectra of $CpRh(CO)_2$ are shown in figure 16. The HeII spectrum of this compound shows that there is not as distinct an energy separation between the metal and ring orbitals as in $CpCo(CO)_2$. It can be seen in figure 16 and Table VII that the peaks at 10.59 and 9.82 both lose intensity compared to the other four peaks in the HeII spectrum. Assuming these two peaks to be the ring ionizations gives them a splitting of 0.77 eV as opposed to 0.36 eV in $CpCo(CO)_2$. The factors which contribute to this increased splitting will be examined. The remaining four metal ionizations have also spread farther apart in energy and overlap considerably with the ring ionization region. The spectrum of the permethylated $Me_5CpRh(CO)_2$ analogue in

figure 17 is helpful. As in $Me_5CpCo(CO)_2$, we can no longer resolve one of the valence ionizations. The 8.61 eV peak clearly loses intensity in the HeII spectrum identifying it as one of the two ring ionizations. The increase in relative area for this peak in the HeII spectrum indicates considerable metal d character. This could result from the overlap of the 10.59 eV (ring) and 10.25 eV (metal) peaks of $CpRh(CO)_2$. The shifts which result from these assignments are shown in Table VIII. The two ring ionizations of $CpRh(CO)_2$ (10.59 and 9.82 eV) shift the most as expected. Of the four remaining ionizations three shift by approximately the same amount while the HOMO at 7.64 eV shifts more, but still less than the ring orbitals. This is further evidence of considerable ring character mixing into this molecular orbital.

Molecular Orbital Description of $CpCo(CO)_2$

In order to fully understand the experimental results described in the previous section, a careful analysis of the orbital interactions associated with the observed molecular ionizations is essential. Qualitative analyses of this kind using the extended Hückel methods have been reported for $C_5H_5M(CO)_2$ (M = Mn and Co).[66] The Fenske-Hall molecular orbital diagram of $C_5H_5Co(CO)_2$ shown in figure 18 is in qualitative agreement with the results of Albright and Hoffmann.[66b] Since the most visible valence ionizations derive from the ring pi and metal d orbitals, a fragment analysis was chosen which would most clearly indicate their contributions to the overall electronic structure. The important metal-ring interactions involve the two highest

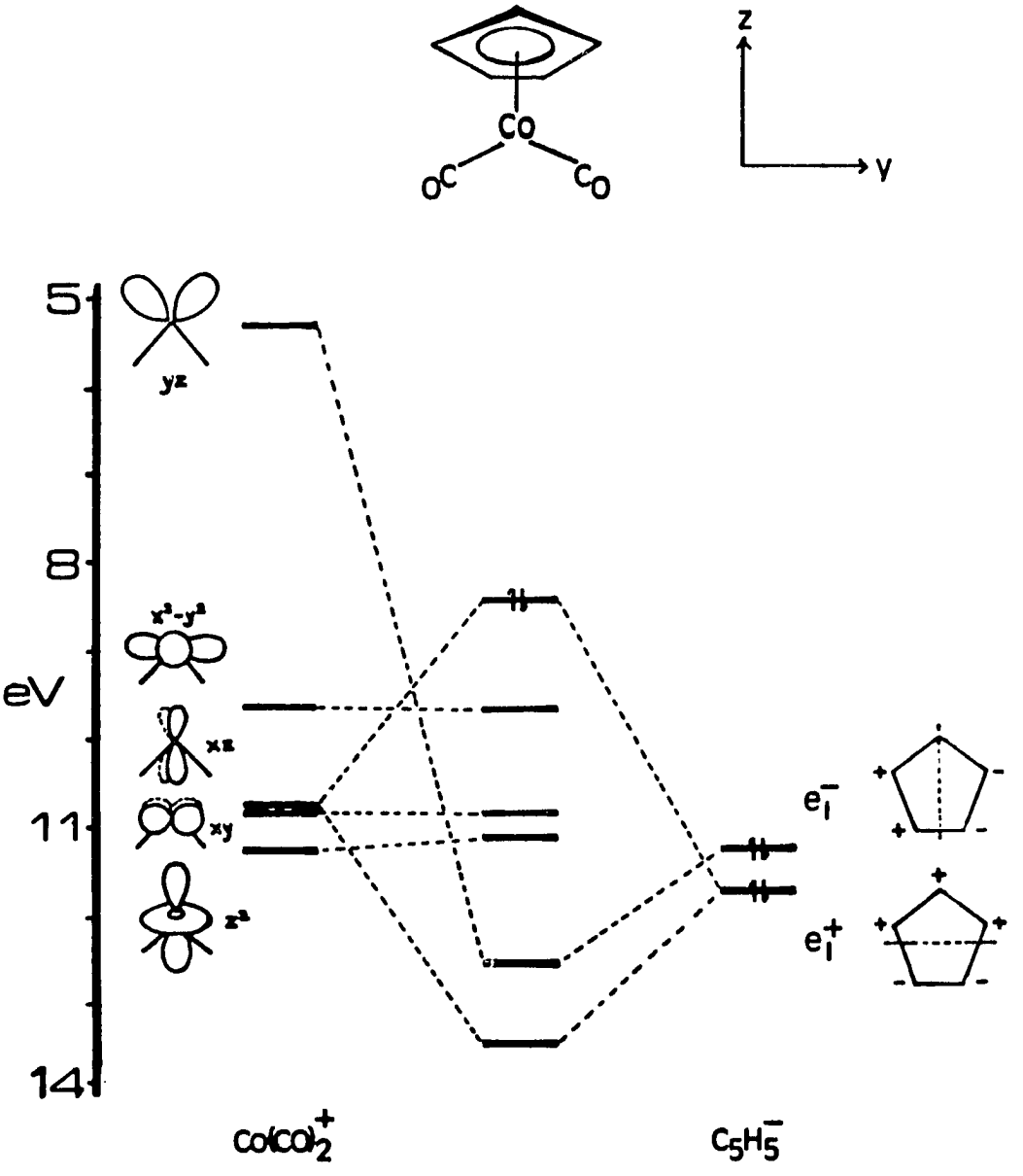

Figure 18 - The Fenske-Hall Molecular Orbital Diagram of $CpCo(CO)_2$

occupied orbitals of the $C_5H_5^-$ fragment which originate from the degenerate e_1'' pair of free $C_5H_5^-$. The diagonal terms for these orbitals on the right of figure 18 show that their degeneracy is lifted in the presence of $Co(CO)_2^+$ (vide infra). The important $Co(CO)_2^+$ orbitals with their atomic components are shown on the left of figure 18. The LUMO of $Co(CO)_2^+$ is primarily derived from the dyz orbital which is pointing straight at the two carbonyl ligands. This orbital is best oriented for accepting electron density from the filled CO 5 sigma donor orbitals. The highest occupied orbital of $Co(CO)_2^+$ is predominantly dx^2-y^2 with a considerable mixing in of dz^2 character. The hybrid possesses good backbonding capability with the in-plane carbonyl pi* orbitals. The HOMO is followed by two closely spaced orbitals which are primarily dxz and dxy respectively. Finally comes the counterpart of the dx^2-y^2/dz^2 hydridized HOMO which is largely dz^2 in character. The molecular orbitals which result from the interaction of these fragments is in agreement with the observed valene ionizations of $CpCo(CO)_2$. The HOMO of $CpCo(CO)_2$ results from the mixing of the out-of-plane dxz orbital with the filled ring e_1^+ orbital. This is a filled-filled interaction and produces filled bonding and antibonding combinations. While the HOMO remains mostly metal d in character, the presence of some ring character causes a small decrease in its HeII peak area (Table VIII) and a slightly larger shift with ring methylation (Table VIII) relative to the following three molecular orbitals which are almost entirely metal d in nature. These orbitals are the dx^2-y^2/dz^2 hybrid pair and the dxy

which have negligible interactions with the ring. The two lowest energy valence orbitals shown in figure[18] are high in ring pi character as was seen in figure[14]. The first of these is the e_1^- ring orbital which is slightly stabilized by its weak interaction with the dyz LUMO of $Co(CO)_2^+$. The lowest energy valence orbital of $CpCo(CO)_2$ is the dxz-e_1^+ bonding counterpart to the antibonding HOMO. In contrast to its antibonding HOMO. In contrast to its antibonding partner, the ring character predominates in this orbital.

The observed effects of changing from Co to Rh are illustrated in figure 19. In both the substituted and unsubstituted cyclopentadienyl analogues the three orbitals which are almost entirely metal d in character shift the most. The largely ring e_1^- orbital and the metal-ring antibonding HOMO hardly shift at all while the dxz, e_1^+ bonding orbital drifts by an intermediate amount. The consistency of these shifts lends further support to our peak assignments.

The final set of peak assignments have been arrived at with some confidence. These assignments have consistently explained HeI/HeII intensity ratio changes, as well as the changes which result from specific chemical perturations (ring methylation and variation of the metal atom).

Localized Bonding within the Coordinated Cyclopentadienyl Ring

As pointed out in Appendix B, the idea of localized bonding within the pi system of coordinated cyclopentadienyl rings has been a persistent point of uncertainty in our understanding of metal-cyclopentadienyl bonding.[67] This situation arises from metal-ring orbital overlaps which result in an unequal pi electron distribution throughout the

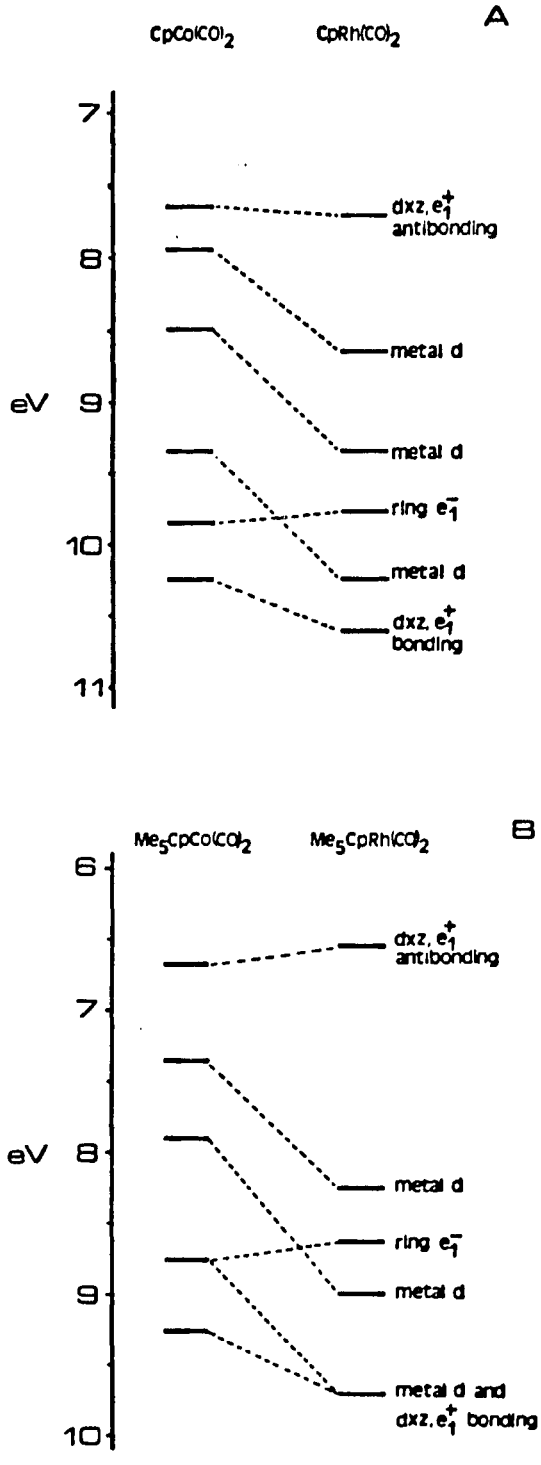

Figure 19 - The Effects of varying the Metal Atom in the A) Cyclopentadienyl and B) Pentamethyl-cyclopentadienyl Analogues

ring. While this should result in unequal ring C-C bond lengths, the small magnitude of this distortion and ring librational motion has hampered efforts to measure this effect. Two recent structural studies have circumvented this problem to obtain statistically valid bond length distortions. A low temperature crystal structure of $CpMn(CO)_3$ which was corrected for libratonal motion indicated a diene type configuration of the ring where two of the C-C bond lengths are shorter than the other three.[68] Alternatively, the use of ring permethylation to minimize librational motion in $Me_5CpCo(CO)_2$, has shown two relatively long ring C-C distances indicating an allyl-ene configuration.[17]

To rule out the possibility of attributing these structural distortions to solid state effects, we have presented the first gas phase evidence for the distortion of coordinated cyclopentadienyl rings from five-fold symmetry.[39] This distortion lifts the degeneracy of the coordinated ring orbitals which originate from the e_1'' HOMO of the free $C_5H_5^-$ anion. This is seen in the UPS spectrum as a splitting in the highest energy ring pi ionization between 8.5 - 10.0 eV. A splitting of 0.36-0.43 eV was measured for the series $(CH_3)_nC_5H_{5-n}M(CO)_3$ where M = Mn; n = 0,1,5 and M = Re; n = 0,5. In these cylindrically-symmetrical d^6 molecules the dxz, dyz orbitals, which interact with the ring pi system, (the z axis is along the metal-ring centroid axis) are unoccupied and degenerate. The noncylindrically-symmetrical d^8 compounds in this study possess a nondegenerate dxz (filled) and dyz (vacant) pair. When these orbitals interact with the ring e_1'' orbitals, they should induce an even greater splitting in these ring orbitals than was observed in the tricarbonyls. This splitting is between the ring e_1^- and dxz/e_1^+

bonding orbitals in figure 19. It can be seen that large splittings are observed for the Rh compounds ($CpRh(CO)_2$ = 0.77 eV, $Me_5CpRh(CO)_2$ = 0.99 eV) as expected. Unexpectedly, the Co analogues have splittings comparable to or even lower than the tricarbonyls ($CpCo(CO)_2$ = 0.36 eV, $Me_5CpCo(CO)_2$ = 0.34 eV). This apparent inconsistency can be attributed to the effects of electron relaxation (see Appendix A). It has been found both experimentally[40,69-71] and theoretically[72,73] that the ionization of d electrons results in large relaxation energies. In addition, it is known that electron relaxation decreases as one descends a column in the periodic table[72] (ab initio calculations show that Co3d ionizations have almost twice the relaxation of Rh4d ionizations).

In the group VII $CpM(CO)_3$ system (Appendix B) there is a distinct separation between the metal d orbitals and the ring pi orbitals. The observed splitting is between two ring orbitals which have very similar atomic composition and relaxation energies and therefore their difference in ionization energy should be very comparable to their ground state splitting due to ring distortion. We have seen in figures 18 and 19 that the split ring orbitals of the group VIII $CpM(CO)_2$ have different atomic compositions. The resulting difference in the relative relaxation energies of these two orbitals affects their observed splitting which would normally be attributed to the ground state ring distortion mentioned above. This is illustrated in figure 20 where the observed splittings of the two mostly ring pi orbitals of $CpCo(CO)_2$ and $CpRh(CO)_2$ are examined in closer detail. Starting from the e_1" degenerate pair of the free $C_5H_5^-$ anion, we have observed the

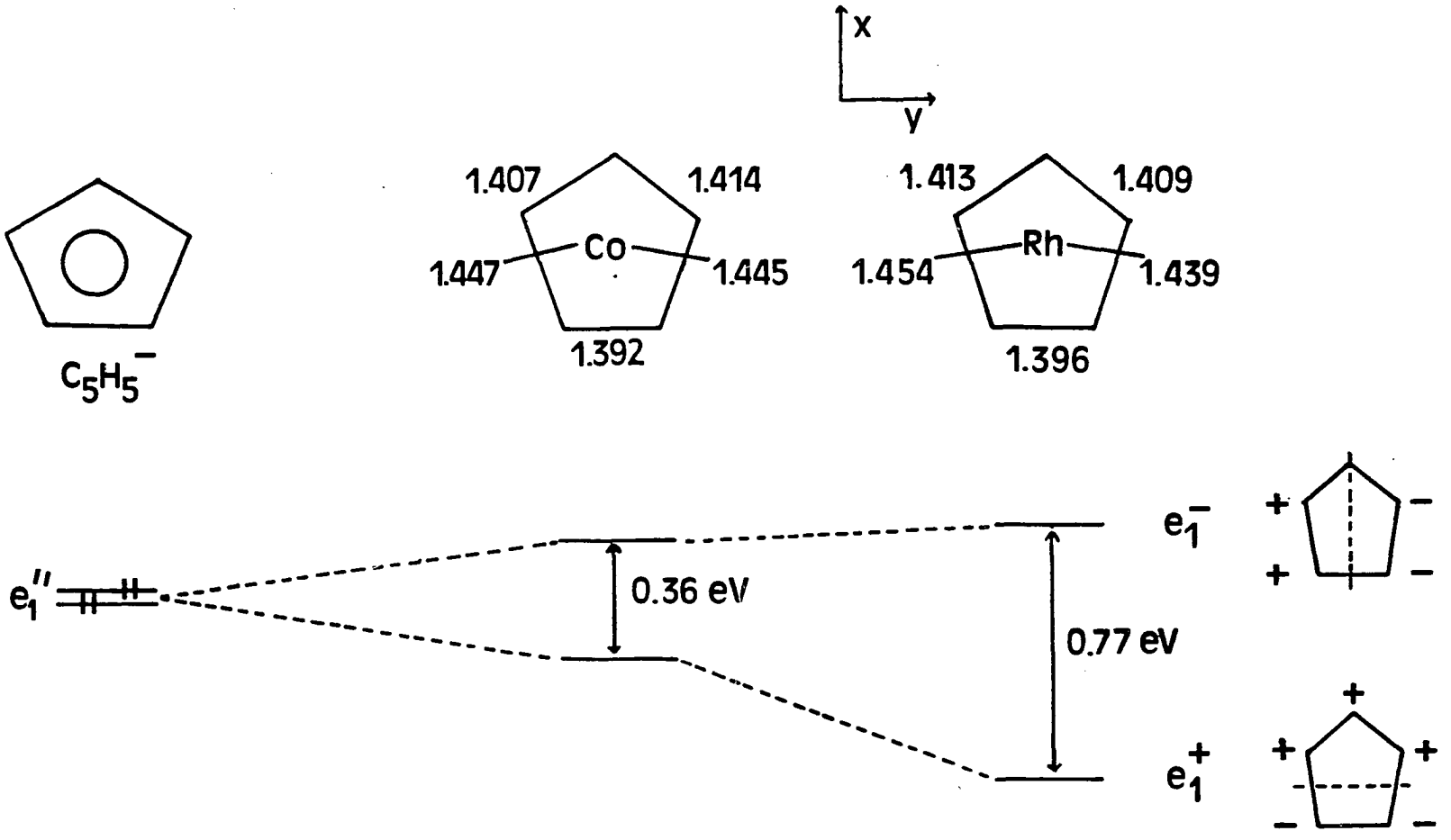

Figure 20 - Observed Loss in Degeneracy in the Ring e_1'' Orbitals Upon Coordination

lifting of this degeneracy in the $CpM(CO)_2$ complexes by the amounts shown. It is important to note that although the measured ring C-C bond lengths for $Me_5CpCo(CO)_2$[17] and $Me_5CpRh(CO)_2$[74] indicate comparable amounts of ring distortion, the splitting of the ring ionization more than double in the Rh analogue. This indicates that ring distortion is not the sole variable in determining the splitting in the ring pi ionization energies. Since there is higher metal d orbital mixing into the lower energy e_1^+ orbital (figures 18 and 19), there is greater relaxation associated with ionization from this orbital than from the e_1^- orbital. In both the Co and Rh compounds this serves to decrease the ionization energy of the e_1^+ relative to the e_1^- orbital and therefore decreases the splitting between their ionization energies. The larger relaxation energy associated with the Co3d ionizations enhances this effect resulting in the unexpectedly small splittings observed for $CpCo(CO)_2$ and $Me_5CpCo(CO)_2$. Since the Rh4d orbitals relax much less, the symmetry-induced nondegeneracy of the ring orbitals dominates and maintains the larger splitting in the Rh compounds. The e_1^+ orbital still relaxes more but not enough to decrease its splitting from the e_1^- to the level observed in the Co compounds.

The above explanation shows that the larger splitting in the ring pi ionizations of the Rh compounds does not necessarily imply greater ring distortion than in the Co analogues. This would be true only in the absence of relaxation effects (as in the group VIII tricarbonyls) in which case ionization energies would be a direct indication of ground state electronic structure.

APPENDIX A

Koopmans' Theorem[5] has had much influence on current concepts and models of chemical behavior. The Theorem equates electron orbital energies with ionization energies, contingent on specific assumptions pertaining to the Hartree-Fock wavefunctions. The ionization energies of atoms and molecules are associated with many aspects of chemistry, including certain thermochemical cycles, models of electronegativity, and parameterization schemes for semi-empirical molecular orbital theories. Koopmans' Theorem provides the theoretical framework for interpreting such physical and chemical properties in terms of ground state electronic structures.

Evidence of the limitations of Koopmans' approximation has followed from the concurrent development of photoelectron spectroscopy and increasingly sophisticated theoretical calculations.[75] One important assumption of the Theorem is that, when an electron is removed from an atom or molecule, the remaining charge distribution does not change. In fact, the remaining charge distribution is contracted or reorganized as a result of the decrease in electron-electron repulsions. In addition, Koopmans' approximation to ionization energies neglects relativistic and electron correlation energies, as a result of the assumptions of the Hartree-Fock model.[76]

Core electron ionizations have received considerable theoretical

investigation,[77-79] and it is found that Koopmans' approximation leads to very large absolute errors. A rough guideline is that Koopmans' predictions of ionization energies are 5% to 10% larger than the experimental ionization energies.[80-82] In the case of valence ionizations, the electron relaxation energy is generally much less, and it is partly compensated by the correction due to neglect of electron correlation. It has been said that Koopmans' predictions of valence ionizations are normally correct within one or two electron volts.[77-83] However, the order of particular ionizations may still be predicted incorrectly, since the relaxation energy is not the same for ionization from each orbital. Several calculational alternatives to Koopmans' approximation have been put forward.[84,85]

There is now evidence of much larger errors in Koopmans' approximation for the valence ionization energies of many molecules. The most striking examples follow from the photoelectron studies of transition metal complexes.[40,41,69,71,86-88] For instance, the first ionization of ferrocene, at 6.8 eV, has been assigned to the $^2E_{2g}$ state of the positive ion.[85] This ionization is associated with removal of an electron from an e_{2g} orbital with high metal d character. From an *ab initio* calculation of the electronic structure of ferrocene, this e_{2g} orbital has an eigenvalue of 14.4eV and is the third orbital below the highest occupied orbital.[86] Such large discrepancies can lead to serious problems in the chemical interpretation of electronic structure.

The errors of Koopmans' approximation for valence ionizations are normally explained in terms of "molecular" characteristics related to the energy of electron charge rearrangement throughout the molecule.

For instance, the errors for metal complexes partly correlate with the degree of localization of the orbital.[69,71,89] A relationship between these errors and the metal character in the orbital has also been noted, and has prompted us to investigate the possibility of explaining certain gross features of the errors of Koopmans' approximation in terms of a simple "atomic" model. We report some characteristic trends in the errors of Koopmans' approximation for valence ionization of atoms. Just as valence ionization energies themselves have well-defined periodic characteristics, it may be anticipated that the relaxation energies display certain periodic properties. The analysis of these properties contributes valuable insight into the ionization energies of molecules.

A Quantitative Approximation of Relaxation Energy

The quantities needed for definition of the relaxation energy are illustrated in figure 21. The self-consistent-field ground state of atom N with orbital structure ϕ is represented as $M(\phi)$. Removal of an electron from the i^{th} atomic orbital without allowing the radial distributions of the remaining electrons to relax produces $M_i^+(\phi)$. $M_i^+(\phi)$ is called the Koopmans' or frozen orbital wavefunction for the positive ion state. Koopmans' Theorem states that the energy difference between these two wavefunctions is equal to the orbital eigenvalue, ϵ_i. This represents

$$E[M_i^+(\phi)] - E[M(\phi)] = -\epsilon_i = \Delta E_{KT} \qquad (1)$$

the Koopmans' approximation to the ionization energy.[90]

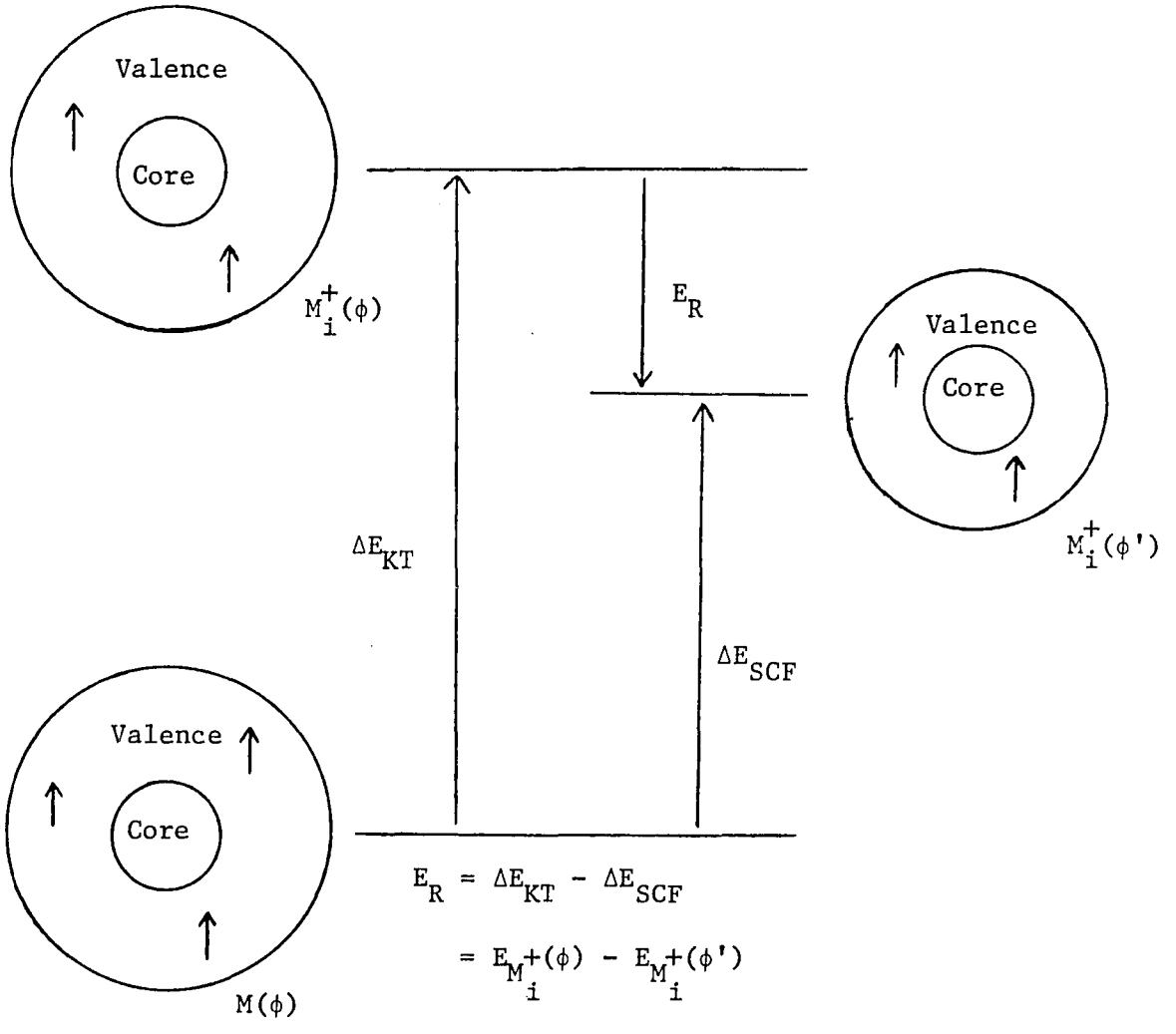

Figure 21 - Schematic Definition of the Electron Relaxation Energy, E_R

The self-consistent-field wavefunction of the positive ion, where the atomic orbitals are optimized according to the actual electron interactions in the ion, is represented as $M_i^+(\phi')$. The energy difference between $M_i^+(\phi')$ and $M(\phi)$ is termed the ΔE_{SCF} approximation to the ionization energy.

$$E[M_i^+(\phi')] - E[M(\phi)] = \Delta E_{SCF} \qquad (2)$$

The relaxation energy, E_R, is defined as the difference between Koopmans' approximation and the self-consistent-field approximation, which is the energy associated with optimization of the orbitals of the positive ion from the frozen orbital representation determined from the ground state.

$$\begin{aligned} E_R &= \Delta E_{KT} - \Delta E_{SCF} \\ &= E[M_i^+(\phi)] - E[M_i^+(\phi')] \end{aligned} \qquad (3)$$

The optimized orbitals of the positive ion are represented in figure 21 as having more contracted radial distribution functions.

It should be emphasized that E_R, the electron relaxation energy, is a precisely defined theoretical consequence of the orbital description of atomic structure. As is well-known, the Hartree-Fock approximation itself is limited by electron correlation and relativistic effects. These correlations should be included in a definition of the ionization energy.

$$\begin{aligned} \text{ionization energy} &= \Delta E_{SCF} + E_{correlation} + E_{relativistic} \\ &= \Delta E_{KT} - E_R + E_{correlation} + E_{relativistic} \end{aligned} \qquad (4)$$

In order to place the magnitude of these corrections in perspective, the contribution of each term for ionization of a 2p electron of carbon is shown in figure 22. The relativistic correction is very small for ionization of a valence electron.[91] The ΔE_{SCF} approximation is often less than the experimental ionization energy due to correlation effects, while neglect of electron relaxation causes ΔE_{KT} to be too large. Figure 22 exemplifies several common generalizations about valence ionizations that are shown in this paper to be violated in specific instances of atomic ionization. First, E_R is only one electron volt. Second, E_R is partly compensated by the correlation correction, thus improving agreement between ΔE_{KT} and the experimental ionization energy. Third, these corrections seem to provide a convenient situation in which ΔE_{KT} and ΔE_{SCF} are upper and lower bounds to the experimental ionization energy.

The periodic trends presented in this paper are obtained from calculations for the atom and the ion that are near the Hartree-Fock limit.[92] These atomic solutions are appropriate since they are often used for the initial construction of molecular wavefunctions. Similar results are found from other calculations.[78b,79,93] The goal of this study is not to critically evaluate the many sophisticated electronic structure theories, but to develop a conceptual interpretation of the relaxation energies. A simple atomic model that aids this purpose is Slater's concept of elecron shielding and effective nuclear charges.[94,95] In this model the origin of the electron relaxation

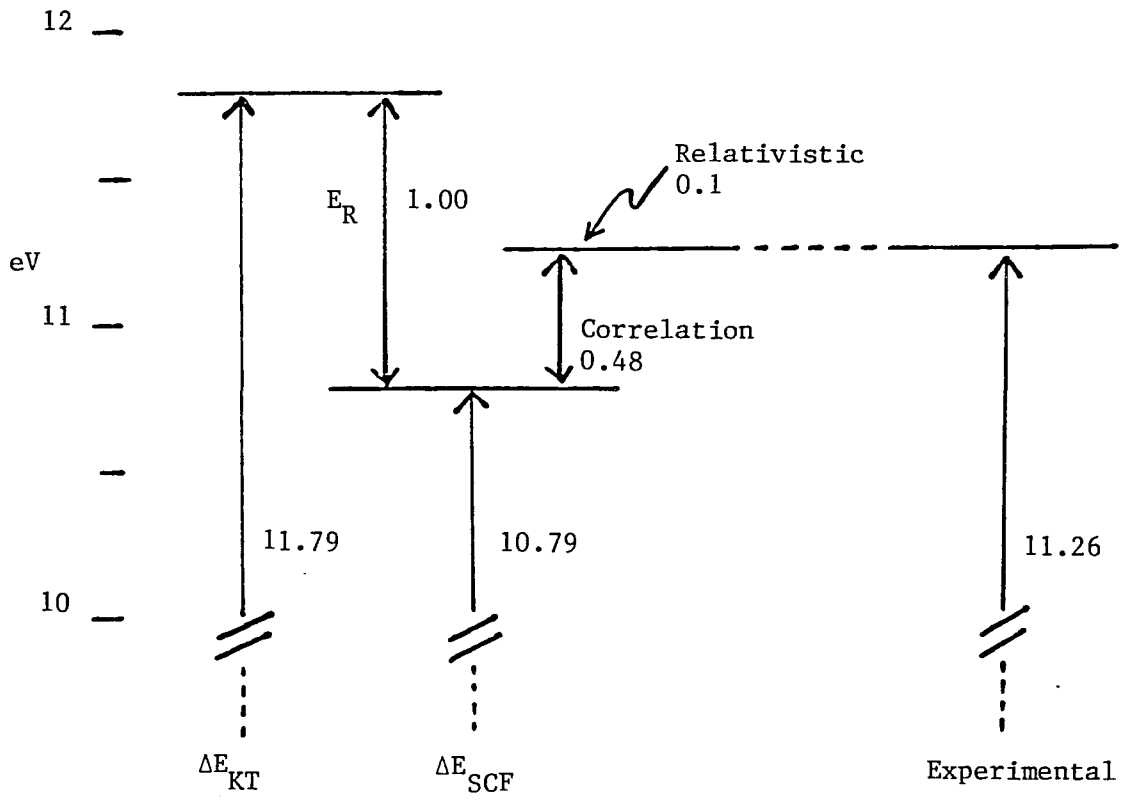

Figure 22 - Relative Energy Contributions from Equation (4) to the Carbon 2p Ionization

energy follows from the different total electron shielding in the positive ion compared to the neutral atom. The total shielding of each electron from the nucleus is defined as the sum of the individual electron shielding factors from all other electrons. This may be written as

$$S_{n\ell} = \sum_{n'} \sum_{\ell'} [N_{n'\ell'} S_{n\ell,n'\ell'}] - S_{n\ell,n\ell} \tag{5}$$

where $S_{n\ell,n'\ell'}$ is the extent an electron with $[n,\ell]$ quantum numbers is shielded by one electron with $[n'\ell']$ quantum numbers, and $N_{n'\ell'}$ is the number of electrons with these quantum numbers (substracting $S_{n\ell,n\ell}$ eliminates an electron shielding itself). Some examples of shielding factors are given in Table IX. It should be remembered that, according to Slater's rules, beyond n=1 the ns and np electrons are grouped together, shielding by electrons in the same group is 0.35, and shielding by electrons in outer groups is zero. The total energy of the atom is written as

$$E[M(\phi)] = -\sum_{n} \sum_{\ell} \frac{N_{n\ell}}{n^2} [Z - S_{n\ell}]^2 \tag{6}$$

where Z is the nuclear charge and the quantity $[Z - S_{n,\ell}]$ is the effective nuclear charge felt by electrons in the $[n\ell]$ shell. The corresponding expression for the self-consistent positive ion state is

$$E[M_i^+(\phi')] = -\sum_{n} \sum_{\ell} \frac{N^+_{n\ell}}{n^2} [Z - S^+_{n\ell}]^2 \tag{7}$$

where $N^+_{n\ell}$ and $S^+_{n\ell}$ correspond to the configuration in the positive ion.

Snyder[96] has derived the following expression for the energy of Koopmans' imaginary positive ion state, which preserves the shielding

Table IX - Slater Shielding Factors $S_{n\ell,n'\ell'}$

$n\ell/n'\ell'$	3s	3p	3d	4s
3s	.35	.35	0	0
3p	.35	.35	0	0
3d	1.0	1.0	.35	0
4s	.85	.85	.85	.35

↑

shielded electron

determined for the neutral atom:

$$E[M_i^+(\phi')] = \sum_{n\ell} \frac{N_{n\ell}^+}{n^2} [Z-S_{n\ell}]^2 - \sum_{n\ell} \frac{N_{n\ell}^+}{n^2} [Z-S_{n\ell}] [Z-S_{n\ell}^+] \quad (8)$$

The electron relaxation energy is now obtained by subtracting equation (7) from equation (8). It follows that

$$E_R = \sum_{n\ell} \frac{N_{n\ell}^+}{n^2} [(Z-S_{n\ell}) - (Z-S_{n\ell}^+)]^2$$

$$= \sum_{n\ell} \frac{N_{n\ell}^+}{n^2} [S_{n\ell}^+ - S_{n\ell}]^2 \quad (9)$$

only those shells that are shielded by the electron which is removed contribute to the relaxation energy, since each term vanishes if the shell is shielded by an equivalent amount in both the neutral atom and the positive ion. According to Slater's rules the electron does not shield electrons that are in deeper shells, so only electrons in the same shell as the electron to be removed, or in outer shells, will experience relaxation. Equation (9) also indicates that the electron relaxation energy is independent of Z.

In the case of core ionizations E_R is generally dominated by the large number of electrons in outer shells that are effectively shielded from the nucleus by the core electron.[78e,96-98] The numerical agreement between calculations of E_R using equation (9) and other estimations is basically good.[77,96] The significance of this equation to the relaxation accompanying valence ionizations has not been discussed in detail previously. In the case of valence electron ionizations there are no outer shell electrons to relax, so only the term for intra-shell

relaxation need be considered. If $N_{valence}$ is defined as a number of electrons in the outer valence shell (defined according to Slater's grouping of orbitals) of the neutral atom, equation (9) is reduced to

$$E_R = (N_{valence}{}^{-1}) \left(\frac{0.35}{n}\right)^2 \qquad (10)$$

The numerical factor 0.35 follows from recognizing that the total shielding of an electron in the valence shell is reduced by 0.35 (except when n=1) when one valence electron is removed. Equation (10) simply says that the total relaxation energy is equivalent to the number of electrons remaining in the valence shell multiplied by a relaxation energy which is related to the extent each electron was shielded by the ionized electron. This equation is the starting point for discussing the characteristics of E_R for valence ionization.

Periodic Trends in E_R

The observed trends in the calculated values of E_R are most clear when these numbers are presented in graphical form. Figure 23 illustrates ΔE_{KT}, ΔE_{SCF}, and the experimental first ionization potentials for atoms from the first row of the periodic table. For each atom, the dashed horizontal line is the experimental ionization energy, the top of the box is ΔE_{KT} and the bottom of the box is ΔE_{SCF}. Therefore the height of the box is equal to E_R for the first ionization of each atom. For lithium, ΔE_{KT}, ΔE_{SCF}, and the experimental energy all coincide within the width of the line. Equation (10) indicates that E_R should be

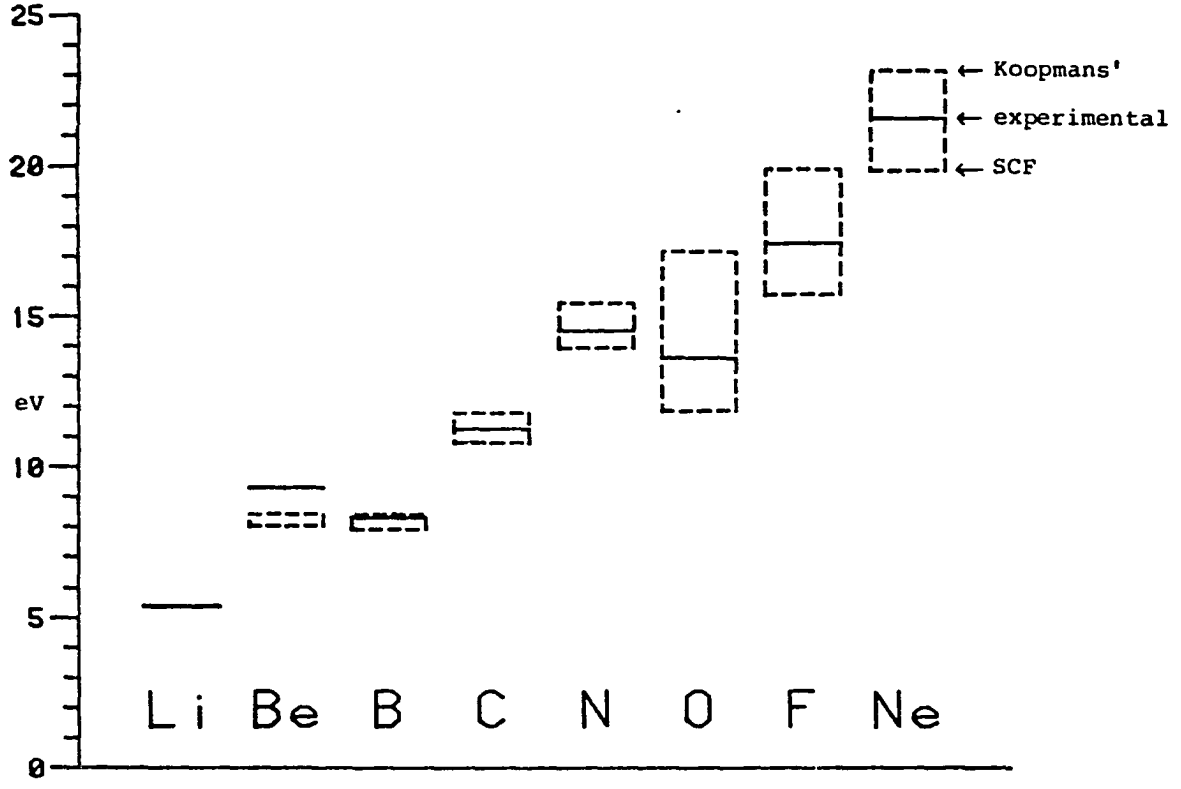

Figure 23 - Comparison of Calculated and Experimental First Ionization Potentials for First Row Atoms. The Dashed Lines are the Experimental Ionization Energies. The Top of Each Box is Koopmans' Approximation. The Bottom is the ΔE_{SCF} Approximation

zero in this case because no electrons are left in this valence shell. The change in correlation energy is also small for the same reason.

Equation (10) also predicts a steady increase in E_R from left to right across a row as the number of electrons remaining in the outer shell increases. While generally larger to the right of the row, E_R actually maximises at oxygen and falls off at fluorine and neon. Of course, the magnitude of E_R for oxygen would be partly diminished if $E[M_i^+(\phi')]$ were taken from a weighted average of the positive ion configurations, but the large increase of E_R from nitrogen to oxygen remains. This increase is related to the corresponding decrease in experimental ionization energies from nitrogen to oxygen. Koopmans' energies as well as effective nuclear charges, indicate a continual increase in the first ionization energy from boron to neon. However, the P^4 configuration of oxygen is the first instance in which the ionized electron is paired with one electron and has spin opposite to the other electrons in the p shell. The larger coulomb integral between electrons in the same spatial orbital and the lack of exchange integrals between electrons with opposite spin leads to a greater average electron repulsion between the ionized electron and the remaining electrons of oxygen. In other words, the ionized electron of a p^4 configuration shields the remaining electrons to a greater average extent. Figure 24 plots the average electron-electron repulsion between the p electron to be ionized and the other p electrons in the shell in terms of the Slater-Condon parameters. The average repulsion remains steady from carbon to nitrogen, maximizes at oxygen and falls off at fluorine and neon, consistent with the relaxation energies.

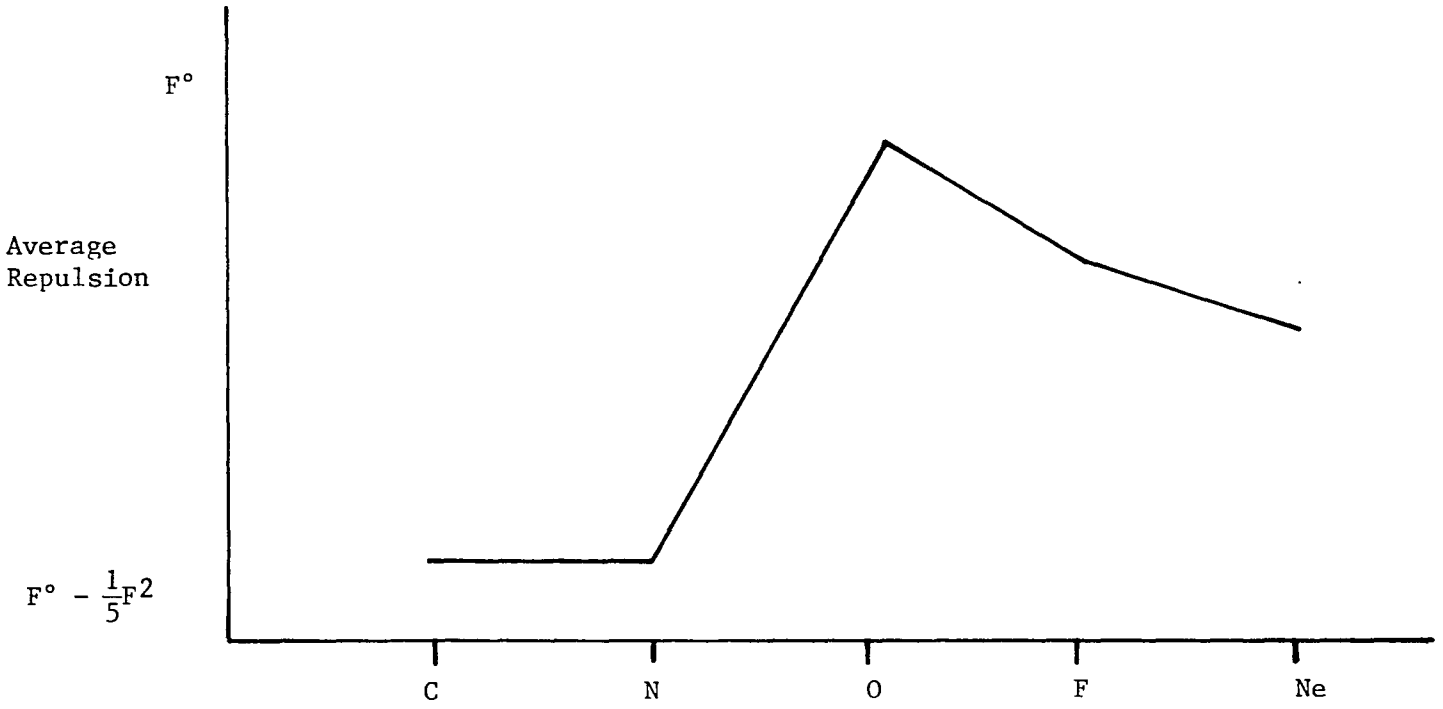

Figure 24 - Average Electron-Electron Repulsion Between 2p Electrons in terms of Slater-Condon Parameters.

Slater's rules for shielding factors are not capable of reproducing this discontinuity, since these rules average the 2s and 2p shells and each electron in these shells shields all others equivalently. Slater's rules indicate that the increase in E_R with each increase in atomic number across the row should be $.35^2/n^2$. It is interesting to compare this with the average change in E_R with atomic number across the rows as found from the self-consistent-field calculations (Table X). Within the averaging imposed by Slater's rules, the two determinations of E_R are in close agreement.

Table X - Average $\Delta E_{R/\Delta N}$

	n=2	n=3	n=4
Slater's rules	0.42	0.19	0.10
Hartree-Fock	0.47	0.19	0.14

Another feature worth noting in figure 23 is that in every case but beryllium, the experimental ionization energy is "bracketed" by the Koopmans' Theorem and ΔE_{SCF} energies. In the case of beryllium the relaxation energy is still relatively small for only one electron remaining in the shell, but the correlation energy change is relatively large for removal of the electron from a paired orbital. This causes both Koopmans' Theorem and ΔE_{SCF} energies to be less than the experimental energy. This situation also occurs for ionization from the $4s^2$ orbital of transition metals.

Figure 25 is a bar graph in the form of a periodic table which illustrates the magnitude of E_R for the first ionizations of elements

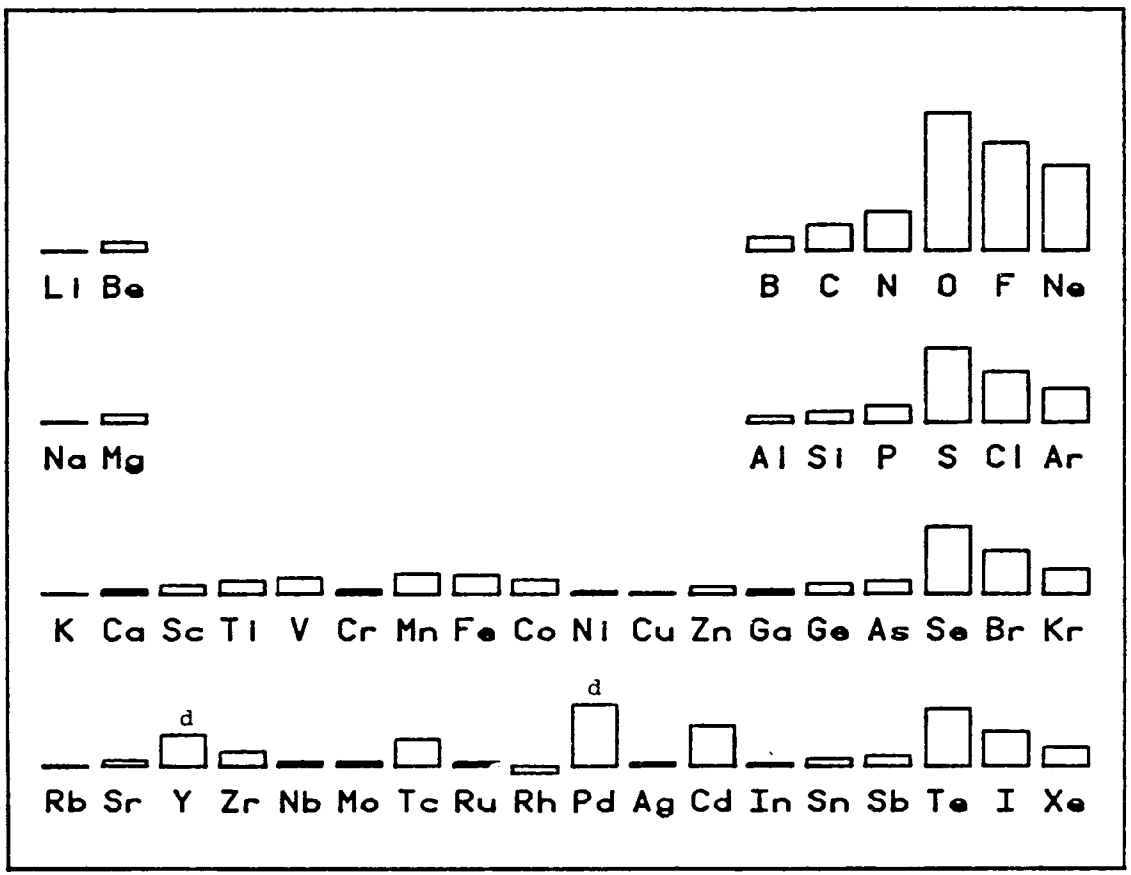

Figure 25 - Periodic Table of E_R, for First Ionizations. The Height of Each Bar is Proportional to E_R. E_R for Carbon is 1.00 eV

with $2 \leq Z \leq 54$. The trends observed for the first row are also observed in subsequent rows. In all cases group I gives very small values of E_R, and each row exhibits a maximum E_R at group VI. As equation (10) predicts, there is in general a smooth decrease in E_R upon descending a column due to increasing n. The transition metals do not appear to follow the trend until one recalls that except for Pd and Y, the first ionization of the transition metals is the loss of an s electron resulting in small E_R values.

The first ionization for Pd and Y is a d electron which gives inordinately high E_R values. Figure 26 compares the electron relaxation energy accompanying d electron ionization for several transition metals. Within each transition metal row E_R is again generally larger on the right than on the left, and there is a maximization of E_R at group VIII, which represents the first electron beyond the half-filled d orbital shell. Also, E_R is not as large in the second transition metal row as in the first. The unexpected feature in terms of Slater's rules for shielding is the large size of the relaxation energies for d ionization.

An explanation of these large relaxation energies is provided by the shielding factors derived by Clementi and Raimondi[99] from their "best atom" self-consistent-field calculations, shown in Table XI. These shielding factors indicate that the 3d electrons shield the 3s and 3p electrons at least as effectively as they shield other 3d electrons. This means that the s and p electrons should be included in the outer relaxation shell with the d electrons, and $N_{valence}$ in equation (10) ranges from 9 to 18 electrons instead of from 1 to 10. The individual

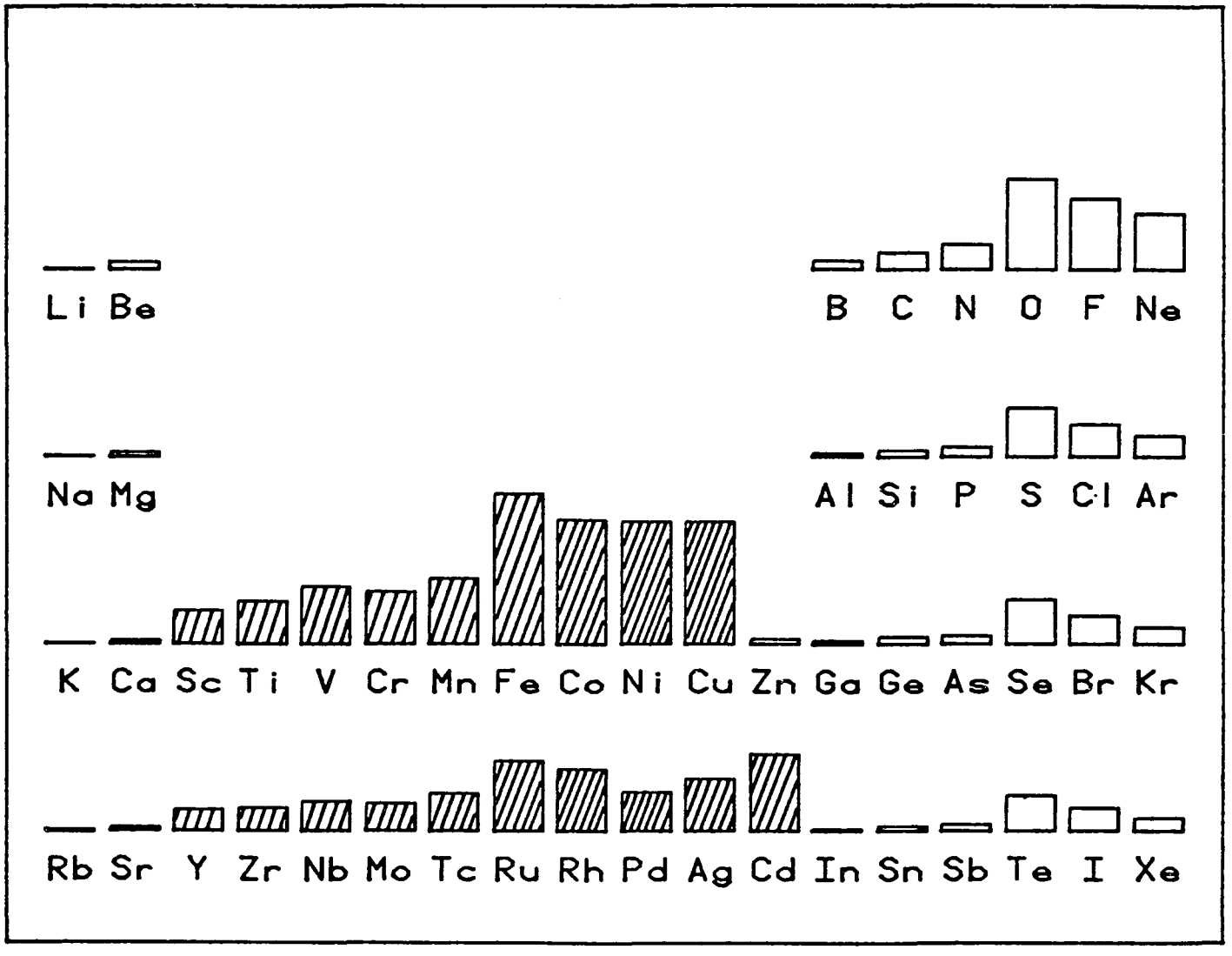

Figure 26 - Periodic Table of E_R for First Ionizations. The Height of Each Bar is Proportional to E_R. E_R for carbon is 1.0 eV. The Shaded Bars Correspond to Removal of a d Electron

Table XI - Clementi and Raimondi's $S_{n\ell,n'\ell'}$

$n\ell/n'\ell'$	3s	3p	3d	4s
3s	.25	.25	.34	.08
3p	†	.38	.33	.05
3d	†	†	.27	0
4s	†	†	.83	.10

↑

Shielded electron

† combined in single term for all inner electrons

contributions of relaxation of the 3s, 3p, 3d, and 4s electrons to the total relaxation energy may be evaluated using equation 9 and Clementi and Raimondi's shielding factors. This predicts the relaxation energies for d ionizations within about 20% if the d electron shell is not more than half filled. If d electrons are paired the predictions are much too low.

The most striking feature of E_R is the large values indicated for atomic 3d ionization. Evidence for similarly large values has been found from ab initio ΔE_{SCF} calculations on several organometallic molecules. This is illustrated in the case of ferrocene in figure 27. The eigenvalues for orbitals which are predominantly metal 3d are calculated much below the predominantly cyclopentadienyl e_1'' (carbon 2p) orbitals, as shown in the Koopmans' Theorem prediction of the ionization potentials. Calculations for the appropriate positive ion states show a much greater relaxation from metal ionization than from carbon ionization, and switches the order of the ionizations in agreement with the assignment of the photoelectron spectrum.

A rough correlation between the % metal character and the magnitude of E_R has also been noted. Figure 28 displays the correlation obtained from calculations in the literature on nine different organometallic complexes.[40,41,69-71,86-88] The vertical bar at 100% metal character is the range of E_R found for d^6-d^{10} metals in the atomic calculations. There is considerable scatter in the data, nonetheless, it is significant that orbitals with more than about 70% metal character have E_R greater than about 5 eV, and orbitals with less than 40% metal character have E_R of only 1 or 2 eV. In the range of 40% to 70% metal

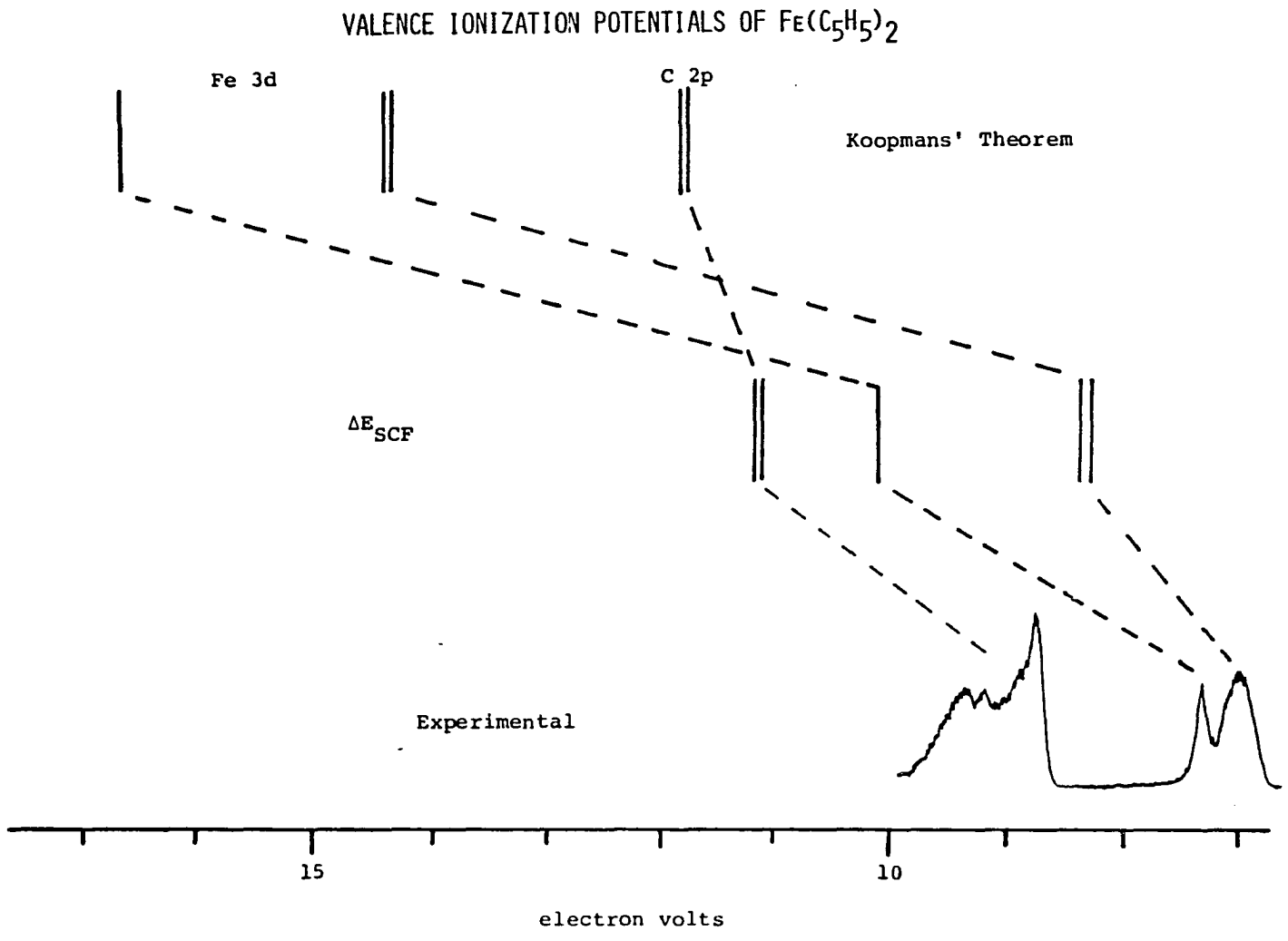

Figure 27 - Comparison of Koopmans' and ΔE_{SCF} Energies of Ferrocene with the Experimental Photoelectron Spectrum

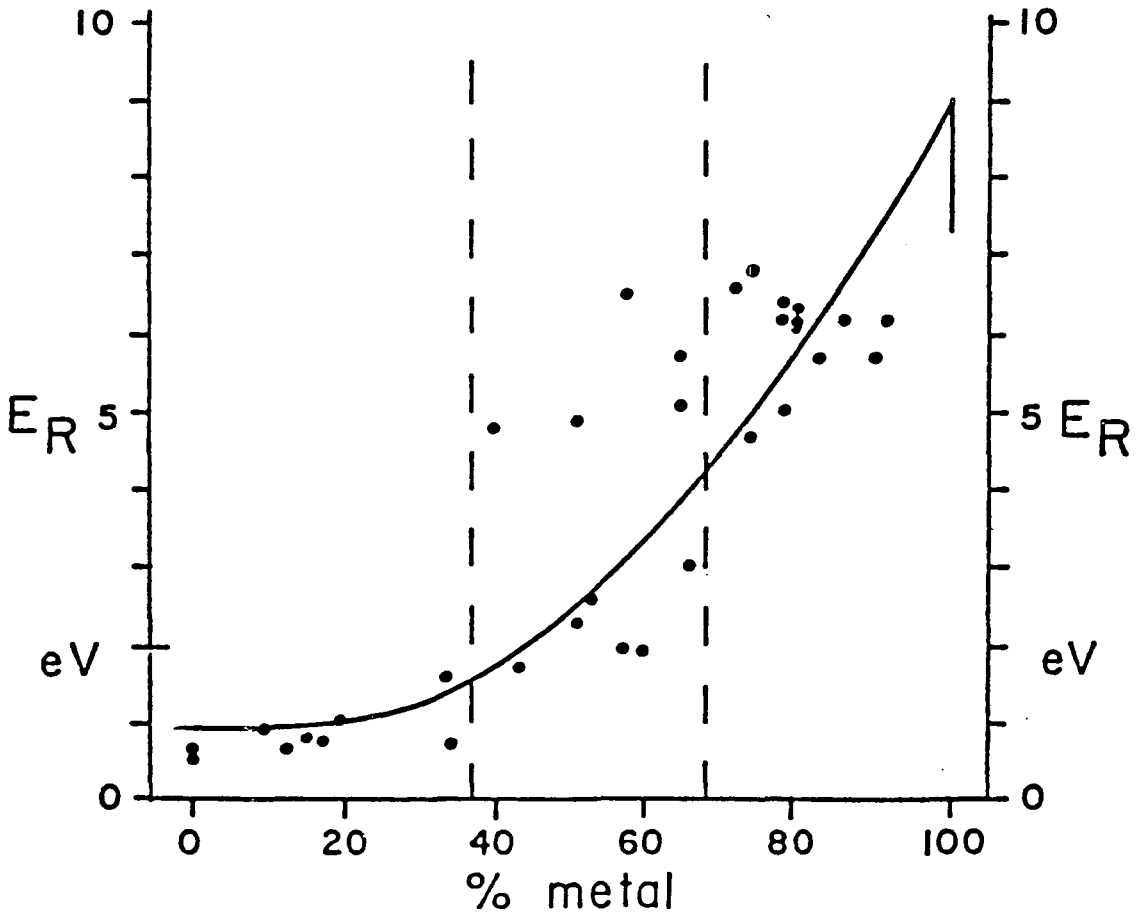

Figure 28 - Comparison of E_R with Percent Metal Character.

character there are much larger deviations from the curve for intra-atomic relaxation, possibly because of greater uncertainties in the contribution of electron reorganization for delocalized orbitals. It should be remembered that these ab initio molecular calculations for metal complexes employ limited basis sets that do not uniformly approximate the Hartree-Fock limit, and it is often difficult to optimize the correct positive ion states for the low symmetry systems. These factors place additional uncertainties on the Koopmans' and ΔE_{SCF} predictions. The important point is that as the metal character approaches 100%, the E_R tends toward the atomic values.

Previous calculations on metal complexes have failed to reveal the atomic nature of the relaxation energies.[69,71] This is partly because basis sets similar to those used in the molecular calculations will fail to indicate the full atomic relaxation energy. This work shows that the atomic orbitals below the valence shell, particularly the 3s and 3p, must have enough variational freedom for full optimization in the atomic calculations. This need is reduced in the molecular calculations by the charge reorganization toward the positive holes in the potential.

Conclusions

The periodic trends in electron relaxation with valence atomic ionization are summarized as follows:

1. The electron relaxation energy decreases down each row of the periodic table.

2. The electron relaxation energy is very low for s electron ionization. It increases across the row to the right until maximizing at group VIA, and then decreases slightly in groups VIIA and VIIIA.

3. The electron relaxation energy is large for metal 3d ionization, especially when the 3d electrons are paired.

These trends have not been recognized previously, but are easily understood in terms of shielding factors between electrons. The relaxation energy increases with the number of electrons that are shielded by the electron to be removed, and with the extent of the shielding. In the case of first ionizations the shielding of electrons in the same outer shell is most important. For removal of 3d electrons it is best to consider the 3s and 3p electrons as also being in the outer shell.

APPENDIX B

THE VALENCE IONIZATIONS OF $CpM(CO)_3$; M = Mn and Re

The cyclopentadienyl ring ligand has played an important role in the development of organometallic chemistry since the discovery of ferrocene in 1952. The significance of the cyclopentadienyl ligand has stimulated interest in investigating the chemistry of other closely related ligands, such as rings in which one or more of the hydrogen atoms are substituted by other groups.[64] The most useful developments in this direction have been the synthesis of pentamethyl-cyclopentadienyl complexes, many of which are analogous to the well-known sandwich and half-sandwich compounds. Although at first glance the permethylation of cyclopentadienyl rings might appear to be a relatively minor alteration, it has proven to be a useful perturbation for mechanistic studies and has uncovered a significantly different chemistry in many systems.[64,100,101] For instance, the permethylated analogues have exhibited altered crystallization characteristics,[102] solubilities,[100a,103] tendencies to form metal-metal bonds,[64,102a,103] stabilities,[100a] susceptibility to attack,[101] sensitivity to oxidation,[104,105] etc. Some of the changes in behavior of pentamethyl-cyclopentadienyl complexes may be attributed to the steric protection provided by the five ring methyl groups and by the chemically different hydrogen atoms present. Another very important factor is the apparent increased

electron density and donor strength of the permethylated ring. One example is the low oxidation potential of decamethylferrocene and its spontaneous oxidation in air, in contract to the air stability of ferrocene.[105]

Photoelectron spectroscopy is currently the best method for quantitatively measuring substituent effects on gas phase oxidation potentials and ionization energies. Some valence ionization studies of ring methylation in biscyclopentadienyl metal complexes have recently been reported.[106,107] The UPS of $(\eta^5\text{-}C_5H_5)Mn(CO)_3$[8] and $(\eta^5\text{-}C_5H_4CH_3)\text{-}Mn(CO)_3$[108] have been previously reported, and comments have been made on the change in valence metal and ring ionizations between these complexes.[69,108] These valence ionizations are found to decrease in energy with ring methylation, and this is generally interpreted in terms of a greater electron-releasing or inductive effect of the methyl groups that increase the electron charge in the ring, thereby increasing the ring's net "basicity".[64,106,107]

An additional interesting result of these ionization studies concerns the proposed distortion from five-fold symmetry for coordinated cyclopentadienyl rings.[17,109] Ring distortions have previously been implicated by IR,[110] Raman,[110] NMR[111] and low-temperature crystal structure results.[68] The valence ionizations examined in this study indicate that these distortions are also present when the molecules are in the gas phase.

These complexes are the foundation for the description of a significant class of organometallic complexes with different molecules and molecular fragments bound to the metal. A detailed knowledge of the

effects of ring methylation on electron distribution, bonding, and ionization characteristics of the present system is essential for later investigations. Chapter 3 demonstrates how the spectral changes caused by cyclopentadienyl methylation can be used as a valuable assignment and interpretation aid in the related (η^5-cyclopentadienyl)$M(CO)_2$(ligand) complexes.

Results and Discussion

The HeI photoelectron spectra of $CpMn(CO)_3$, $MeCpMn(CO)_3$, and $Me_5CpMn(CO)_3$ are presented in figure 29. In this notation Cp is η^5-$C_5H_5^-$, MeCp is η^5-$C_5H_4CH_3^-$, and Me_5Cp is η^5-$C_5(CH_3)_5$. The general shift of the ionizations to lower binding energy with increasing ring methylation can be seen. All three spectra have three major ionization regions in agreement with expectations based on molecular orbital theory.[8,42,112] The broad, intense band from 16 to 12 eV results from the overlap of CO 5σ and 1π, and ring σ and $a_2''(\pi)$ ionizations. The large number of closely-spaced orbitals in this region makes meaningful interpretation difficult. A distinct shoulder between 11 and 13 eV is present in the methyl-substituted compounds. This peak increases in intensity and shifts to lower energy with an increase in the number of ring methyl groups, suggesting ionization from an orbital which is high in ring methyl character. The two lowest binding energy bands at 9.0-10.5 eV and 7.5-8.5 eV exhibit the greatest sensitivity to ring methylation in these systems. The results of curve-fit analyses of these two bands are shown in figure 30 and the peak parameters are

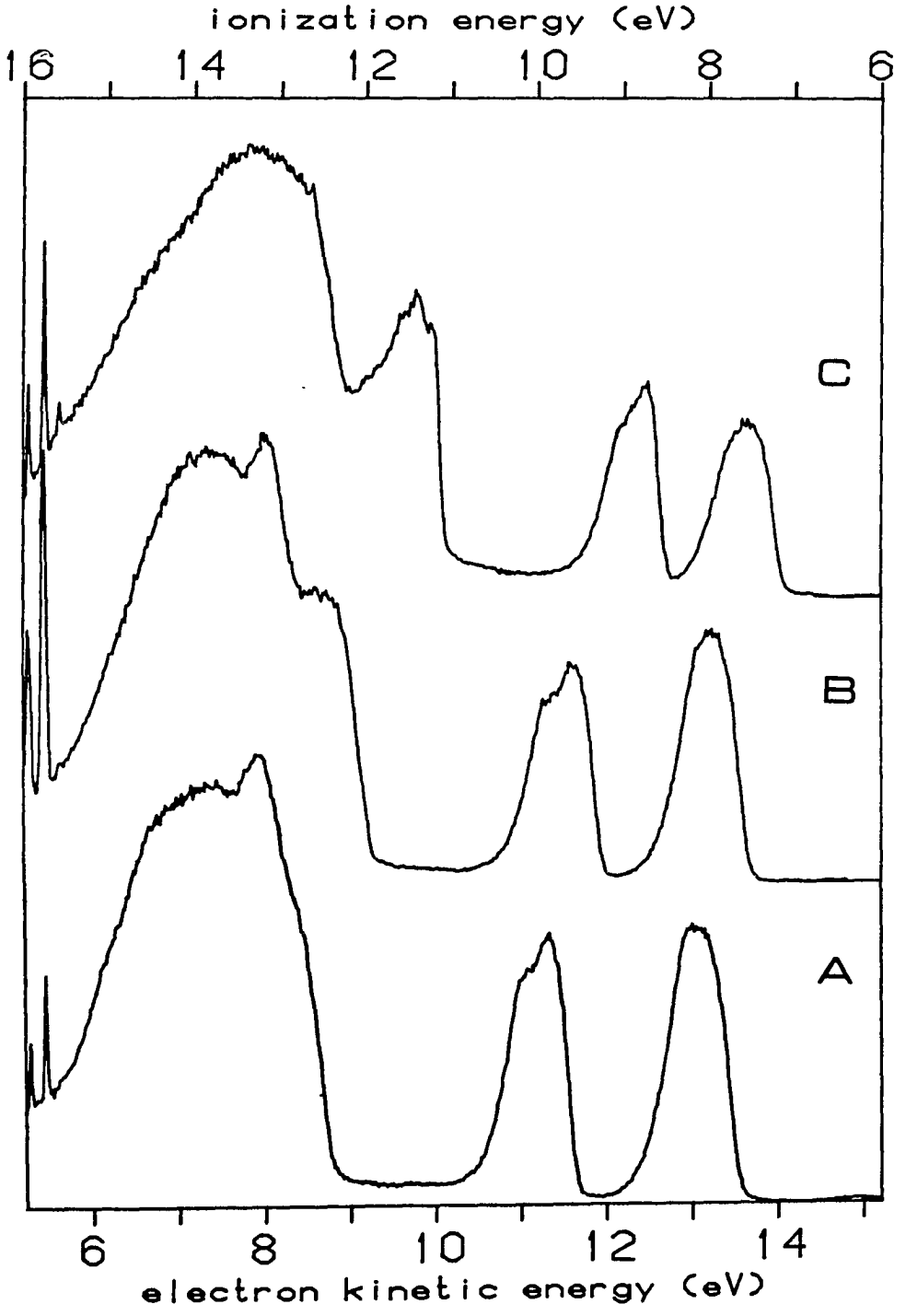

Figure 29 - The HeI Photoelectron Spectra of A) $CpMn(CO)_3$, B) $MeCpMn(CO)_3$ and C) $Me_5CpMn(CO)_3$

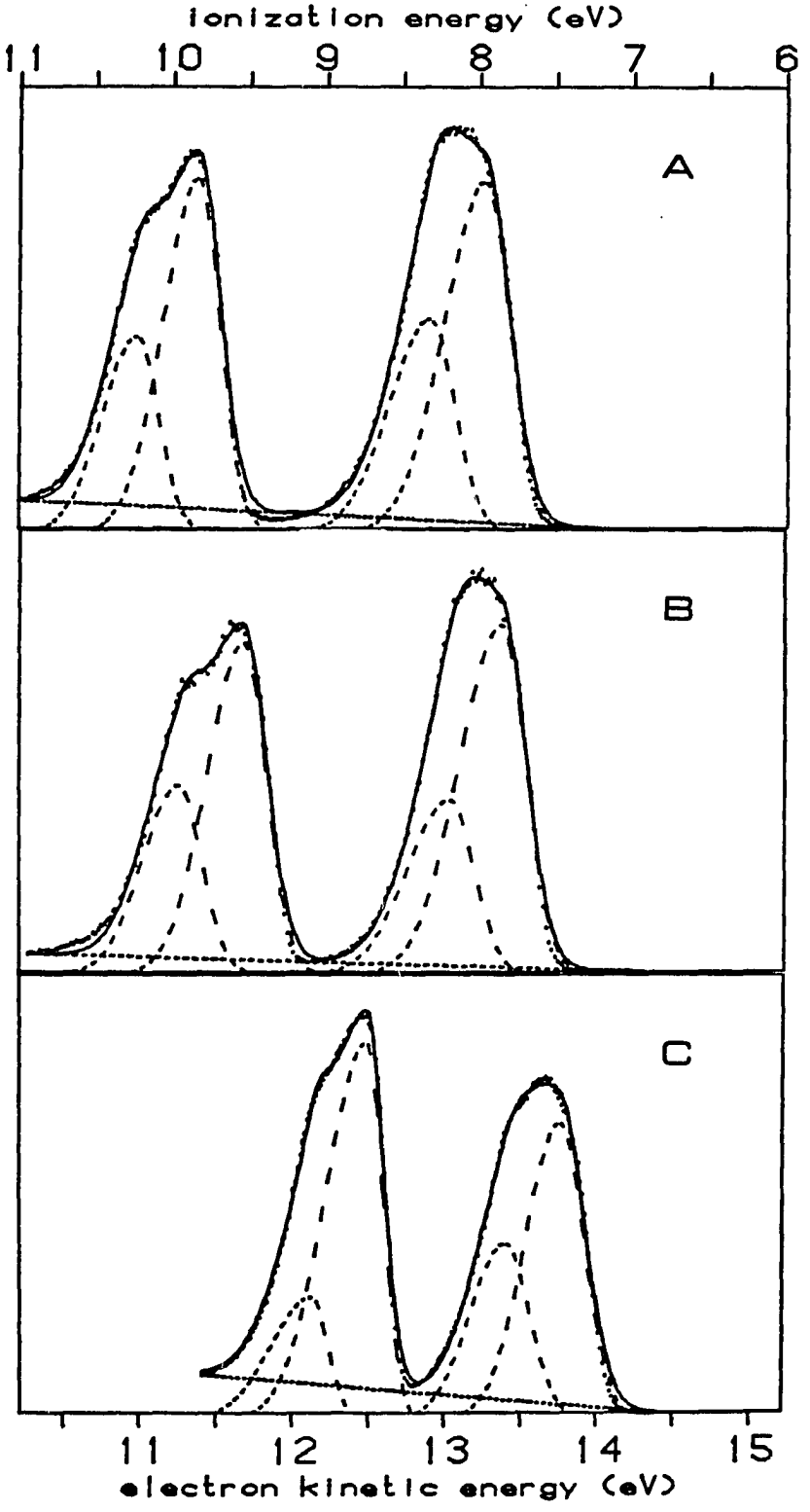

Figure 30 - Low Ionization Energy HeI Spectra of A) $CpMn(CO)_3$, B) $MeCpMn(CO)_3$ and C) $Me_5CpMn(CO)_3$

listed in Table XII. The ionization band at 9.0-10.5 eV has previously been assigned to the predominantly ring e_1'' ionization.[8] This band has a shoulder on its high binding energy side that has been observed in the spectra of a large number of cyclopentadienyl-containing compounds. The consistency of the splitting in this band for a variety of d^6 $CpM(CO)_2L$ complexes is shown in Table XIII. This distinctive band-shape will be one focal point of the discussion.

Figure 31 illustrates the differences in relative band intensitites in the HeI and HeII spectra of these complexes. These spectra are corrected for the increased analyzer transmission at higher kinetic energy. The HeII spectrum is also corrected for secondary HeIIβ and HeIIγ emissions in the source. It is clear that the first ionization band, from 7.5 to 8.5 eV, increases in intensity relative to the band in the 9.0 to 10.5 eV region. By analogy with the spectra of other metal complexes, this indicates that the first band is from an orbital which is high in metal d character.[40,41]

The HeI spectra of $CpRe(CO)_3$ and $Me_5CpRe(CO)_3$ in figure 32 provide further peak assignment information. These spectra have the same general features as their Mn analogues except for the considerable splitting observed in the lowest energy ionization. This splitting can be attributed to spin-orbit coupling in the third row metal,[8,113] and is an additional indication of high metal character in this ionization. The increased relative intensity of this band also reflects the known larger metal d ionization cross-section for third row metals compared to first row metals.[70] The closeup of this ionization for $CpRe(CO)_3$ is shown in figure 33. The plot of the absolute value of the first

Table XII - HeI Ionization Data. W_h and W_ℓ are the High and Low Binding Energy Halfwidths as Defined in the Experimental Section

	Vertical Ionization Energy (eV)	W_h	W_ℓ	Relative Amplitude	Relative Area
$C_5H_5Mn(CO)_3$	8.05	0.60	0.37	1.0	0.49
	8.40	0.60	0.37	0.6	
	9.90	0.50	0.3	1.21	0.51
	10.29	0.50	0.33	0.71	
$CH_3C_5H_4Mn(CO)_3$	7.89	0.65	0.38	1.0	0.52
	8.23	0.65	0.38	0.5	
	9.57	0.57	0.36	0.96	0.48
	10.00	0.57	0.36	0.57	
$(CH_3)_5C_5Mn(CO)_3$	7.46	0.54	0.38	1.0	0.50
	7.82	0.54	0.38	0.6	
	8.72	0.64	0.25	1.27	0.50
	9.09	0.64	0.25	1.41	
$C_5H_5Re(CO)_3$	8.05	0.40	0.19	1.0	0.60
	8.44	0.52	0.18	1.30	
	8.72	0.52	0.18	0.53	
	10.11	0.67	0.31	0.84	0.40
	10.54	0.67	0.31	0.41	
$(CH_3)_5C_5Re(CO)_3$	7.57	0.42	0.21	1.0	0.58
	7.92	0.50	0.16	1.13	
	8.23	0.50	0.16	0.59	
	9.07	0.55	0.27	1.08	0.42
	9.42	0.55	0.27	0.48	

Table XIII - The Measured Splittings in the Cp pi Ionization (eV)

Complex	Splitting (eV)	Reference
$CpMn(CO)_3$	0.39	this work
$MeCpMn(CO)_3$	0.43	this work
$Me_5CpMn(CO)_3$	0.37	this work
$CpRe(CO)_3$	0.43	this work
$Me_5CpRe(CO)_3$	0.35	this work
$MeCpMn(CO)_2(C_2H_4)$	0.46	this work
$MeCpMn(CO)_2(C_3H_6)$	0.42	this work
$Me_5CpMn(CO)_2(C_2H_4)$	0.38	this work
$CpMn(CO)_2SO_2$	0.43	108
$MeCpMn(CO)_2SO_2$	0.42	108
$CpMn(CO)_2N_2$	0.39	12
$CpMn(CO)_2CS$	0.36	13
$CpFe(CO)_2I$	0.36	8
$CpFe(CO)_2CH_3$	0.36	8
$CpCr(CO)_2NO$	0.38	46
$CpCr(CO)_2NS$	0.42	46

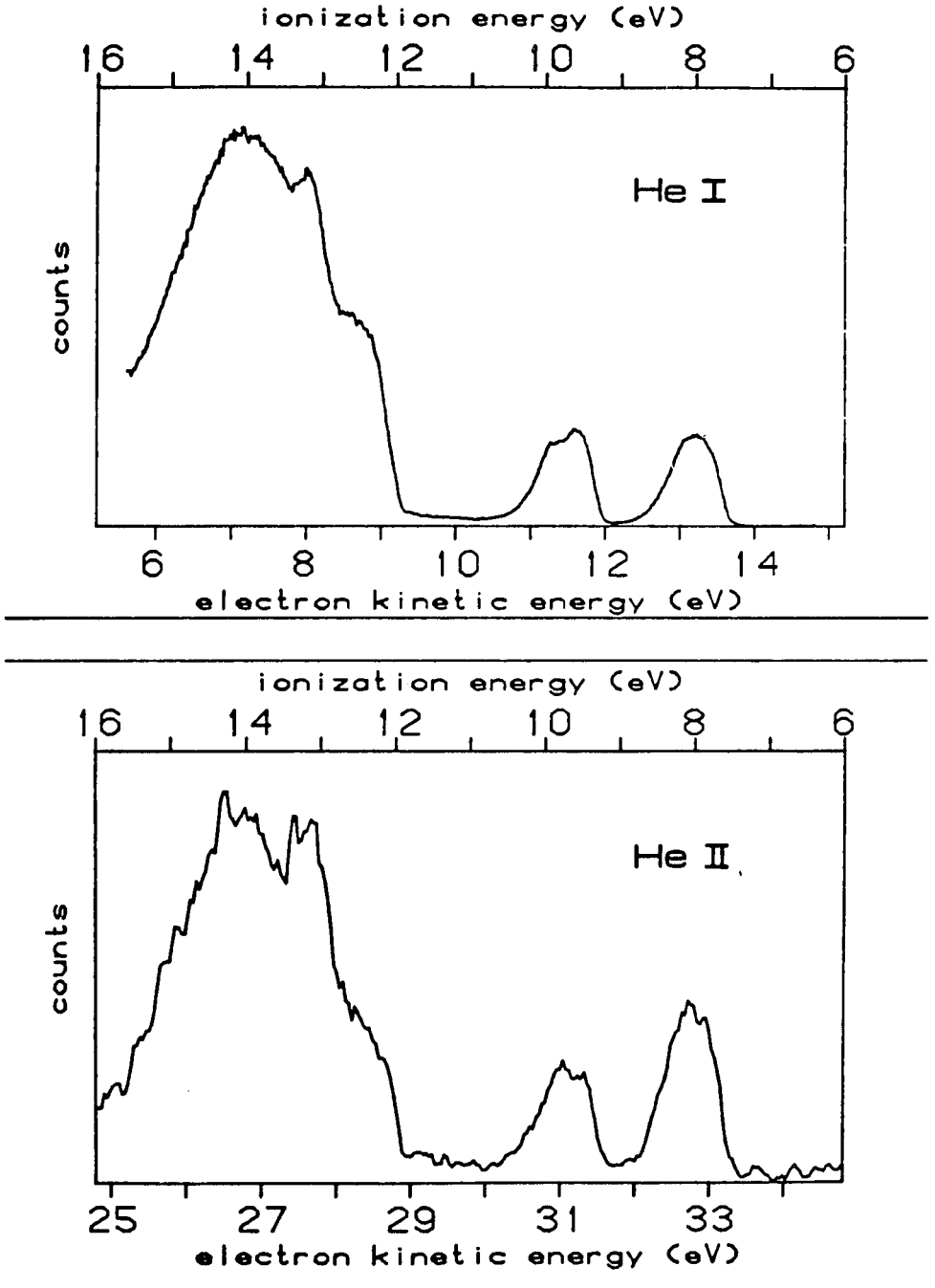

Figure 31 - HeI and HeII Photoelectron Spectra of $MeCpMn(CO)_3$

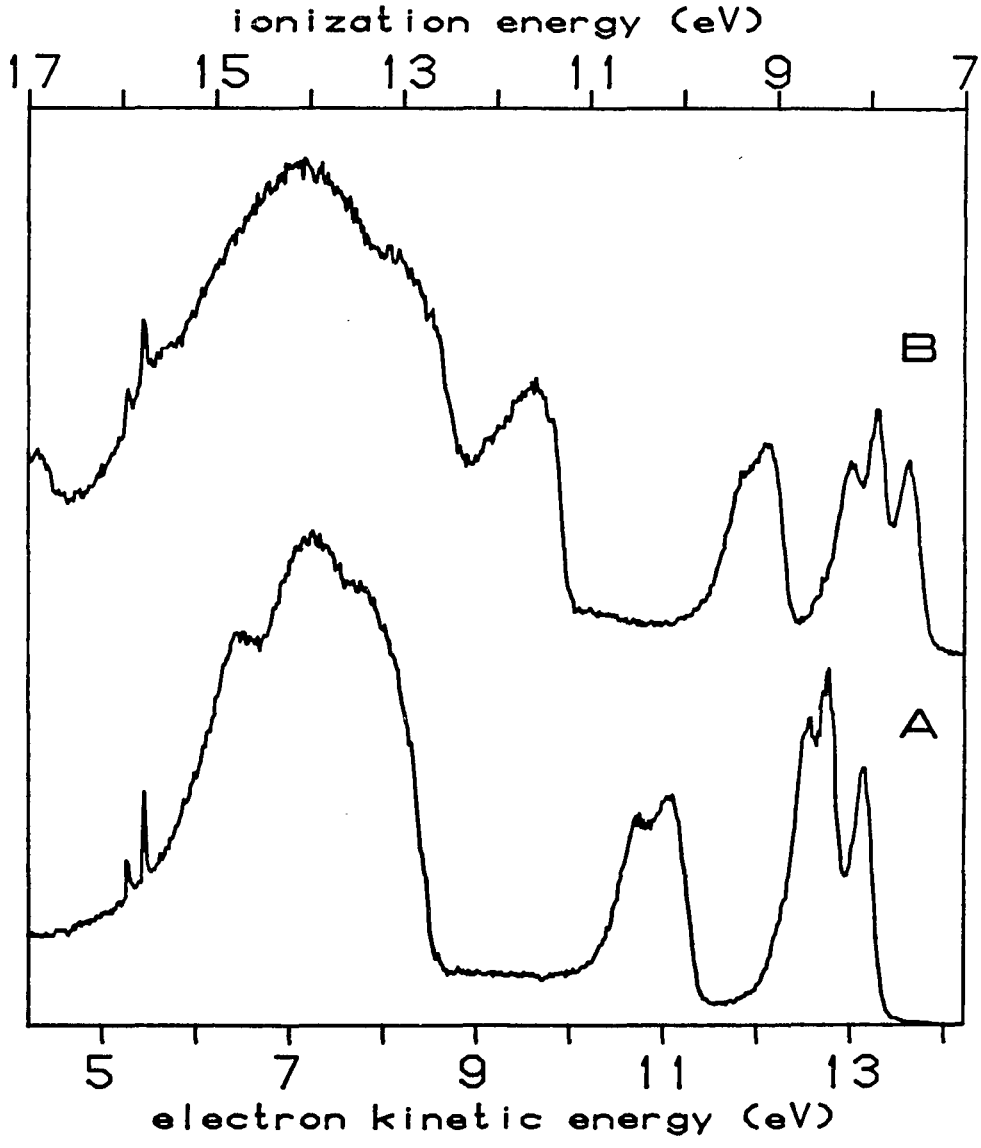

Figure 32 - The HeI Photoelectron Spectra of A) $CpRe(CO)_3$ and B) $Me_5CpRe(CO)_3$

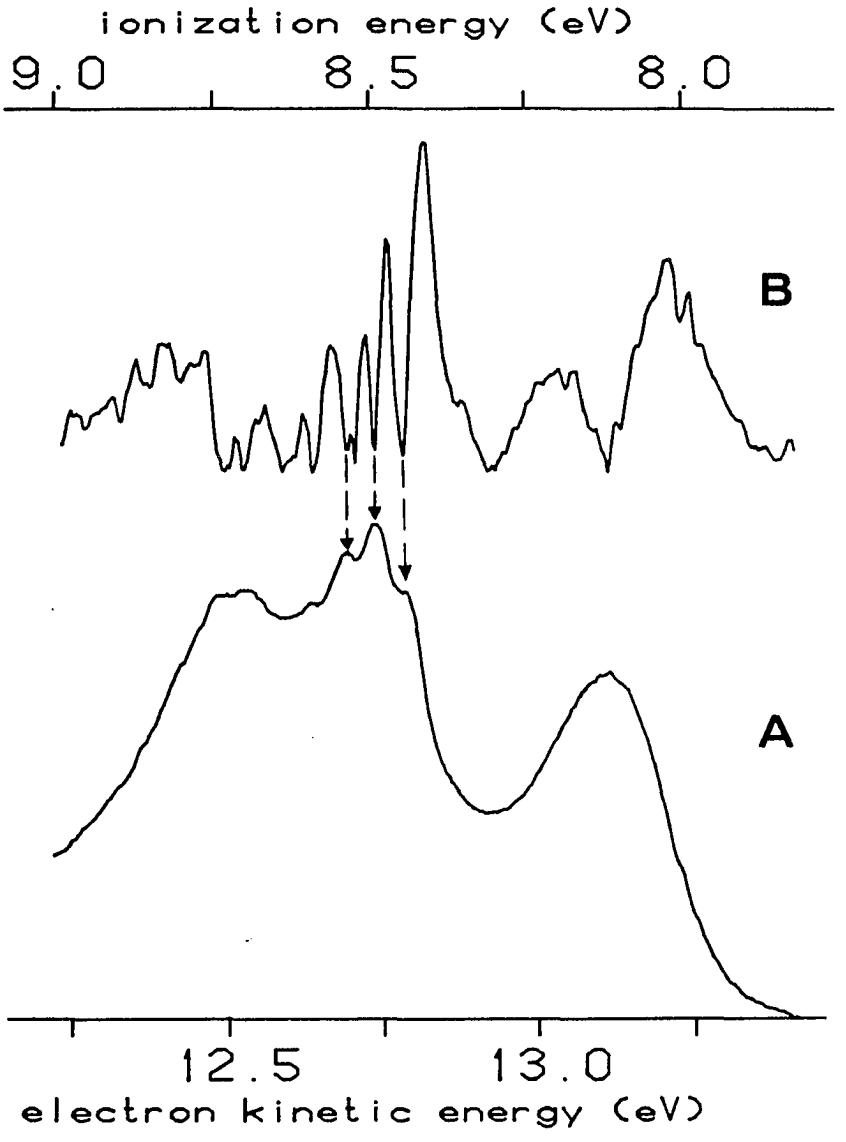

Figure 33 - A) Close-up of the Metal Ionization Region of $CpRe(CO)_3$, B) Absolute Value of the First Derivative of A

derivative of the spectrum accentuates the vibrational fine structure which can be observed on the middle peak and extends into the third peak. The measured vibrational splitting is 400±5 cm^{-1}. The observation of this vibrational fine structure has important consequences for the detailed description of the metal orbital interactions in these complexes (vide infra).

The measured effects of ring methylation are presented in Table XIV. As would be expected, ring methylation shifts the ring pi ionization much more than (by a factor of 2) the metal d ionizations. Comparison of the effect of one methyl group with that of five indicates that the inductive effect is not additive as indicated by published results on permethylated metallocenes.[106] It is important to note that the ring pi orbital is destabilized by more than 1 eV upon permethylation. This is a relatively large shift for any valence ionization between two similar molecules. The practical applications of this shift as a peak assignment aid and in uncovering unresolved ionization features is demonstrated in Chapters 3 and 5.

Table XIV - Decrease in Valence Ionization Energies (eV) with Methyl Substitution

	$CpMn(CO)_3$ ↓ $MeCpMn(CO)_3$	$CpMn(CO)_3$ ↓ $Me_5CpMn(CO)_3$	$CpRe(CO)_3$ ↓ $Me_5CpRe(CO)_3$
ring	0.31	1.19	1.08
metal	0.16	0.59	0.50

Tricarbonyl-η^5-cyclopentadienyl metal complexes have been the subject of several previous theoretical and ionization studies.[8,42,112] These studies agree in their general interpretation of the ionizations and electronic structure of these species, such as the observation that the first ionization band is predominantly associated with metal d orbital electrons and the second ionization is associated with the highest energy ring pi electrons. However, there are some very important questions that could not be answered from previous experiments. One concerns a definitive determination of the pattern of valence metal ionizations. Reasonably precise knowledge of these ionizations is needed for understanding the relative bonding characteristics of other small molecule ligands in similar complexes. Another question concerns the unusual but characteristic band envelope of the mostly ring pi ionization. The experimental results reported here provide information for interpreting these features. These points will be discussed before focusing on the effects of Cp ring methylation.

Metal Ionization Pattern. The occupied metal d orbitals of a d $Mn(CO)_3^+$ fragment transform as a_1(mostly dz^2) and e (mostly dx^2-y^2, dxy) representations.[114] Molecular orbital calculations show that the a orbital is only slightly more stable than the e orbitals in the $Mn(CO)_3^+$ fragment, and that these orbitals are perturbed very little by the addition of the Cp^- ring.[8] The a_1 and e ionizations are not fully resolved in the spectra of the manganese complexes, but bandshape analysis (figure 30) does show that the bandwidths and profiles are at least

consistent with the expected e before a_1 pattern. Additional evidence is provided by the spin-orbit splitting of these ionizations which is easily observed in the spectra of the rhenium complexes (figure 32). Analysis of the spin-orbit terms gives one interpretaton that assigns the outer metal ionizations to the spin-orbit components of the e orbitals. The middle ionization band then derives from the a_1 orbital, which has only slight spin-orbit mixing with the e components. The pattern of ionizations is obtained if the e orbitals are about 0.4 eV less stable than the a_1 orbital before spin-orbit splitting. This interpretation is consistent with the theoretical expectations. However, it was not possible in earlier studies to rule out other intepretations based on different assignments of the rhenium ionizations.[8]

A definitive assignment is now possible because of our ability to observe fine structure in the central ionization of the rhenium metal band. This ability has been developed from separate high resolution ionization studies of metal-carbonyl complexes.[115] This is the first report of such structure in the spectrum of an organometallic complex. Briefly, the structure is associated with the symmetric metal-carbon (of CO) stretch in the positive ion. We have found that this structure is observable in the ionization of a predominantly metal d orbital that is symmetrically backbonding to the carbonyls. In $CpRe(CO)_3$ this would be the a_1 orbital, which is mostly dz^2 in character. This orbital is directed between the tricarbonyl tripod with the carbonyls near the nodal surface, so that it backbonds equally to the three carbonyls. The observation of strong structure on the central ionization and very

little structure on the outer ionizations is direct support for assigning this middle peak of the spin-orbit split band to the predominantly a_1 ionization.

Two features of the vibrational fine structure also provide direct evidence for the magnitude of backbonding from the rhenium to the carbonyls in this orbital. First, the measured vibrational spacing in the positive ion is 400±5 cm^{-1}. The decrease of this frequency from 502 cm^{-1} in the neutral molecule[116] reflects the decrease in Re-C(O) bond order when one metal pi electron is removed. If backbonding were not significant one would expect a slight increase in bond energy from the improved sigma donation of the carbonyls. The other important feature is that a true progression in the vibrations is obtained. If the orbital were truly nonbonding, then the first or adiabatic vibrational mode would be most intense.[59] The vertical transition is actually to the third or fourth vibrational mode, indicating an increase in the equilibrium Re-C(O) distance in the positive ion compared to the neutral molecule.

Cyclopentadienly pi Ionization. In all of the spectra reported in this study and those of the compounds listed in Table XIII, the predominantly Cp pi ionizatoin between 9-10.5 eV displays a shoulder on its high binding energy side separated by 0.40 ±.05 eV from the main peak. Although the consistency of this bandshape has made it a very useful peak assignment aid in the photoelectron spectra of complexes of this type, the origin of this bandshape has not been explained. These orbitals originate from the e_1'' HOMO of the free ring. The lack of symmetry in

these complexes (C_s) will contribute to the splitting in this ionization band by lifting the degeneracy of any fragment orbitals of e symmetry. However, the results in Table XIII indicate no systematic change in this splitting as molecular symmetry is further lowered by ring methylation and CO substitution. It is also apparent that symmetry arguments alone do not explain the differences in intensity of the two split bands which results in the overall bandshape of this envelope (see figure 30). It appears that the general splitting and characteristic bandshape must be a more fundamental consequence of the coordination of Cp^- to a d^6 ML_3 group.

In previous studies it was noted that the separation in the ring pi ionization is consistent with the frequency of the carbon-hydrogen stretching mode, and that perhaps this splitting is a short progression in this vibrational mode.[8] This possibility is now eliminated because the same bandshape is found in the spectrum of $Me_5CpM(CO)_3$, in which there are no ring carbon-hydrogen bonds. Autoionization is another process that can give rise to unusual band envelopes, but this process is now ruled out because the shoulder is still observed when HeII excitation is used.[59]

The existence of Jahn-Teller splitting of the nearly degenerate Cp e_1"-type orbitals in the positive ion is also a possibility.[117] If the Jahn-Teller coupling is important in this case it should also be important in other high-symmetry Cp-metal complexes. A splitting is not observed in the spectrum of CpNiNO,[118] and current assignments are not in favor of Jahn-Teller splittings in metallocenes.[106] Alternatively,

a proposed Jahn-Teller splitting of 0.1 - 0.2 eV has been reported for the $^2E_1$ states of CpBeX (X = CH_3, C_2H, C_3H_3,Cl, Br).[119] A Jahn-Teller splitting is generally dependent on the vibrational energy of the molecule.[117,120] We have recorded ionization spectra of $MeCpMn(CO)_3$ from 25° to 150°C without any detectable change in the bandshape. The excited state Jahn-Teller type effect may still contribute to the total splitting, but it is difficult to support as the dominant cause of our observed 0.40 ± 0.05 eV splitting.

Since excited state or positive ion effects are unable to satisfactorily account for the bandshape of the predominantly Cp e_1'' ionization, it is appropriate to consider certain ground state effects in more detail. In particular, the possibility of a ground state distortion of the coordinated Cp^- ring, which would split the e_1'' ionization, should be carefully considered. Over the past ten years an increasing amount of spectroscopic evidence has accumulated which indicates that distortions of the coordinated Cp^- ring do occur,[68,110,111] but the distortions are apparently small and have been difficult to unambiguously observe within the certainty of crystal structure determinations.[68,109] The additional problems of packing forces and other solid state electronic effects further complicate the issue. An advantage of our gas phase ionization experiments is that there are no solid state effects. Also, the time scale of the electronic transitions is fast compared to nuclear motions, so thermal and librational motions are not a concern. It should be noted that small distortions in the coordinated Cp^- ring might be easily detected by UPS since the splitting

of the e_1'' eigenvalues will have an even greater effect on the separation of the positive ion states than on the stability of the ground state.

This point is supported by molecular orbital calculations on these systems. Figure 34 illustrates the results of parameter-free Fenske-Hall calculations for the coordination of the Cp^- ring. When the free Cp^- ring with D_{5h} symmetry (34a) is coordinated to $Mn(CO)_3^+$ with C_{3v} symmetry, the initially degenerate e_1'' orbital eigenvalues split by just 0.04 eV from the descent to C_s symmetry of the full complex (34b). Thus, just as there is no evidence for significant splitting of the e orbitals of $M(CO)_3^+$ in coordination to the Cp^- ring (previous section), the calculations show that the e orbitals of the Cp^- ring are not significantly split upon coordination to $M(CO)_3^+$. An important observation is that the five carbon-carbon overlap populations in the ring are no longer the same. The carbon-carbon bonds that are not eclipsed by the carbonyls of $Mn(CO)_3$ have clearly larger overlap populations, and there will be a tendency for these bonds to be shorter than the others. The Cp^- ring is susceptible to small distortions because one component of the e_1'' is stabilized while the other is destabilized with little net change in total energy. A model calculation was performed using a C_{2v}-distorted ring in which two C-C bond lengths were shorteded by 0.03 Å. The mostly e_1'' orbitals in this calculation are split into b_1 and a_2 orbitals (C_{2v}) with a separation of 0.36 eV, in good agreement with the measured splittings in

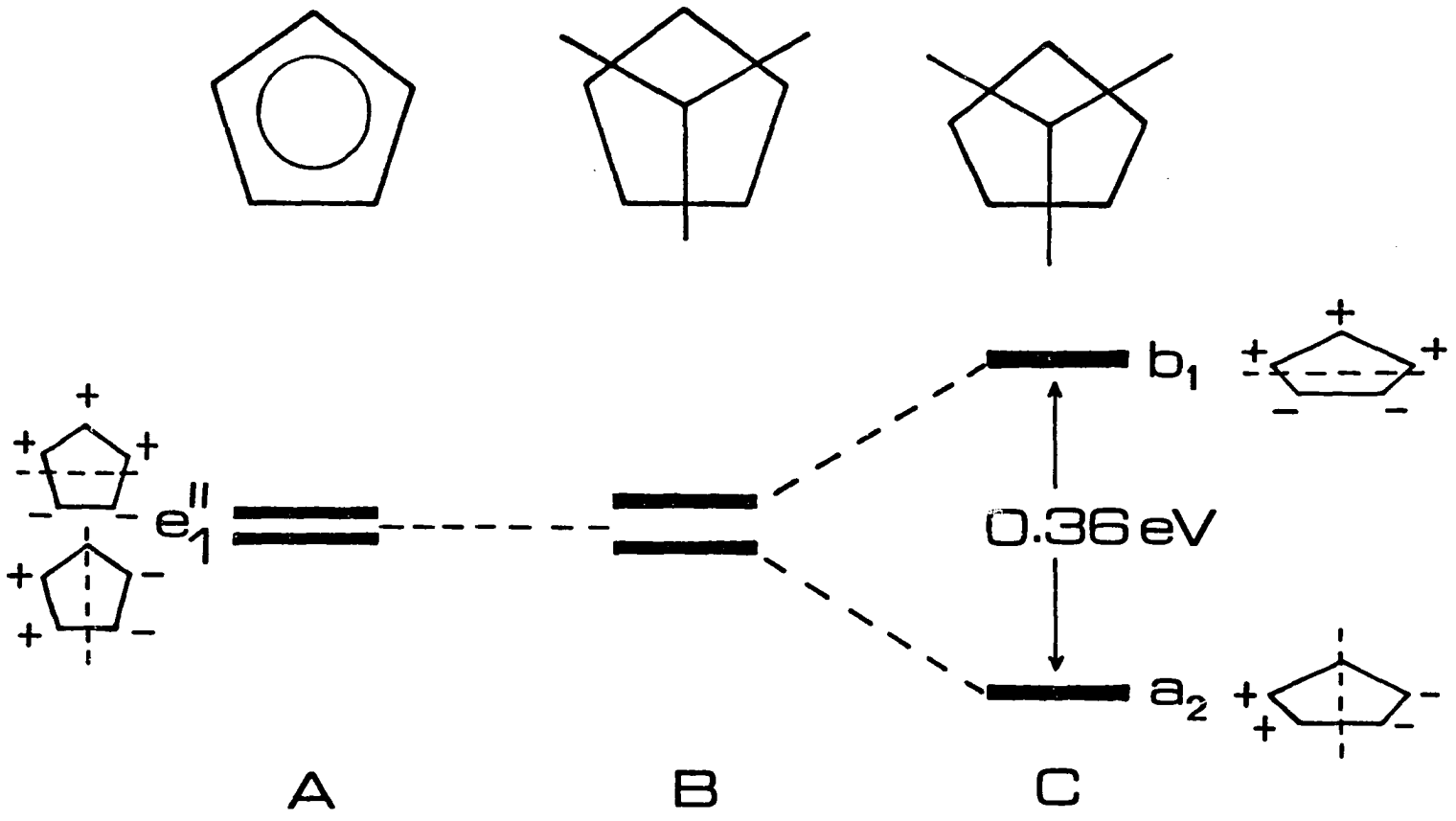

Figure 34 - The Effects of Coordination and the Loss of Five-Fold Symmetry on the e_1'' HOMO of Free $C_5H_5^-$. A) Free $C_5H_5^-$ B) $CpMn(CO)_3$ in Which the Local Five-Fold Symmetry of the Ring is Maintained (Splitting in e_1'' is 0.04 eV), C) $CpMn(CO)_3$ in Which Two of the Ring C-C Bond Lengths Have Been Shortened by 0.03Å (C_{2v} Symmetry Labels)

Table XIII. This distortion is similar in symmetry and in magnitude to that found from recent crystal structure determinations of $CpMn(CO)_3$ and $CpRe(CO)_3$.[68] Although complete optimization of the ring geometry was not pursued in our calculations, it is clear that an average deviation of C-C bond distances of only about 0.01 to 0.02 Å is sufficient to account for the observed splitting in the e_1'' ionization.

The intensity pattern of the two individual bands in the Cp pi ionization envelope is also consistent with this analysis. A shortening of two ring C-C bonds, as shown in figure 34, increases the bonding nature of the a_2 orbital while decreasing that of the b_1 orbital. Orbitals with more bonding character generally have broader vibrational envelopes.[59] Figure 35 shows a fit of the predominantly Cp pi ionization in which the two components are constrained to have equal ionization areas. The greater halfwidth of the higher bonding energy component is evident.

Conclusions

In the course of this investigation we have obtained additional fundamental experimental observations relating to coordinated cyclopentadienyls and carbonyls. The Cp e_1'' ionization bandshape is probable evidence of small (.01 - .02 Å) distortions from five-fold symmetry of the Cp^- ring when coordinated to d^6 ML_3^+ groups in the gas phase. The observation of Re-(CO) vibrational fine structure in the spin-orbit split valence metal ionizations, provide direct evidence of the extent

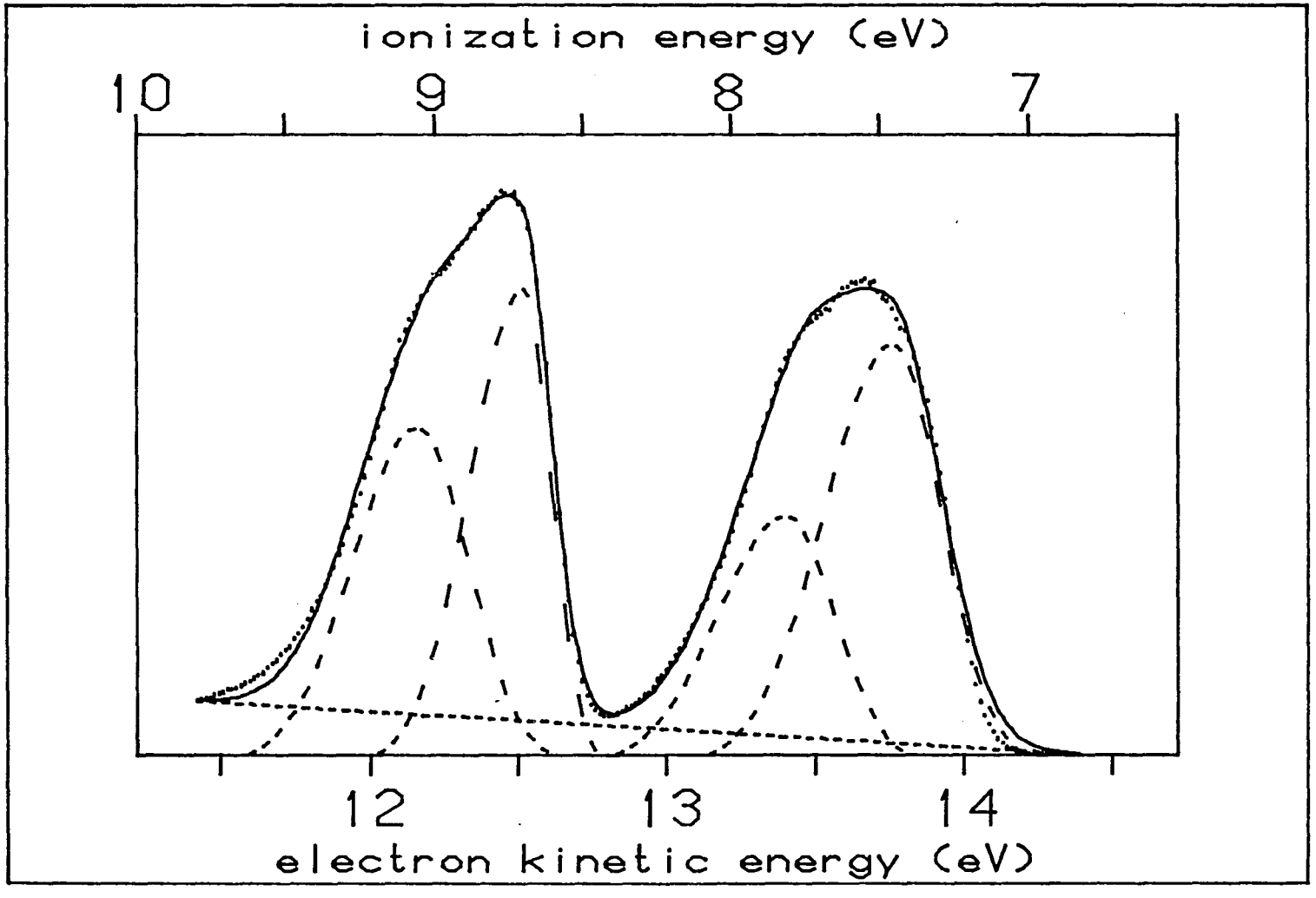

Figure 35 - Curve-Fit Analysis of $Me_5CpMn(CO)_3$ in Which the Ring pi Ionization Between 8.5 → 9.5 eV is Fit with Two Gaussians of Equal Area

of rhenium to carbonyl pi back-bonding. These observations also allow definitive interpretation of the pattern of metal ionizations.

The magnitude of the valence ionization energy shifts for the permethylated compounds are large on the energy scale of these experiments. This is an indication of considerable change in the electronic structure of these compounds and shows that electronic effects should, in general, receive equal attention to steric effects in explaining reactivity differences between substituted and unsubstituted cyclopentadienyl complexes.

REFERENCES

(1) Turner, D.W. "Molecular Photoelectron Spectroscopy", Wiley-Interscience, New York, 1970.

(2) Rabalais, J.W. "Principles of Ultraviolet Photoelectron Spectroscopy", Wiley, New York, 1977.

(3) Brundle, C.R. and Baker, A.D. "Electron Spectroscopy: Theory, Techniques and Applications", Academic Press, London, 1977.

(4) Briggs, D., ed. "Handbook of X-ray and Ultraviolet Photoelectron Spectroscopy", Heyden, Philadelphia, 1977.

(5) Koopmans, T.A.; Physica, (1934), 1, 104.

(6) See Appendix A and references therein.

(7) Lancaster, G.M.; Taylor, J.A.; Ignatiev, A. and Rabalais, J.W. J. Elect. Spect. Rel. Phen. (1978), 14, 143.

(8) Lichtenberger, D.L. and Fenske, R.F. J. Amer. Chem. Soc. (1976) 98, 50.

(9) Howell, J.; Rossi, A.; Wallace, D.; Haraki, K. and Hoffmann, R. QCPE (1977), 11, 344.

(10) Hall, M.B. and Fenske, R.F. Inorg. Chem. (1972) 11, 768.

(11) a) Richardson, J.W.; Nieuwport, W.C., Powell, R.R. and Edgell, W.F. J. Chem. Phys. (1962), 36, 1057; b) Clementi, E. J. Chem. Phys. (1964) 40, 1944.

(12) Lichtenberger, D.L.; Sellmann, D. and Fenske, R.F. J. Organometal. Chem. (1976) 117, 253.

(13) Lichtenberger, D.L. and Fenske, R.F. Inorg. Chem. (1976), 15, 2015.

(14) a) Granoff, B. and Jacobson, R.A. Inorg. Chem (1968), 7, 2328; b) LeBorgne, P.G.; Genetric, E. and Grandjean, D. Acta. Cryst. (1975), B31, 2824; c) Zeigler, M. Z. Anorg. Allg. Chem. (1967), 355, 12; d) Benson, I.B.; Knox, S.A.R.; Stansfield, R.F.D. and Woodward, P. Chem. Comm. (1977), 404.

REFERENCES (continued)

(15) Ittel, S.D. and Ibers, J.A. Adv. Organomet. Chem. (1976), 14, 33.

(16) Creswick, M.; Bernal, I. and Herrmann, W.A. J. Organomet. Chem. (1979), 172, C39.

(17) Byers, L.R. and Dahl, L.F. Inorg. Chem. (1980), 19, 277.

(18) Threlkel, R.S. and Bercaw, J.E. J. Organomet. Chem. (1977), 136, 1.

(19) Angelici, R.J. and Loewen, W. Inorg. Chem. (1967), 6, 682.

(20) Eisch, J.J. and King, R.B. "Synthesis of Organometallic Compounds", Academic Press, New York, vol. 1, p. 118..

(21) a) Rausch, M.D. and Genetti, R.A. J. Org. Chem. (1970), 35, 3888; b) King, R.B. and Bisnette, M.B. J. Organomet. Chem. (1967), 8, 287.

(22) Fischer, E.O. and Bittler, K. Z. Naturoforsch. (1961), 16b, 225.

(23) a) Cramer, R. Inorg. Synth. (1974), 15, 17; b) McCleverty, J.A. and Wilkinson, G. Inorg. Synth. (1966) 8, 211.

(24) Kang, J.W. and Maitlis, P.M. J. Organomet. Chem. (1971), 26, 393.

(25) a) Dewar, M.J.S. Bull. Soc. Chim. (1951), 18, C79; Ann. Rep. Chem. Soc. (1951), 48, 112; b) Chatt, J. and Duncanson, L.A. J. Chem. Soc. (1953), 2339

(26) Upton, T.H. and Goddard, W.A. III J. Amer. Chem. Soc. (1978), 100, 321.

(27) Rosch, N.; Messmer, R.P. and Johnson, K.H. J. Amer. Chem. Soc. (1974), 96, 3855.

(28) Norman, J.G. Jr. Inorg. Chem. (1977), 16, 1328.

(29) a) Baerends, E.J.; Ellis, D.E. and Ros, P. Theor. Chim. Acta (1972), 27, 339; b) Murrell, J.N. and Scollary, C.E. J. Chem. Soc., Dalton Trans. (1977), 1034.

(30) Sakaki, S.; Kudou, N. and Ohyeshi, A. Inorg. Chem. (1977), 16, 202.

REFERENCES (continued)

(31) a) Demuth, J.E. and Eastman, D.E. Phys. Rev. B (1976), 13, 1523; b) Demuth, J.E. Phys. Rev. L (1978), 40, 409; c) Demuth, J.E. Surf. Sci. (1978), 76, L603.

(32) Green, J.C.; Jackson, S.E. and Higginson, B. J. C. S. Dalton (1975), 403.

(33) Baerends, E.J., Oudshoorn, Ch. and Oskam, A. J. Elect. Spect. Rel. Phen. (1975), 6, 259.

(34) Flamini, A.; Semprini, E.; Stefani, F.; Cardaci, G.; Bellachioma, G. and Andreocci, M. J. C. S. Dalton (1978), 695.

(35) VanDam, H. and Oskam, A. J. Elect. Spect. Rel. Phen. (1979), 16, 307.

(36) VanDam, H. and Oskam, A. J. Elect. Spect. Rel. Phen. (1979), 17, 357.

(37) Hill, W.E.; Ward, C.H.; Webb, T.R. and Worley, S.D., Inorg. Chem. (1979), 18, 2029.

(38) VanDam, H.; Terpstra, A.; Stufkens, D.J. and Oskam, A. Inorg. Chem. (1980), 19, 3448.

(39) See Appendix B and; Calabro, D.C.; Hubbard, J.L.; Blevins, C.H. II; Campbell, A.C. and Lichtenberger, D.L. J. Amer. Chem. Soc. (1981) 103, 6839.

(40) Connor, J.A.; Derrick, L.M.R.; Hillier, I.H.; Guest, M.F.; Lloyd, D.R. Molec. Phys. (1976), 31, 23.

(41) Connor, J.A.; Derrick, L.M.R.; Hall, M.B.; Hillier, I.H.; Guest, M.F.; Lloyd, D.R. Molec. Phys. (1974), 28, 1193.

(42) Herberhold, M. "Metal π-Complexes", vol. II, Elsevier, N.Y., 1972.

(43) Schilling, B.E.R.; Hoffmann, R. and Lichtenberger, D.L. J. Amer. Chem. Soc. (1979), 101, 585.

(44) Schilling, B.E.R.; Hoffmann, R. and Faller, J.W. J. Amer. Chem. Soc. (1979), 101, 592.

REFERENCES (continued)

(45) For clarity we have retained the labels of the $CpMn(CO)_2$ fragment orbitals shown in figure 3.

(46) Hubbard, J.L. and Lichtenberger, D.L. Inorg. Chem. (1980), 19, 1388.

(47) Albright, T.A.; Hoffman, R.; Thibeault, J.C. and Thorn, D.L. J. Amer. Chem. Soc. (1979), 101, 3801.

(48) Although it is difficult from these measurements to absolutely determine the charge density on the coordinated ethylene, comparison of metal and ring ionization energies for the CO and ethylene complexes does show that the net charge density on coordinated ethylene is less than the charge density on coordinated CO. The net charge density is even less on a coordinated propylene.

(49) McWeeney, R.; Mason, R. and Towl, A.D.C. Disc. Faraday Soc. (1969), 47, 20.

(50) Porzio, W. and Zocchi, M. J. Amer. Chem. Soc. (1978), 100, 2048.

(51) Herrmann, W.A.; Reiter, B. and Biersack, H. J. Organomet. Chem. (1975), 97, 245.

(52) Masters, C. Adv. Organomet. Chem. (1979), 17, 61.

(53) Biloen, P.; Helle, J.N. and Sachtler, W.M.H. J. Catal. (1979), 58, 95.

(54) Brady, R.C. III and Pettit, R. J. Amer. Chem. Soc. (1980), 102, 6181.

(55) a) Schultz, A.J.; Williams, J.M.; Calvert, R.B.; Shapley, J.R. and Stucky, G.D. Inorg. Chem. (1979), 18, 319; b) Halbert, T.R.; Leonowicz, M.E. and Maydonovitch, D.J. J. Amer. Chem. Soc. (1980), 102, 5101; and references therein.

(56) Herrmann, W.A. Angew. Chem. Int. Ed. Engl., (1978), 17, 800; and references therein.

(57) Granozzi, G.; Tondello, E.; Casarin, M. and Ajo, D. Inorg. Chim. Acta. (1981), 48, 73.

REFERENCES (continued)

(58) a) Evans, S; Green, J.C.; Green, M.L.H.; Orchard, A.F. and Turner, D.W. Discuss. Faraday Soc. (1969), 47, 112; b) Bursten, B.E.; Cotton, F.A.; Cowley, A.H.; Hanson, B.E.; Lattman, M; and Stanley, G.G. J. Amer. Chem. Soc. (1979), 101, 6244; c) Guest, M.F.; Garner, C.D.; Hillier, I.H. and Walton, I.B. Faraday Trans. II (1978) 2092.

(59) Baker, A.D. and Brundle, C.R. "Electron Spectroscopy: Theory, Techniques and Applications", Academic Press, N.Y., (1977), Vol. I, Chap. 1.

(60) a) Block, T.F. and Fenske, R.F. J. Am. Chem. Soc. (1977), 99, 4321; b) Goddard, R.J.; Hoffmann, R. and Jemmis, E.D. J. Am. Chem. Soc. (1980), 102, 7667.

(61) Hofmann, P. Angew. Chem. Int. Ed. Engl. (1979), 18, 554.

(62) a) Redhouse, A.D. J. Organomet. Chem. (1975), 99, C29; b) Hadicke, E and Hoppe, W. Acta. Cryst. (1971), B27, 760.

(63) a) Shaik, S. and Hoffmann, R. J. Am. Chem. Soc. (1980), 102, 1194; b) Jemmis, E.D.; Pinhas, A.R. and Hoffmann, R. J. Am. Chem. Soc. (1980), 102, 2576. c) Shaik, S.; Hoffmann R.; Fisel, C.R. and Summerville, R.H. J. Am. Chem. Soc. (1980), 102, 4555.

(64) a) King, R.B. Coord. Chem. Rev. (1976), 20, 155; b) Fagan, P.J.,; Manriquez, M.J. and Marks, T.J. in "Organometallics of f Elements", D. Reidel, Dordrecht, 1979, p. 113.

(65) Green, J.C. Struct. Bonding (1981), 43, 37.

(66) a) Hofmann, P. Ang. Chem. (1977), 16, 536; b) Albright, T.A.; Hoffmann, R. Chem. Ber. (1978), 111, 1578.

(67) a) Dahl, L.F. and Wei, C.H. Inorg. Chem. (1963), 2, 713; b) Gerloch, M.R. and Mason, R. J. Chem. Soc. (1965), 296; c) Bennett, M.J.; Churchill, M. R.; Gerloch, M. and Mason R. Nature (London) (1964), 201, 1318; d) Churchill, M.F. and Kalra, K.L. Inorg. Chem. (1973), 12, 1650; e) Smith, A.E. Inorg. Chem. (1972), 11, 165; f) Bernal, I.; Korp, J.D. and Rusier, G.M. J. Organomet. Chem. (1977), 139, 321.

(68) Fitzpatrick, P.J.; LePage, Y.; Sedman, J. and Butler, I.S. Inorg. Chem. (1981), 20, 2852.

(69) a) Evans, S.; Guest, M.F.; Hillier, I.H. and Orchard, A.F. J. C. S. Faraday Trans. II (1974), 417.

REFERENCES (continued)

(70) Higginson, B.R.; Lloyd, D.R.; Burroughs, P.; Gibson, D.M. and Orchard, A.F. Molec. Phys. (1974), 27, 215.

(71) Hillier, I.H.; Guest, M.F.; Higginson, B.R. and Lloyd, D.R. Molec. Phys. (1975), 29, 113.

(72) Calabro, D.C. and Lichtenberger, D.L. Inorg. Chem. (1980), 18, 1732.

(73) a) Coutiere, M.M.; Demuynick, J. and Veillard, A. Theor. Chim. Acta. (1972), 27, 281; b) Bagus, P.S.; Walgren, U.I. and Almlof, J. J. Chem. Phys. (1976), 64, 2324.

(74) Blevins, C.H. II; Lichtenberger, D.L. submitted for publication.

(75) a) Schwarz, M.E. "Electronic Structure Theory", Vol. 4, edited by Henry F. Schaefer III, Plenum Press, New York, 1977, and references therein; b) Ferreira, R. Structure and Bonding (1976), 31, 1.

(76) Richards, W. G. Int. J. Mass Spec. Ion Phys. (1969), 2, 419.

(77) Ellison, F.O. and White, M.G. J. Chem. Ed. (1976), 53, 431.

(78) a) Gubanov, V.A. J. Electron Spectrosc. (1976), 9, 85; b) Beck, D.R. and Nicolaides, C.A. J. Electron Spectrosc. (1976), 8, 249; c) Pireaux, J.J.; Svenson, S.; Basilier, E.; Malmquist, P.A.; Gelius, U.; Cavdano, R., and Siegbahn, K. Physical Review (1976), 14, 2133; d) Davis, D.W. and Shirley, D.A. Chem. Phys. Letters (1972), 15, 185; e) Hedin, L. and Johansson, A. J. Phys. B (1969), 2, 1336; f) Clark, D.T. and Cromarty, B.J. Chem. Phys. Lett. (1977), 49, 137; g) Kowalczyk, S.P.; Ley, L; McFeely, F.R.; Pollack, R.A. and Shirley, D.A. Phys. Rev. B (1974), 9, 381.

(79) Goscinski, O.; Pickup, B.T. and Purvis, G. Chem. Phys. Lett. (1973), 22, 167.

(80) Brundle, C.R.; Robin, M.B. and Basch, H. J. Chem. Phys. (1970), 53, 2196.

(81) Hall, M.B.; Guest, M.F. and Hillier, I.H. Chem. Phys. Letters (1972), 15, 592.

(82) Kellerer, B.; Cederbaum, L.S. and Hohlneicher, G. J. Electron Spectrosc. (1974), 3, 107.

REFERENCES (continued)

(83) "Molecular Photoelectron Spectroscopy," D.W. Turner, Ed., Wiley-Interscience, New York, 1970, page 7.

(84) Many examples are referenced in VonNiessen, W.; Diereksen, G.H.F. and Cederbaum, L.S. J. Chem. Phys. (1977), 67, 4124.

(85) "Electron Spectroscopy," Edited by C.R. Brundle and A.D. Baker, Academic Press, New York, 1977, page 305 and references therein.

(86) a) Coutiere, M.M.; Demuynik, J. and Veillard, A. Theoret. Chim. Acta (1972), 27, 281; b) Rabalais, J.W.; Werme, L.O.; Bergmark, T.; Karlsson, L.; Hussain, M. and Seigbahn, K. J. Chem. Phys. (1960), 32, 245.

(87) a) Rohmer, M.M. and Veillard, A. J. Chem. Soc. D (1973), 250; b) Veillard, A. Chem. Commun. (1969) 1022.

(88) Veillard A. and Demuynik J. "Modern Theoretical Chemistry," Edited by H.F. Schaefer III, Plenum Press, New York, 1977, page 207.

(89) Brogli, F.; Clark, P.A. and Heilbronner, E. Angew. Chem. Int. Ed. (1973), 12, 422.

(90) These statements strictly apply to single determinant wavefunctions for closed-shell molecules. The concept has been extended to include differences between average energies with frozen orbitals. J.C. Slater, "Quantum Theory of Atomic Structure," Vol. II, McGraw-Hill, 1970.

(91) a) Fraga, S.; Saxena, K.M.S. and Karwowski, J. Can. J. Phys. (1973), 51, 2063; b) Fraga, S.; Saxena, K.M.S.; Karwowski, J. and Bray, B. Can. J. Phys. (1975), 53, 2415.

(92) Where possible, the necessary values $E[M(\phi)]$, $E[M_i^+(\phi')]$, and ϵ_i were taken from the tables of E. Clementi and C. Roetti, Atomic Data and Nuclear Data Tables (1974) 14, 177. The experimental ionization energies are from C. E. Moore, NSRDS-NB534, National Bureau of Standards, Washington, D.C., 1970. Except where noted the configurations correspond to those of Moore.

(93) a) Richardson, J.W.; Blackman, M.J. and Ranochak, J.E. J. Chem. Phys. (1973), 58, 3010; b) Maly, J. and Hussonnois, M. Theoret. Chim. Acta (1973), 31, 137; c) Williams, A.R. and Lang, N.D. Phys. Rev. Letters (1978), 40, 954.

REFERENCES (continued)

(94) Slater, J.C. Physical Review (1930), 36, 57.

(95) See for instance "Inorganic Chemistry", Edited by J.E. Huheey, Harper and Row, New York, 1972, page 40.

(96) Snyder, L.C. J. Chem. Phys. (1971), 55, 95.

(97) Kowalczyk, S.P.; Ley, L.; McFeely, F.R.; Pollak, R.A. and Shirley, D.A. Phys. Rev. B (1974), 9, 381.

(98) Shirley, D.A. Chem. Phys. Letters (1972), 17, 312; Phys. Rev. A (1973), 7, 1520.

(99) a) Clementi, E. and Raimondi, D.L. J. Chem Phys. (1963), 38, 2686; b) Clementi, E.; Raimondi, D.L. and Reinhardt, W.P. J. Chem. Phys. (1967), 47, 1300.

(100) a) Bercaw, J.E.; Marvich, R.H.; Bell, L.G. and Brintzinger, H.H. J. Amer. Chem. Soc. (1972), 94, 1219; b) Bercaw, J.E. J. Amer. Chem. Soc. (1974), 96, 5087.

(101) a) Thomas, J.L. and Brintzinger, H.H. J. Amer. Chem. Soc. (1972), 94, 1386; b) Thomas, J.L. J. Amer. Chem. Soc. (1973), 95, 1838.

(102) a) King, R.B. and Bisnette, M.B. J. Organomet. Chem. (1967), 8, 287; b) Kang, J.W.; Moseley, K. and Maitlis, P.M. J. Amer. Chem. Soc. (1969), 91, 5970; c) Kang, J.W. and Maitlis, P.M. J. Organomet. Chem. (1972), 26, 393.

(103) King, R.B. and Efraty, A. J. Amer. Chem. Soc. (1972), 94, 3773.

(104) King, R.B.; Efraty, A. and Douglas, W.M. J. Organomet. Chem. (1973), 56, 345.

(105) Nesmeyanov, A.N.; Materikova, R.B.; Lyatifov, I.R.; Kurbanov, T.K. and Kochetkova, N.S. J. Organomet. Chem. (1978), 145, 241.

(106) Cauletti, C.; Green, J.C.; Kelly, M. Ruth; Powell, P.; VanTilborg, J.; Robbins, J. and Smark, J. J. Elect. Spectr. Rel. Phen. (1980), 19, 327.

(107) a) Fragala, I.; Marks, T.J.; Fagan, P.J. and Manriquez, J.M. J. Elect. Spectr. Rel. Phen. (1980), 20, 249; b) Evans, S.; Green, M.L.H.; Jewitt, B.; Orchard, A.F. and Pyall, C.F. J. C. S. Faraday II (1972), 68, 1847.

REFERENCES (continued)

(108) Campbell, A.C.; M.S. Thesis, University of Arizona, 1980.

(109) a) Wheatly, P.J. in "Perspectives in Structural Chemistry", Dunitz, J.D.; Ibers, J.A., Eds., Wiley, New York, 1967, Vol. 1, p. 1; b) Teller, R.G. and Williams, J.M. Inorg. Chem. (1980), 19, 2770.

(110) a) Adams, D.M. and Squire, A. J. Organomet. Chem. (1973), 63, 381; b) Parker, D.J. J. Chem. Soc. Dalton Trans. (1974), 155.

(111) a) Lindon, J.C. and Dailey, B.P. Mol. Phys. (1971), 22, 465; b) Bailey, D.; Buckingham, A.D.; McIvor, M.C. and Rest, A.J. Mol. Phys. (1973), 25, 479; c) Khetrapal, C.L.; Kunwar, A.C. and Saupe, A. Mol. Cryst. Liq. Cryst. (1976), 35, 215.

(112) a) Brown, D.A.; Fitzpatrick, N.J. and Mathews, N.J. J. Organomet. Chem. (1975), 88, C27; b) Fitzpatrick, N.J.; Savariault, J.M. and Labarre, J.F. J. Organomet. Chem. (1977), 127, 325.

(113) Hall, M.B. J. Amer. Chem. Soc. (1975), 97, 2057.

(114) a) Elian, M. and Hoffmann, R. Inorg. Chem. (1975), 14, 1058; b) Elian, M.,; Chen M.M.L; Mingos, D.M.P and Hoffman, R. Inorg. Chem. (1976), 15, 1148.

(115) Hubbard, J.L. and Lichtenberger, D.L., Abstracts, Pacific Conference on Chemistry and Spectroscopy, Pasadena, California, 1979.

(116) Lokshin, B.V.; Klemenkova, Z.S. and Marakov, Yu. V. Spectrochim. Acta (1972), 28A, 2209.

(117) a) Sturge, M.D. Solid State Physics (1967), 20, 92; b) Englman, R. "The Jahn-Teller Effect in Molecules and Crystals", Wiley-Interscience, N.Y., 1972; c) Rabalais, J.W.; Bergmark, T.; Werme, L.O.; Karlsson, L. and Siegbahn, K. Physica Scripta (1971), 3, 13; d) Rowland, C.G. Chem. Phys. Lett. (1971), 9, 169.

(118) a) Evans, S.; Guest, M.F.; Hillier, I.H. and Orchard, A.F. J. C. S. Faraday Trans. II (1974), 417; b) Hubbard, J.L. and Lichtenberger, D.L., unpublished results.

(119) Böhm, M.C.; Gleiter, R; Morgan, G.L.; Lusztyk, J. and Starawieyski, K.B. J. Organomet. Chem. (1980), 194, 257.

(120) Lichtenberger, D.L., Abstracts, Pacific Conference on Chemistry, Anaheim, California, 1977.